UNIVERSITAT POLITÈCNICA
DE CATALUNYA
BARCELONATECH

Cellular networks for smart grid communication

Charalampos Kalalas

UNIVERSITAT POLITÈCNICA DE CATALUNYA
BARCELONATECH
Departament de Teoria del Senyal
i Comunicacions

Centre Tecnològic
de Telecomunicacions de Catalunya

Doctoral Thesis

Cellular Networks for Smart Grid Communication

Radio Access Design
Towards Massive and Reliable Connectivity

Charalampos Kalalas

Advisor: Dr. Jesus Alonso-Zarate
Centre Tecnològic de Telecomunicacions de Catalunya

Tutor: Prof. Luis Alonso
Universitat Politècnica de Catalunya

Submitted in fulfillment of the requirements
for the degree of Doctor of Philosophy in the

Department of Signal Theory and Communications
Universitat Politècnica de Catalunya

Barcelona, May 2018

This work was supported in part by the ADVANTAGE Project (FP7-PEOPLE-2013-ITN) under Grant 607774 and in part by the Catalan Government under Grant 2014-SGR-1551.

Abstract

The next-generation electric power system, known as smart grid, relies on a robust and reliable underlying communication infrastructure to improve the efficiency of electricity distribution. Cellular networks, e.g., LTE/LTE-A systems, appear as a promising technology to facilitate the smart grid evolution. Their inherent performance characteristics and well-established ecosystem could potentially unlock unprecedented use cases, enabling real-time and autonomous distribution grid operations. However, cellular technology was not originally intended for smart grid communication, associated with highly-reliable message exchange and massive device connectivity requirements. The fundamental differences between smart grid and human-type communication challenge the classical design of cellular networks and introduce important research questions that have not been sufficiently addressed so far. Motivated by these challenges, this doctoral thesis investigates novel radio access network (RAN) design principles and performance analysis for the seamless integration of smart grid traffic in future cellular networks. Specifically, we focus on addressing the fundamental RAN problems of network scalability in massive smart grid deployments and radio resource management for smart grid and human-type traffic. The main objective of the thesis lies on the design, analysis and performance evaluation of RAN mechanisms that would render cellular networks the key enabler for emerging smart grid applications.

The first part of the thesis addresses the radio access limitations in LTE-based networks for reliable and scalable smart grid communication. We first identify the congestion problem in LTE random access that arises in large-scale smart grid deployments. To overcome this, a novel random access mechanism is proposed that can efficiently support real-time distribution automation services with negligible impact on the background traffic. Motivated by the stringent reliability requirements of various smart grid operations, we then develop an analytical model of the LTE random access procedure that allows us to assess the performance of event-based monitoring traffic under various load conditions and network configurations. We further extend our analysis to include the relation between the cell size and the availability of orthogonal random access resources and we identify an additional challenge for reliable smart grid connectivity. To this end, we devise an interference- and load-aware cell planning mechanism that enhances reliability in substation automation services. Finally, we couple the problem of state estimation in wide-area monitoring systems with the reliability challenges in information acquisition. Using our developed analytical framework, we quantify the impact of imperfect communication reliability in the state estimation accuracy and we provide useful insights for the design of reliability-aware state estimators.

The second part of the thesis builds on the previous one and focuses on the RAN problem of resource scheduling and sharing for smart grid and human-type traffic. We introduce a novel scheduler that achieves low latency for distribution automation traffic while resource allocation is performed in a way that keeps the degradation of cellular users at a minimum level. In addition, we investigate the benefits of Device-to-Device (D2D) transmission mode for event-based message exchange in substation automation scenarios. We design a joint mode selection and resource allocation mechanism which results in higher data rates with respect to the conventional transmission mode via the base station. An orthogonal resource partition scheme between cellular and D2D links is

further proposed to prevent the underutilization of the scarce cellular spectrum.

The research findings of this thesis aim to deliver novel solutions to important RAN performance issues, i.e., massive and reliable random access, efficient resource sharing and scheduling, that arise when cellular networks support smart grid communication. With the emergence of smart grid paradigm, the results of this thesis are expected to provide fundamental RAN design guidelines for future cellular networks and fulfill the smart grid potential. In addition, our research outcomes and drawn insights may also prove useful for other applications envisioned for 5G which rely on massive and reliable information acquisition, e.g., intelligent transportation systems, industrial automation and mobile health-care services.

Keywords: Cellular networks, 3GPP LTE, Radio Access Network (RAN), Random Access CHannel (RACH), Radio Resource Management (RRM), Device-to-Device (D2D), Massive Machine-Type Communication (mMTC), Reliability, Smart grid, Distribution automation, Substation automation, Wide-area Monitoring Systems.

Resumen

La próxima generación del sistema eléctrico de potencia, conocido como smart grid, se basa en una infraestructura de comunicaciones robusta y fiable que permita mejorar la eficiencia en la distribución de energía eléctrica. Las redes celulares, p.e., los sistemas LTE/LTE-A, aparecen como una tecnología prometedora para facilitar la evolución de la smart grid. Sus características de rendimiento inherentes y un ecosistema bien establecido pueden permitir la realización de casos de uso sin precedentes, haciendo posible la operación autónoma y en tiempo real de la red de distribución eléctrica. Sin embargo, la tecnología celular no fue pensada originalmente para las comunicaciones en la smart grid, asociadas con el intercambio fiable de mensajes y con requisitos de conectividad de un número masivo de dispositivos. Las diferencias fundamentales entre las comunicaciones en la smart grid y la comunicación de tipo humano desafían el diseño clásico de las redes celulares e introducen importantes cuestiones de investigación que hasta ahora no se han abordado suficientemente. Motivada por estos retos, esta tesis doctoral investiga los principios de diseño y analiza el rendimiento de una nueva red de acceso radio (RAN) que permita una integración perfecta del tráfico de la smart grid en las redes celulares futuras. En concreto, nos centramos en los problemas fundamentales de escalabilidad de la RAN en despliegues de smart grid masivos, y en la gestión de los recursos radio para la integración del tráfico de la smart grid con el tráfico de tipo humano. El objetivo principal de la tesis consiste en el diseño, el análisis y la evaluación del rendimiento de los mecanismos de las RAN que convertirán a las redes celulares en el elemento clave para las aplicaciones emergentes de las smart grids.

La primera parte de la tesis aborda las limitaciones del acceso radio en redes LTE para la comunicación fiable y escalable en smart grids. En primer lugar, identificamos el problema de congestión en el acceso aleatorio de LTE que aparece en los despliegues de smart grids a gran escala. Para superar este problema, se propone un nuevo mecanismo de acceso aleatorio que permite soportar de forma eficiente los servicios de automatización de la distribución eléctrica en tiempo real, con un impacto insignificante en el tráfico de fondo. Motivados por los estrictos requisitos de fiabilidad de las diversas operaciones en la smart grid, desarrollamos un modelo analítico del procedimiento de acceso aleatorio de LTE que nos permite evaluar el rendimiento del tráfico de monitorización de la red eléctrica basado en eventos bajo diversas condiciones de carga y configuraciones de red. Además, ampliamos nuestro análisis para incluir la relación entre el tamaño de celda y la disponibilidad de recursos de acceso aleatorio ortogonales, e identificamos un reto adicional para la conectividad fiable en la smart grid. Con este fin, diseñamos un mecanismo de planificación celular que tiene en cuenta las interferencias y la carga de la red, y que mejora la fiabilidad en los servicios de automatización de las subestaciones eléctricas. Finalmente, combinamos el problema de la estimación de estado en sistemas de monitorización de redes eléctricas de área amplia con los retos de fiabilidad en la adquisición de la información. Utilizando el modelo analítico desarrollado, cuantificamos el impacto de la baja fiabilidad en las comunicaciones sobre la precisión de la estimación de estado, y proporcionamos información útil para el diseño de estimadores de estado que tienen en cuenta la fiabilidad en las comunicaciones.

La segunda parte de la tesis se basa en la anterior y se centra en el problema de scheduling y compartición de recursos en la RAN para el tráfico de smart grid y el tráfico

de tipo humano. Presentamos un nuevo scheduler que proporciona baja latencia para el tráfico de automatización de la distribución eléctrica, mientras que la asignación de recursos se realiza de un modo que mantiene la degradación de los usuarios celulares en un nivel mínimo. Además, investigamos los beneficios del modo de transmisión Device-to-Device (D2D) en el intercambio de mensajes basados en eventos en escenarios de automatización de subestaciones eléctricas. Diseñamos un mecanismo conjunto de asignación de recursos y selección de modo que da como resultado tasas de datos más elevadas con respecto al modo de transmisión convencional a través de la estación base. Finalmente, se propone un esquema de partición de recursos ortogonales entre enlaces celulares y D2D para evitar la infrautilización del espectro celular escaso.

Los hallazgos de esta tesis tienen como objetivo la entrega de soluciones a importantes problemas de rendimiento de la RAN, tales como el acceso aleatorio masivo y fiable, el scheduling y la compartición de recursos de forma eficiente, los cuales aparecen cuando las redes celulares deben soportar el tráfico de smart grid. Con la aparición del paradigma de la smart grid, se espera que los resultados de esta tesis proporcionen directrices fundamentales para el diseño de la RAN en las redes celulares futuras y alcanzar el potencial de la smart grid. Además, los resultados de nuestra investigación y los conocimientos adquiridos también pueden ser útiles para otras aplicaciones previstas en 5G que se basan en la adquisición de información masiva y fiable, por ejemplo, en sistemas de transporte inteligentes, automatización industrial, y servicios móviles de atención médica.

Palabras clave: Cellular networks, 3GPP LTE, Radio Access Network (RAN), Random Access CHannel (RACH), Radio Resource Management (RRM), Device-to-Device (D2D), Massive Machine-Type Communication (mMTC), Reliability, Smart grid, Distribution automation, Substation automation, Wide-area Monitoring Systems.

Acknowledgments

This thesis was a wonderful journey of about three-and-a-half years and I feel indebted to a number of people, whose support and advice have been invaluable to the success of my efforts.

First and foremost, I would like to express my sincere gratitude to my advisors Dr. Jesus Alonso-Zarate and Prof. Luis Alonso for their invaluable guidance, suggestions and constructive criticism throughout the development of this thesis. Their insightful comments encouraged me to push my limits and discover not only an exciting research area but also a new vision of engineering in general. Further, I would like to extend my gratitude to Prof. Petar Popovski and Prof. Cedomir Stefanović for giving me the opportunity to visit their research group at Aalborg University, for their mentoring and openness to ideas. I am also grateful to Mr. Linus Thrybom and Dr. Gargi Bag for all the technical advice and fruitful discussions during my stay at ABB Corporate Research.

I would like to deeply thank my co-authors Dr. Francisco Vázquez-Gallego (special thanks for your help in translating the abstract of the thesis!), Dr. Andrés Laya, Dr. Carles Antón-Haro, Dr. Lazaros Gkatzikis and Prof. Carlo Fischione for all the stimulating technical discussions and collaborations that have allowed me to substantially develop my knowledge.

Further, I would like to take the opportunity to thank Prof. Toktam Mahmoodi, Prof. Ferran Adelantado and Prof. David Rincón for agreeing to serve in this thesis' examining committee. My gratitude also extends to Dr. Agapi Mesodiakaki, Dr. Konstantinos Ntontin and Dr. Angelos Antonopoulos for conducting the preliminary assessment and quality review of the thesis.

Throughout the last years, I had the opportunity to interact and work with many talented colleagues at CTTC. Thank you all for the precious knowledge exchange. A special acknowledgment goes to project ADVANTAGE for the financial support of my doctoral studies and my research visits. I would like to especially thank my ADVANTAGE colleagues Mirsad, Marko, Pierre, Anna and Achilleas, for all the nice moments we shared during the project and their friendship. I am also indebted to my "old-school" friends Dimosthenis, Ioannis C., Ioannis Z., Konstantinos N., Konstantinos Z., Theodoros and many others, who have made my life enjoyable.

This thesis is dedicated to my beloved family. I would like to express my deepest gratitude to my parents and my sister for their continuous encouragement in every stage of my life and for their endless support despite the distance, especially during the tough moments of this journey. Last, but by no means least, I would like to thank Jackeline for her unconditional kindness, patience and love.

Thank you!

Charalampos Kalalas
Barcelona, May 2018

Contents

List of Figures

List of Tables

List of Acronyms

3GPP	3rd Generation Partnership Project
ACB	Access Class Barring
AMI	Advanced Metering Infrastructure
CDF	Cumulative Distribution Function
CI	Configuration Index
CP	Cyclic Prefix
D2D	Device to Device
DER	Distributed Energy Resource
EC-GSM-IoT	Extended Coverage GSM Internet of Things
EIT	European Institute of Innovation and Technology
EPC	Evolved Packet Core
EPS	Evolved Packet System
FDD	Frequency Division Duplexing
FLISR	Fault Location, Isolation and Service Restoration
GBR	Guaranteed Bit Rate
GOOSE	Generic Object Oriented Substation Event
GPS	Global Positioning System
HARQ	Hybrid Automatic Repeat reQuest
HTC	Human Type Communication
HTTP	HyperText Transfer Protocol
IEC	International Electrotechnical Commission
IED	Intelligent Electronic Device
IoT	Internet of Things
ISM	Industrial, Scientific and Medical
LAN	Local Area Network
LTE	Long Term Evolution
LTE-A	Long Term Evolution Advanced
MAC	Medium Access Control
MAP	Markovian Arrival Process
MIMO	Multiple Input Multiple Output
MMPP	Markov-Modulated Poisson Process
MMS	Manufacturing Messaging Specification
MSRA	Mode Selection and Resource Allocation

MTC	Machine Type Communication
NAN	Neighborhood Area Network
NB-IoT	NarrowBand Internet of Things
NR	New Radio
OFDM	Orthogonal Frequency Division Multiplexing
OFDMA	Orthogonal Frequency Division Multiple Access
OSI	Open Systems Interconnection
PAPR	Peak-to-Average Power Ratio
PDN-GW	Packet Data Network Gateway
PMU	Phasor Measurement Unit
QCI	Quality of Service Class Identifier
QoE	Quality of Experience
QoS	Quality of Service
RACH	Random Access CHannel
RADA	Random Access for Distribution Automation
RAN	Radio Access Network
RAR	Random Access Response
RRC	Radio Resource Control
RRM	Radio Resource Management
SC-FDMA	Single Carrier Frequency Division Multiple Access
SINR	Signal-to-Interference-plus-Noise Ratio
TDD	Time Division Duplexing
TTI	Transmission Time Interval
UDP	User Datagram Protocol
UE	User Equipment
URLLC	Ultra-Reliable Low-Latency Communications
V2X	Vehicle-to-everything
VoIP	Voice over IP
ZC	Zadoff-Chu

Chapter 1

Introduction

1.1 Motivation

The smart grid can be defined as an integrated, fully inter-operable and communication-enabled electrical system which aims at revolutionizing traditional power systems through the support of a wide range of applications including automated meter reading, demand response, real-time monitoring, and renewable integration. This ongoing modernization of the aging electrical system mainly relies on the evolution of the power distribution grid into a fully automated and interconnected network at medium-voltage level. In recent years, two key building blocks have emerged for the realization of the future distribution grid: *i*) large-scale information acquisition and *ii*) reliable monitoring, protection and control. The former entails the massive installation of smart metering devices, forming Advanced Metering Infrastructure (AMI) systems that involve deployments spanning widespread geographical areas. The latter requires the use of Intelligent Electronic Devices (IEDs) capable of exchanging mission-critical communication for real-time situational awareness and rapid detection of system faults. In addition, the emergence of Distributed Energy Resources (DERs) results in larger power system dynamics and, thus, in a growing need for real-time supervision of the grid behavior to ensure stability.

Instrumental to this power system evolution is the underlying communication technology selected to support extensive and timely information exchange in the distribution grid. Among many existing alternatives to realize communication, cellular networks relying on LTE-based standards have been identified as a promising technology to meet the stringent requirements of emerging functionalities in the distribution grid, such as distribution automation, inter-substation communications and outage management [1]. The evolution of cellular networks through global standardization via the 3GPP offers a widely-deployed and future-proof technology that is provisioned to act as the catalyst for advanced -currently unrealizable- functionalities in the power distribution grid. The inherent technical characteristics of LTE, namely ubiquitous coverage, low end-to-end latency, high throughput, and Quality-of-Service (QoS) differentiation, unlock novel use cases and contribute significantly to the actual operation and management of the overall power grid. The use of licensed bands renders LTE-based networks robust to interference and to security threats which may compromise the quality and privacy of energy data. Leaving technical reasons apart, the distribution system operators may benefit

from the existing public cellular infrastructure without the need to install and maintain a proprietary communication network or have trust in uncontrolled and/or unlicensed communications for sensitive applications.

However, cellular technology was not initially intended for distribution grid applications and the peculiar characteristics of smart grid communication are fundamentally different from Human-Type Communication (HTC) generated by conventional LTE subscribers. Instead, cellular networks were designed for human-centric broadband services with a moderate number of users per eNodeB, i.e., the base station. Besides massive traffic volume, smart grid messages are short with sporadic activity patterns while automation services, e.g., fault location, isolation and service restoration (FLISR), are associated with unprecedented stringent requirements, in terms of latency and reliability, that challenge the classical design principles of cellular networks. Although cellular networks are considered mature for traditional HTC with well-established ecosystems, the 3GPP has already raised the need to revisit the design of next-generation cellular networks in order to make them capable of supporting Machine-Type Communication (MTC) [2]. Ongoing 3GPP standardization efforts aim at making cellular networks the dominant connectivity technology for MTC. Recent standard releases (i.e., Rel-13, Rel-14 and ongoing Rel-15) aim at providing radio interface enhancements for MTC and bring a major mentality shift on the operation of cellular systems. Three solutions for MTC services, optimized for lower complexity and power consumption, enhanced coverage, and higher device density, are introduced: *i*) enhanced Machine-Type Communications (eMTC, often referred to as LTE-M), *ii*) NarrowBand Internet of Things (NB-IoT), and *iii*) Extended Coverage GSM Internet of Things (EC-GSM-IoT). However, significant improvements over 4G radio interface, in terms of both massive connectivity provisioning and reliability/latency performance, are yet needed for the efficient support of the envisioned real-time distribution grid services in the smart grid [3].

In particular, in order to meet the stringent requirements associated with the reliable message exchange among numerous smart grid entities, i.e., ranging from IEDs to Phasor Measurement Units (PMUs) and massive-scale smart meter infrastructure, radical enhancements are required for the radio access design and architecture of the current cellular networks. In this context, 3GPP 5G standardization of the New Radio (NR) interface, launched in Rel-13, is expected to support two new MTC services: *i*) massive Machine-Type Communications (mMTC), aiming at further enhanced device connectivity with performance guarantees, and *ii*) Ultra-Reliable Low-Latency Communications (URLLC), targeting at handling reliably mission-critical links. As standardization work is underway and the transition towards 5G mobile networks is emerging, cellular technologies based on 3GPP standards are anticipated to provide a strong foundation for the Internet-of-Things (IoT) paradigm in the short term.

Motivated by the foreseen potential of cellular networks for supporting distribution grid applications, in this thesis we aim to address the identified cellular connectivity limitations for massive and reliable information acquisition in the smart grid. In particular, we investigate Radio Access Network (RAN) design principles for next-generation cellular networks supporting smart grid traffic. Our focus lies on the design and performance analysis of random access mechanisms and Radio Resource Management (RRM) techniques when LTE-based networks constitute the underlying communication enabler of challenging distribution grid operations. The reliable support of the stringent smart

grid requirements would facilitate the transformation of the aging distribution grid into a modernized and fully automated power distribution system.

1.2 Research Challenges and Objectives

Smart grid communication poses important design challenges for the cellular network architecture and protocols, originally designed for legacy HTC, that have not been sufficiently addressed so far. The fundamentally different characteristics of MTC in the smart grid render indispensable a major mentality shift on the way cellular systems operate nowadays. One of the key RAN components is the Medium Access Control (MAC) layer which is responsible for deciding who, when, and how a network device is granted access to the wireless channel; a shared medium. The reliable support of the stringent communication requirements of distribution grid operations, such as optimized fault management to reduce power outages, integrated distributed generation to limit voltage fluctuations, and fast FLISR, requires a significant reconsideration of the MAC design principles of cellular networks. A number of open issues and technical challenges need to be addressed to overcome the connectivity limitations related to the massive channel access and ensure a fair coexistence of smart grid traffic in shared cellular networks with performance guarantees.

This thesis investigates two fundamental MAC layer procedures for the seamless integration of smart grid communication in LTE-based networks: *i*) the initial network association phase, where smart grid devices request transmission resources or re-establish a connection to the eNodeB and *ii*) the data transmission phase, where the actual transfer of smart grid information is performed over a communication link. The former entails a random access procedure between each device and the eNodeB, initiated in several cases such as device transition from idle to connected state, radio link failure, handover and uplink synchronization. The latter requires a transmission scheduling mechanism at the eNodeB, responsible for allocating the scarce radio resources among the various devices present in the system.

Our main objective lies on the design of key RAN techniques explicitly tailored to support massive and reliable smart grid communication in LTE-based networks. In particular, we focus on the performance analysis of the LTE random access procedure and we identify its performance limitations for massive connectivity in the smart grid. In turn, we develop radio access mechanisms that mitigate the signaling overhead related to the initial access of numerous smart grid devices and enhance the network reliability. To ensure an efficient resource assignment and sharing between the smart grid devices and the conventional HTC subscribers in shared LTE networks, we propose RRM techniques that guarantee the overall performance and prevent the underutilization of the scarce resources. Resource allocation schemes are designed in a way that enable smart grid data scheduling without jeopardizing the regular LTE traffic, especially when network resources tend to become limited. We further aim to leverage the advantages of network-assisted Device-to-Device (D2D) communication, in an effort to enable unprecedented decentralized smart grid functionalities that rely on distributed (peer-to-peer) information exchange. Through direct communication links and bypassing the cellular infrastructure, decision making could be pushed closer to the grid and response times could be expedited yielding a near-autonomous operation of the distribution grid units.

In overall, this thesis aims to provide novel methodologies and RAN design guidelines for future cellular systems towards massive and reliable information acquisition in fundamental distribution grid operations. Our contributions lie on the interdisciplinary area of smart grid with an ultimate goal of providing highly reliable, robust and scalable communication solutions especially for real-time mission-critical applications.

1.3 Outline and Contributions

This thesis investigates RAN design principles and performance analysis of future cellular networks for reliable support of smart grid communication. Specifically, our focus lies on fundamental MAC/RRM issues related to *i*) massive network access due to the large volume of smart grid devices and *ii*) radio resource sharing and scheduling for smart grid and human-type traffic with performance guarantees.

The remainder of the thesis is organized as follows. Chapter 2 provides an overview of the connection establishment and data transmission procedures in LTE-based networks. A comprehensive review and classification of existing related works in LTE for smart grid applications is also presented, leading to the identification of research gaps for contribution. Chapter 3 is devoted to the problem of radio access congestion in LTE-based networks and presents our contributions on the design, analysis and performance evaluation of radio access enhancements for massive and reliable smart grid connectivity. Chapter 4 studies the resource scheduling and sharing problem between smart grid and human-type traffic in shared LTE networks and investigates the benefits of direct D2D communication as a key enabler of mission-critical smart grid operations. Finally, our concluding remarks on the main research outcomes of the thesis are provided in Chapter 5 along with an outline of possible directions for future work.

In the following subsections, a summary of the main contributions of the thesis (Chapters 3 and 4) is provided.

1.3.1 Random Access for Smart Grid Communication

Chapter 3 focuses on the congestion problem in the radio access of LTE-based networks due to the sheer scale of smart grid devices attempting channel access for initial network association. The cornerstone of such study is the establishment of a mathematically tractable yet accurate model for the contention-based LTE random access procedure which allows for a detailed performance assessment of event-driven smart grid communication.

In the first section of Chapter 3, we identify the connectivity limitations for large-scale smart grid deployments due to the limited capacity of the LTE Random Access CHannel (RACH) compared to the increased resource demand. In particular, we first propose a traffic model that captures the bursty behavior of monitoring traffic in event-driven distribution grid operations. Unlike the majority of existing literature where delta traffic or simple Poisson models are used to represent the aggregate smart grid traffic, our modeling approach accounts for the frequency and duration of a burst traffic generation. The impact of smart grid communication in real-time monitoring and wide-area metering applications is investigated in terms of access delay and blocking probability under different network configurations and traffic characteristics. The performance assessment of realistic network-overload scenarios reveals that the standard LTE random access proce-

dure becomes highly susceptible to congestion when a high number of smart grid entities request channel access in a highly-synchronized manner. In addition, the bursty nature of monitoring traffic may result in severe performance degradation.

Motivated by this feasibility study, in the second section of Chapter 3, we devise a novel random access mechanism to enable the integration of distribution automation services in public LTE networks. The IEC-61850 standard for power utility automation has been used for modeling the communication in the distribution grid. Based on the continuous monitoring of the network loading state by the eNodeB, a flexible partition of the available resources, i.e., the random access preambles, into different traffic classes is applied. In turn, in capacity-overload conditions, a dynamic access barring scheme for delay-tolerant smart metering traffic is employed. The RACH congestion is further relieved by a load-shedding scheme at the eNodeB that discards unnecessary preamble transmissions originated from neighboring IEDs. Our proposed mechanism rigorously considers the stringent latency constraints imposed by distribution automation traffic while guaranteeing the performance of contending network entities, i.e., cellular users and smart meters.

The challenging communication requirements of monitoring traffic call for a rigorous reliability analysis of the contention-based LTE random access procedure. To this end, in the third section of Chapter 3, we leverage tools from Markov chain theory to develop a tractable analytical framework of the LTE random access mechanism enhanced with an access class barring (ACB) scheme for the connection establishment of a high number of monitoring devices. We derive an accurate reliability expression as a function of the monitoring traffic characteristics and the RACH/ACB parameters. The performance assessment clarifies the achieved reliability levels under different network and traffic configurations and provides useful guidelines for the design of traffic-aware random access protocols for the reliable support of smart grid monitoring traffic.

In the fourth section of Chapter 3, we investigate the relation between the cell size and the number of preambles generated from a single or multiple root sequences and we study their impact on the achieved reliability. In particular, the fact that the number of orthogonal preambles available for contention decreases as the cell radius increases has not been considered in the literature. This relation reveals an important limitation for cells with large radius and imposes an additional challenge for the reliable support of wide-area smart grid traffic due to the non-orthogonality of preambles originated from different root sequences. To address this research gap, we introduce an interference- and load-aware cell planning mechanism that efficiently allocates the root sequences among multiple cells and regulates the traffic load to guarantee reliable channel access of a high density of distribution automation devices. In addition, we extend our traffic model to accurately capture the spatiotemporal correlation of event-driven substation automation traffic that may result in interdependent packet interarrival times. A performance evaluation of a power distribution automation scenario under network-overload reveals the superior performance of our proposed mechanism in terms of RACH reliability against benchmarking network deployment schemes. Our derived insights for the design of such cellular systems can be generalized in network scenarios of industrial communication where event-driven MTC needs to be supported with reliability guarantees.

Finally, the fifth section of Chapter 3 applies the analytical frameworks and insights of the previous sections to investigate the impact of the LTE RACH reliability on the

accuracy of information acquisition in smart grid monitoring systems relying on PMUs. The deployment of the PMUs, providing linear measurement functions, can significantly improve the state estimation performance via precise and synchronized measurements. We consider two representative network deployment scenarios that involve acquisition of PMU information, namely *i*) a shared LTE network, where PMUs contend for the random access resources along with a high number of smart metering devices present in the system, and *ii*) a dedicated LTE network, where the selected range of an LTE cell that provides coverage solely to PMUs, determines the availability of the orthogonal random access preambles. In both scenarios, we demonstrate that the state estimation accuracy critically depends on the achieved RACH reliability levels for PMU communication. However, in some cases, the additional installation of PMUs may help reduce the state estimation uncertainty and desensitize the estimation error to the effect of a low communication reliability. Therefore, useful design guidelines can be drawn for state estimation schemes when the problem of estimation is coupled with the reliability limitations in information acquisition.

Chapter 3 is based on the following published papers or manuscripts under preparation for submission [1, 4, 5, 6, 7, 8, 9]:

[J-1] **C. Kalalas**, L. Thrybom and J. Alonso-Zarate, "Cellular Communications for Smart Grid Neighborhood Area Networks: A Survey," in *IEEE Access*, vol. 4, no. 1, pp. 1469–1493, March 2016.

[J-2] A. Laya, **C. Kalalas**, F. Vazquez-Gallego, L. Alonso and J. Alonso-Zarate, "Goodbye, ALOHA!," in *IEEE Access*, vol. 4, no. 1, pp. 2029–2044, April 2016.

[J-3] **C. Kalalas**, C. Stefanovic, P. Popovski and J. Alonso-Zarate, "Reliable Vehicle Discovery based on Code-Expanded Random Access," *under preparation for submission*, 2018.

[C-1] **C. Kalalas**, F. Vazquez-Gallego and J. Alonso-Zarate, "Handling Mission-Critical Communication in Smart Grid Distribution Automation Services through LTE," in *Proc. of IEEE International Conference on Smart Grid Communications 2016 (IEEE SmartGridComm '16)*, Sydney, Australia, November 2016.

[C-2] **C. Kalalas**, F. Vazquez-Gallego and J. Alonso-Zarate, "Performance Evaluation of the Contention-Based Random Access of LTE under Smart Grid Traffic," in *Proc. of EAI International Conference on Smart Grid Inspired Future Technologies 2017 (EAI SmartGIFT '17)*, London, UK, March 2017.

[C-3] **C. Kalalas** and J. Alonso-Zarate, "Reliability Analysis of the Random Access Channel of LTE with Access Class Barring for Smart Grid Monitoring Traffic," in *Proc. of IEEE International Conference on Communications, Workshop on Integrating Communications, Control, and Computing Technologies for Smart Grid 2017 (IEEE ICC '17, ICT4SG)*, Paris, France, May 2017.

[C-4] **C. Kalalas** and J. Alonso-Zarate, "Efficient Cell Planning for Reliable Support of Event-Driven Machine-Type Traffic in LTE," in *Proc. of IEEE Global Communications Conference 2017 (IEEE Globecom '17)*, Singapore, December 2017.

[C-5] A. Tsitsimelis, **C. Kalalas**, J. Alonso-Zarate and C. Antón-Haro, "On the Impact of LTE RACH Reliability on State Estimation in Wide-Area Monitoring Systems," in *Proc. of IEEE Wireless Communications and Networking Conference 2018 (IEEE WCNC '18)*, Barcelona, Spain, April 2018.

1.3.2 Resource Scheduling for Smart Grid and Human-Type Traffic

In Chapter 4, we turn our attention to the RRM problem in shared LTE-based networks. RRM is generally used in wireless systems in a broad sense to cover all functions that are related to the assignment and the sharing of radio resources among the users/devices of the wireless network. Our focus lies on the design of efficient scheduling and resource allocation policies for smart grid traffic while attempting to keep the degradation of conventional HTC at a minimum level.

In the first section of Chapter 4, we focus on the design of an appropriate LTE scheduler to support IEC-61850 communication services. Since such time-critical applications are not adequately supported by current LTE implementations [10], we propose a novel LTE scheduling policy that prioritizes automation traffic with minimum impact on background traffic. We further extend existing bibliography via *i*) a characterization of the performance constraints that distribution automation tasks introduce in the LTE scheduling process and *ii*) an analysis of the impact of smart grid traffic prioritization on the performance of the human-centric and real-time LTE services. Our extensive simulations in a realistic radio system simulator demonstrate that properly designed LTE schedulers can successfully meet the performance requirements of IEC-61850 services with negligible impact on background traffic.

Motivated by the stringent requirements of substation automation, in the second section of Chapter 4, we explore the potential of D2D technology for IED local data exchange in an effort to achieve higher performance with respect to traditional cellular communication. In particular, we propose D2D communication over dedicated cellular resources, i.e., D2D-overlay mode, as a key enabling technology for reliable information exchange in power distribution grids. We jointly address two fundamental issues: *i*) the seamless transition from cellular (i.e., communication via the eNodeB) to D2D-overlay mode for smart grid entities upon detection of a surge of channel access attempts and *ii*) the efficient orthogonal resource partition for cellular and D2D links. An analytical framework capturing the event-driven nature of substation automation traffic and both phases of uplink communication is introduced based on the technical analyses and insights of Chapter 3. The joint problem of mode selection and resource allocation (MSRA) is then formulated as a sum-rate maximization problem and a dynamic heuristic mechanism is proposed to adaptively allocate uplink resources for D2D links and prevent spectrum underutilization while guaranteeing a minimum rate requirement for cellular users. The performance of our proposed scheme is evaluated through extensive simulations under different performance criteria and numerical results demonstrate the rate gains of a dynamic switch between D2D-overlay and conventional cellular mode for substation automation traffic.

Chapter 4 is based on the following published papers [1, 11, 12]:

[J-1] **C. Kalalas**, L. Thrybom and J. Alonso-Zarate, "Cellular Communications for Smart Grid Neighborhood Area Networks: A Survey," in *IEEE Access*, vol. 4, no. 1, pp.

1469–1493, March 2016.

[C-6] **C. Kalalas**, L. Gkatzikis, C. Fischione, P. Ljungberg and J. Alonso-Zarate, "Enabling IEC 61850 Communication Services over Public LTE Infrastructure," in *Proc. of IEEE International Conference on Communications 2016 (IEEE ICC '16)*, Kuala Lumpur, Malaysia, May 2016.

[C-7] **C. Kalalas**, J. Alonso-Zarate and G. Bag, "On the Transmission Mode Selection for Substation Automation Traffic in Cellular Networks," in *Proc. of IEEE International Conference on Smart Grid Communications 2017 (IEEE SmartGridComm '17)*, Dresden, Germany, October 2017.

1.3.3 Other Research Contributions

Besides the main contributions of the thesis outlined in the previous subsections, additional research work has been carried out while this thesis was prepared. The following publications are beyond the scope of the thesis, but contain related materials and applications [13, 14, 15]:

[J-4] F. Vazquez-Gallego, **C. Kalalas**, L. Alonso and J. Alonso-Zarate, "Contention Tree-based Access for Wireless Machine-to-Machine Networks with Energy Harvesting," in *IEEE Transactions on Green Communications and Networking*, vol. 1, no. 2, pp. 1–12, April 2017.

[C-8] A. Pouttu, J. Haapola, P. Ahokangas, Y. Xu, M. Kopsakangas-Savolainen, E. Porras, J. Matamoros, **C. Kalalas**, J. Alonso-Zarate, F. D. Gallego, J. M. Martín, G. Deconinck, H. Almasalma, S. Clayes, J. Wu, M. Cheng, F. Li, Z. Zhang, D. Rivas, S. Casado, "P2P Model for Distributed Energy Trading, Grid Control and ICT for Local Smart Grids," in *Proc. of European Conference on Networks and Communications (EuCNC '17)*, Oulu, Finland, June 2017.

[C-9] J. Haapola, S. Ali, **C. Kalalas**, J. Markkula, N. Rajatheva, A. Pouttu, J. M. Martín Rapún, I. Lalaguna, F. Vazquez-Gallego, J. Alonso-Zarate, G. Deconinck, H. Almasalma, J. Wu, C. Zhang, E. Porras Muñoz, F. David Gallego, "Peer-to-Peer Energy Trading and Grid Control Communications Solutions' Feasibility Assessment based on Key Performance Indicators," in *Proc. of IEEE Vehicular Technology Conference (VTC 2018-Spring): Workshop on Enabling Internet via Machine type Wireless Communications*, Porto, Portugal, June 2018.

1.4 Methodology

In the parts of the thesis where simulations are used, realistic assumptions have been made to choose an appropriate level of abstraction as well as the suitable simulation platform for performance assessment. In cases where realistic timing of LTE standard was needed, the discrete-event NS-3 network simulator has been used. The NS-3 simulator constitutes an open-source platform, that currently implements a wide range of protocols in C++, making it useful for cross-layer design and analysis. In the context of the thesis, the mapping of IEC-61850 communication stack with LTE radio protocol stack has

been implemented in NS-3 along with the traffic generation of IEC-61850 communication services. The IEC-61850 packet traces were captured and saved for post-processing using Wireshark network protocol analyzer. These traffic traces have been further used for validation (i.e., parameter estimation) of our proposed smart grid traffic models throughout the thesis. In particular, for model fitting purposes, the expectation-maximization algorithm [16, 17] has been used as an iterative method of finding the maximum-likelihood estimates of the traffic model parameters.

In the context of the thesis, the LTE LENA software tool, initially implemented based on 3GPP Rel-8 standard features, has been properly extended with the development of random access modules in order to provide a widely-accepted reference evaluation environment for our proposed analytical models [4]. The implemented random access modules are based on the architecture and design patterns of LTE LENA and maintain a high level of backwards compatibility with the source code. For validation purposes, the simulation conditions of the original 3GPP Technical Report 37.868 [18] have been replicated to guarantee a high level of accuracy. On the other hand, in cases where functionalities of recent LTE standard releases were not implemented in NS-3 by the time of writing this thesis (e.g., lack of a D2D communication module) or when the level of modules' complexity was considered too high and a less detailed model would suffice, custom MATLAB code was used. In order to ensure statistically sound simulations over the performance metrics of interest, the results were based on the average values of multiple simulation iterations while the duration of simulations and the number of simulation runs is set in a way that the 95% confidence intervals are non-overlapping with results that are concluded to be different.

Chapter 2

Background

In Chapter 2, we overview the smart grid communication architecture and the essential MAC layer procedures for connection establishment and data transmission in LTE-based networks which constitute the main research areas of the thesis. We further provide a comprehensive review of the most relevant architectural and protocol LTE enhancements for smart grid communication that can be found in the literature to date. In particular, Section 2.1 discusses the role of communications in the evolution of the power grid. Section 2.2 provides a general description of the initial network association phase and data transmission phase for communication in LTE/LTE-A systems. Section 2.3 provides an in-depth and comprehensive study on the applicability of cellular technology for fundamental operations in the power distribution grid. The current state of the art related to the ongoing research works on LTE-based systems for smart grid applications is thoroughly presented and discussed. Based on this survey of the recent works in the field and the classification of existing approaches, Section 2.4 summarizes the identified gaps for research contributions.

2.1 Communication in the Smart Grid

The transformation of the existing power distribution grid into an automated smart grid would significantly benefit from a reliable and scalable communication technology that can support advanced and autonomous grid functionalities. The smart grid paradigm consists in building a flexible communication architecture where geographically dispersed IEDs, as well as sensors, smart meters, protective relaying devices and circuit breakers, exchange their status information and control instructions in an automated and distributed manner to efficiently operate the electrical grid [19]. By enabling direct interactions between consumers and the power distribution system operators, it would be possible to develop new services and operations capable of efficiently satisfying the instantaneous demand-response. In addition, the increasing penetration of DERs, photovoltaic cells, storage batteries, and wind energy generators located in widespread areas, introduces several challenges for achieving seamless and reliable communication within the power grid. Therefore, distributed control and real-time bidirectional communication are necessary to support fundamental grid functions which often involve the transmission of mission-critical protection messages and/or massive amount of metering information [20].

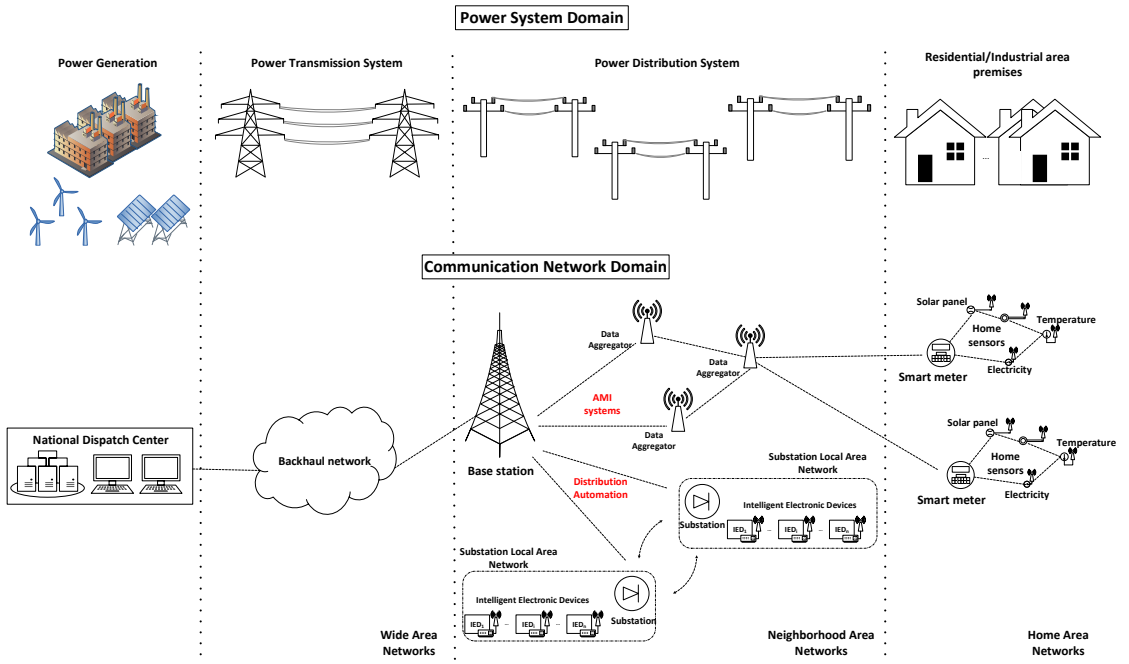

Figure 2.1: Hierarchical smart grid architecture. Two parallel interdependent domains, the power system and the communication network, form the infrastructure of the smart grid. The power distribution grid along with the corresponding NAN constitute the heart of the new power system. In the figure, two fundamental NAN applications, the distribution automation and AMI are illustrated. Distribution automation data between substation local area networks and aggregated metering information from spatially dispersed home area networks, need to be transmitted through a reliable communication infrastructure.

Figure 2.1 depicts the common hierarchical structure of an electrical grid network. Residing at the heart of the smart grid communication network, Neighborhood Area Networks (NANs) constitute the communication infrastructure for the distribution of electricity at medium voltage, between the power transmission system at high voltage and the final residential/industrial consumers at low voltage [1]. NANs involve communication between diverse electric devices, e.g., IEDs and data aggregation points, which are deployed in large and potentially complex geographical areas. Communication in the power distribution grid already exists at a local level to support basic small-scale automatic operations [21]. However, large-scale operations that involve deployments spanning long distances, e.g., wide-area monitoring, protection and control systems, still rely on extensive human intervention. This is the case, for example, of FLISR where field technicians may need to move on site and perform restoration operations. Message exchange between substations, responsible for conducting the voltage transformation and control, is also enabled at the distribution level.

The distinct communication segments in the smart grid employ different network technologies and protocols to ensure service performance at each level, end-to-end interoperable management, and deployment/maintenance costs. Nowadays, communication in

the transmission and distribution systems typically relies on robust wired broadband links. Communication at the consumer side is in principle based on short-range technologies with relaxed QoS requirements. In the smart grid paradigm, the distribution domain is expected to be partitioned into smaller, more-manageable, and potentially autonomous operating units that require a flexible and widely adopted communication infrastructure [22]. If a reliable communication network is available, then advanced operations such as distribution automation and AMI, will be efficiently supported.

Distribution automation deals with system automatic functionalities that require communication interactions among IEDs, such as [22], [23]:

1. Distributed control and protection, involving the introduction of time-critical communication exchanges between substation Local Area Networks (LANs) and measurement equipment installed along the distribution network, e.g., PMUs. A fundamental protection operation is fault detection and localization, including the use of IEDs capable of exchanging protection-relevant messages and reporting events to control centers for rapid diagnosis of system faults and initiation of control commands.

2. Wide-area monitoring systems, involving the use of combined PMU information collected over many substation LANs to perform fast decision-making and switching/isolation actions to avoid the extensive propagation of disturbances to the entire power system. Thus, self-healing and system reconfiguration can be achieved.

3. Monitoring of distribution equipment, including real-time situational awareness and supervision of capacitor bank controllers, fault detectors, re-closers, switches, and voltage regulators within substations [24].

In addition, the envisioned large-scale integration of DERs within the power grid will result in a two way power flow in contrast to the traditional one way power flow, thus adding more complexity to all aforementioned functionalities [20]. The conventional centralized power delivery logic is shifted to a more distributed one and new challenges are created for the protection, control and monitoring of the distribution grid. Distribution automation applications are generally associated with stringent communication network requirements in terms of network latency and reliability [25, 26].

Regarding metering data delivery, a typical AMI system uses smart meters to communicate information between consumers and power utilities for monitoring, operating, and billing purposes [27]. Hierarchical communication network structures have been proposed [28] to handle the data, where concentrator units aggregate consumer meter information before forwarding them to the meter management systems at the utility end for processing. In this case, latency requirements are more lenient compared to distribution automation functionalities. Typically, AMI systems require infrequent uplink transmissions of small-sized data packets. The bandwidth requirements for an individual user are relatively low; however, the overall requirements in a NAN increase considerably due to the large number of customer premises. In AMI deployments, network scalability is of crucial importance. The challenge for the communication network is therefore to allocate efficiently its bandwidth resources to many spatially separated nodes.

2.2 Medium Access Control Layer Procedures

2.2.1 Random Access Mechanism

The future distribution grid is expected to be a flexible and fully dynamic environment equipped with a large number of measurement devices ranging from legacy remote terminal units to PMUs and massive-scale smart meter infrastructure. The number of devices joining the communication network will rapidly evolve, i.e., frequent entries/re-entries, while the sporadic activity patterns of smart grid traffic may result in a loss of uplink synchronization with the eNodeB during periods when no data is transferred. In LTE/LTE-A systems, the random access procedure is used for initial network association of uncoordinated devices in the following cases [29]:

1. Upon initial network access, i.e., device transition from *idle* state to *connected* state for association with the base station (eNodeB).
2. Synchronization for new data transmission or reception, e.g., event-triggered measurement report. An LTE device can only be scheduled for uplink data transmission if its uplink transmission timing is synchronized.
3. Upon transmission of new data when no dedicated scheduling-request resources are assigned.
4. In the case of handover from the current serving cell to a target cell.
5. After radio link failures, for connection re-establishment.

The physical RACH is formed by a periodic reservation of uplink time-frequency resource blocks, the random access slots, for the transmission of access requests. The RACH time-frequency resources are semi-statically allocated within the physical uplink shared region and repeat periodically. The eNodeB broadcasts the periodicity of the random access slots by means of a variable referred to as the RACH configuration index. The random access slot periodicity is configured from once in every LTE subframe (1ms) to once every two LTE frames (20ms) and is periodically broadcast by the eNodeB [30]. The time-duration of the random access slots depends on the format of the access requests, whereas in the frequency domain, each random access slot consists of 6 consecutive resource blocks. The random access procedure in LTE-based networks can be either contention-free or contention-based. In the contention-free mode, the eNodeB is able to prevent collisions by allocating dedicated access resources for requests that require high probability of success, e.g., handover and downlink data arrival. In this thesis, we focus on the contention-based random access operation, where LTE devices contend for network access by establishing a four-way message exchange with the eNodeB, as illustrated in Figure 2.2. In particular, it involves the sequential transmission of the following messages:

- *RACH preamble.* According to LTE standard terminology, a preamble constitutes a pseudo-random digital signature that a device randomly selects to transmit over the first available random access slot of the RACH. A subset of preambles is often reserved for contention-free access and their availability for contention-based access is periodically broadcast by the eNodeB. A collision occurs in case more than one device attempts access with the same preamble over the same random access slot.

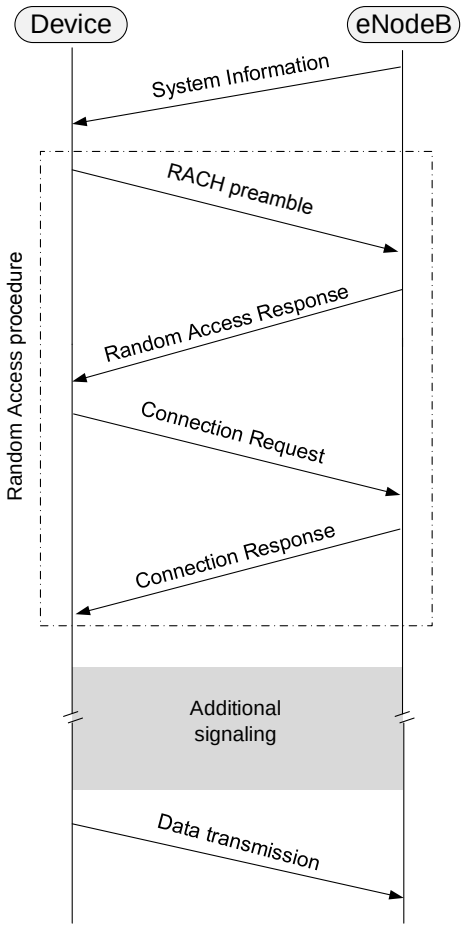

Figure 2.2: Contention-based random access procedure in LTE. Connection establishment normally involves a four-message handshake between the device and the eNodeB. Based on the system information broadcast by the eNodeB, random access preambles are used by the devices to contend in the available random access slots. A channel access request is completed if the four messages are successfully exchanged.

- *Random Access Response (RAR).* In turn, the eNodeB processes the preambles received on a specific random access slot and provides feedback in a RAR message - transmitted over the physical downlink shared channel - to all the devices with preamble transmission on this random access slot. In case at least one device transmits a RACH preamble, the preamble is denoted as activated. Typically, in this step the eNodeB cannot distinguish how many devices have activated a specific preamble; if multiple devices sent the same preamble over the same time-frequency resource, the eNodeB will provide a RAR to every activated preamble and the same RAR information will be decoded by more than one devices. In this case, the contention is resolved in the next step. The RAR message includes an identifier of each successfully decoded preamble, timing information for synchronization, a temporary device identifier and an uplink resource grant for devices

to transmit a connection request, the next message of the handshake. The device expects to receive the RAR within a time window, of which the start and end are configured by the eNodeB as part of the cell-specific system information. If the device does not receive a RAR within the configured time window, it retransmits the preamble. In case a device receives a RAR without the identifier of the preamble it used, it is signaled, via a backoff indicator attached to the RAR, to wait for a random time until the next preamble transmission attempt.

- *Connection request.* Upon receiving the resource grant in RAR, the device transmits a connection request message to the eNodeB, conveying the device identifier and the establishment cause, e.g., scheduling resources request, Radio Resource Control (RRC) connection request, tracking area update. The message also contains configuration information for uplink power control, radio bearer establishment and the channel quality. A retransmission mechanism (Hybrid Automatic Repeat reQuest (HARQ)) is enabled to protect the message delivery. In case of undetected preamble collision in the previous step, more than one devices will transmit in the same time-frequency resource their connection request message. This may result in such interference that no colliding message can be decoded, and the devices restart the random access procedure until reaching the maximum number of HARQ retransmissions. However, if one device is successfully decoded, the contention remains unresolved for the other devices. The subsequent downlink message allows for a quick resolution of this contention.
- *Connection response*: In response to a successfully received connection request message, the eNodeB transmits a connection response message as an acknowledgment for contention resolution. The completion of this step renders the random access attempt successful. Otherwise, if the message is not received by a device within a predefined time window, the random access procedure is declared as failed and the device needs to restart from the first step until the limit for its allowed preamble retransmissions is reached.

According to the LTE preamble design principles, the random access signatures are generated by one or several Zadoff-Chu (ZC) root sequences and their cyclic shifts. A number of 64 different preambles is available per cell and a total of 838 root sequences are defined for LTE/LTE-A systems. Each preamble consists of a cyclic prefix (CP) and a preamble sequence, as illustrated in Figure 2.3. The CP is identical to the end of the sequence, and it is appended at the start of the preamble to enable a periodic correlation at the RACH receiver. Four preamble formats are defined for LTE Frequency Division Duplexing (FDD) operation and they differ in the length of the preamble, as specified in [29]. The preamble length has been designed to be shorter than the random access slot to provide a guard time and absorb the propagation delay. The length of the CP and the guard time shall cover the maximum round trip delay. Figure 2.3 shows two preambles at the receiver with different timings due to the variation in their propagation delay. The relation between the cell size and the number of orthogonal preambles is investigated in detail in Subsection 3.4.2.

One of the major limitations towards an efficient and scalable radio access for massive MTC stems from the deficiencies of the RACH procedure, a key building block of mobile access networks. Currently, the LTE access procedure is designed to enable connection establishment for a relatively low number of accessing devices. As smart grid capabilities expand dramatically, a sheer scale of communicating devices are installed to provide real-time measurements of the grid behavior and to perform monitoring, pro-

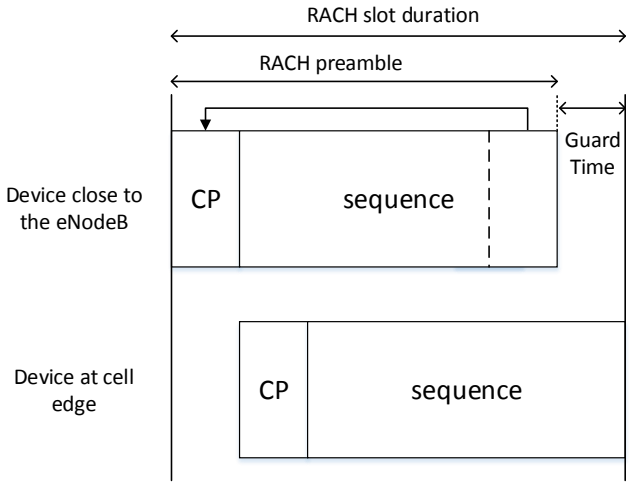

Figure 2.3: Random access preamble received at the eNodeB [29].

tection and control functionalities. The integration of smart grid traffic in LTE-based networks may result in severe scalability issues since the RACH needs to accommodate the near-simultaneous access requests of a high density of devices. The limited random access opportunities (64 preambles) compared to the increased resource demand render the standard LTE access mechanism highly susceptible to congestion, due to the high probability of collision in the transmission of the preambles. In use cases where the LTE network is shared with regular LTE subscribers generating conventional HTC, the resulting harsh contention environment leads to a highly degrading network performance. To this end, massive connectivity and channel overload control constitute topics currently under development for standardization in future releases of LTE systems. In addition, the scalability shortcomings of LTE random access procedure to meet the growing MTC traffic demand has triggered intense research activities worldwide over the last years.

2.2.2 Data Transmission Scheduling

As illustrated in Figure 2.2, the data transmission phase follows after the connection establishment phase for each device. During this stage, the data transmission scheduling and resource allocation mechanisms constitute the key components for the achievement of an optimal and efficient utilization of the available radio resources. In this context, the LTE MAC scheduler is responsible for allocating the shared data resources among the competing devices. Scheduling in LTE is performed at the eNodeB. The scheduling policy needs to accommodate the broad range of air interface features and the wireless channel quality whilst simultaneously optimizing the system capacity and ensuring fairness/QoS among the devices. Upon performing the scheduling decisions, the eNodeB informs users about the dedicated radio resources for their data transmission. The role of the MAC scheduler is even more significant in situations of limited network resources

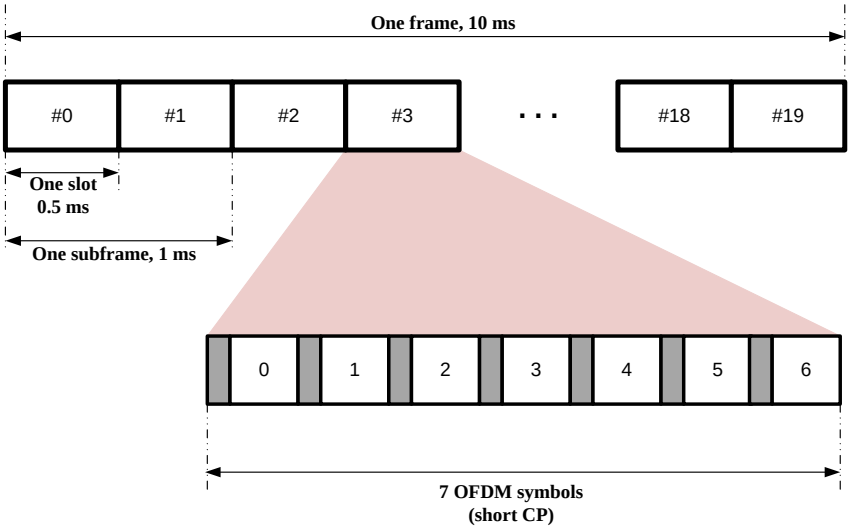

Figure 2.4: LTE frame structure [29].

when numerous devices, associated with diverse performance requirements, are competing simultaneously for data resource scheduling. For instance, on top of the high data rate human-based services, a shared cellular network needs to handle a wide range of smart grid traffic characteristics, from low-rate sporadic metering data to bursty protection information exchange. Traffic prioritization is therefore an essential feature of the MAC scheduler for resolving the contention among the smart grid and cellular entities competing for radio resources.

In LTE uplink, the Single Carrier-Frequency Division Multiple Access (SC-FDMA) scheme is used as multi-carrier access technique. The SC-FDMA constitutes a variation of Orthogonal Frequency Division Multiple Access (OFDMA) and incorporates the advantages of OFDM, i.e., multiple devices can be scheduled for data transmission simultaneously, while achieving a low Peak-to-Average Power Ratio[1](PAPR). This advantage of low power requirement is largely realized when resource contiguity in the frequency domain (i.e., adjacent resource block pairs) is satisfied in the allocation of every single device [31]. The contiguous uplink resource allocation introduces an additional constraint for the scheduling process and has resulted in numerous enhancements proposed in subsequent standard releases.

Both LTE/LTE-A systems support FDD and Time Division Duplexing (TDD) modes. In FDD, different frequency bands are utilized for the downlink and uplink transmissions, while in TDD the downlink and uplink share the same frequency bands but are separated in time. As illustrated in Figure 2.4, all transmissions are organized into radio frames of 10ms each, with each frame further divided into ten equally-sized subframes. In turn, a subframe is divided into two equally sized slots of 0.5ms. In uplink, the basic LTE radio resource is defined as a time-frequency resource block that spans 0.5ms in time and 12 contiguous SC-FDMA subcarriers with a total bandwidth of 180kHz. The resource

[1]The OFDMA solution leads to high PAPR requiring increased power amplifier linearity requirements which in turn leads to reduced power efficiency on the transmitter side.

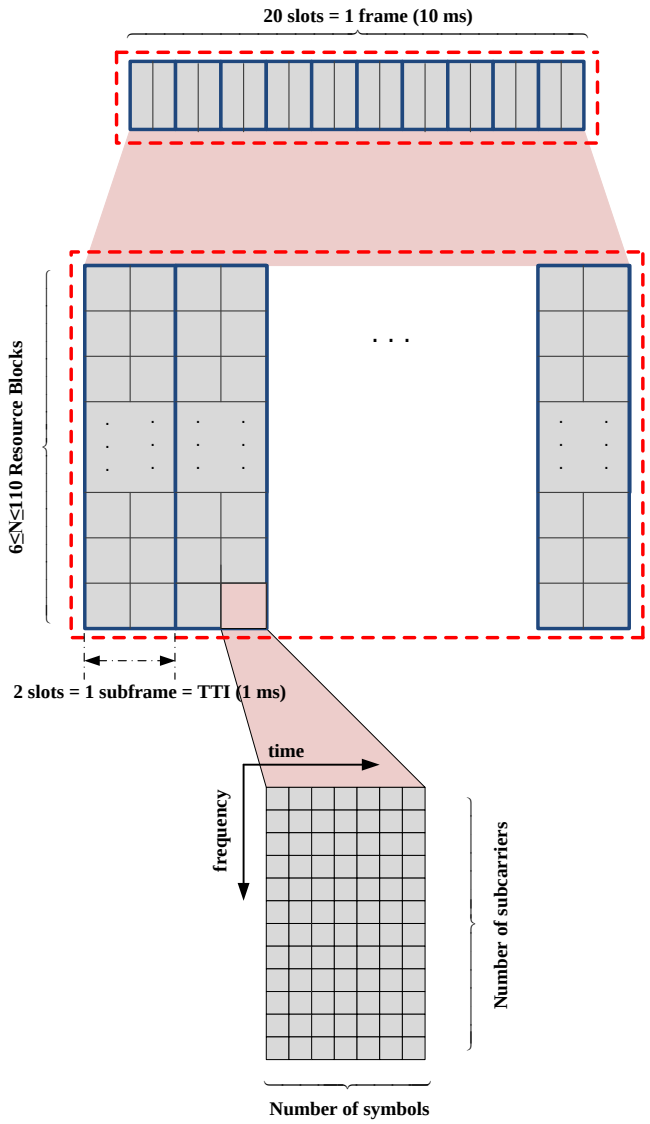

Figure 2.5: LTE radio resource grid. In LTE, the available bandwidth can be seen as a time-frequency grid of physical resource blocks. In each TTI, resource block pairs are assigned to a number of competing users.

block would use either six or seven OFDM symbols depending on whether a normal or extended CP is employed. As shown in Figure 2.5, two time-consecutive resource blocks form a resource block pair, which is the minimum scheduling unit that can be allocated to a device in every Transmission Time Interval (TTI). This granularity of scheduling is intended to facilitate low-latency data transfer. Hence, data scheduling decisions are periodically taken once every TTI (1ms) and resource blocks are always allocated in pairs that form a 180kHz×1ms resource block pair.

Resource allocation needs to consider the demanding latency and throughput require-

Table 2.1: Standardized QoS class identifiers in LTE standard and their basic quantitative characteristics [32].

QCI	Resource type	Priority level	Packet delay budget (ms)	Packet loss rate	Example services
1	Guaranteed Bit Rate	2	100	10^{-2}	Conversational Voice
2		4	150	10^{-3}	Conversational Video (Live Streaming)
3		3	50	10^{-3}	Real Time Gaming, V2X messages
4		5	300	10^{-6}	Non-Conversational Video (Buffered Streaming)
65		0.7	75	10^{-2}	Mission critical user plane Push To Talk voice
66		2	100	10^{-2}	Non-Mission-critical user plane Push To Talk voice
75		2.5	50	10^{-2}	V2X messages
5	Non-Guaranteed Bit Rate	1	100	10^{-6}	IMS Signaling
6		6	300	10^{-6}	Video (Buffered Streaming), TCP-based (e.g. www, e-mail, ftp, p2p file sharing, etc.)
7		7	100	10^{-3}	Voice, Video (Live Streaming), Interactive Gaming
8		8	300	10^{-6}	Video (Buffered Streaming), TCP-based (e.g. www, e-mail, ftp, p2p file sharing, etc.)
9		9			
69		0.5	60	10^{-6}	Mission critical delay sensitive signaling
70		5.5	200	10^{-6}	Mission critical data (e.g. example services as QCI 6/8/9)
79		6.5	50	10^{-2}	V2X messages

ments that smart grid traffic imposes, while ensuring a fair resource sharing. Based on the adopted scheduling policy, a differentiated data handling can be achieved while guaranteeing the QoS of various traffic classes. The QoS framework of LTE is designed in a way that provides an end-to-end QoS support. In particular, the class-based QoS mechanism for LTE relies on the concepts of data flows and bearers. LTE classifies flows into Guaranteed Bit Rate (GBR) and non-GBR flows. Data flows are then mapped to bearers, with three individual bearers (Radio, S1, and S5/S8) combined to provide end-to-end QoS support via the Evolved Packet System (EPS) bearer [29]. A bearer can be considered as a set of multiple QoS requirements which are indicated by the QoS Class Identifier (QCI). In LTE architecture, bearers are mapped to a limited number of discrete classes. A set of nine QoS classes has been prescribed in 3GPP specifications for LTE development, corresponding to an equal number of standardized QCI profiles, as illustrated in Table 2.1. Mobile services (conversational voice and video, streaming video, gaming, IMS signaling) are classified based on the resource type, priority order, packet delay budget and packet loss rate characteristics [32].

Except for defining two types of scheduling (semi-persistent and non-persistent), 3GPP does not explicitly specify how resource block pairs should be allocated, and thus the de-

sign of the MAC scheduler is subject to vendor implementation. In general, the scheduling policy can be designed in a way that *i*) maximizes the spectral efficiency, *ii*) maximizes the overall network throughput, *iii*) minimizes the inter-cell interference or *iv*) ensures fairness. LTE uplink schedulers can be thus categorized into the following main categories [33]:

- *QoS-based*: A QoS-aware MAC scheduler aims to distribute the available data resources to the users within the cell such that their QoS requirements are met. QoS provisioning is mainly achieved when traffic prioritization is included in the scheduler's utility function. The utility function accommodates different QoS measures, such as maximum delay budget or minimum required data rate.

- *Best-effort*: In contrast to a QoS-based discipline, a best-effort scheduler aims to optimize the utilization of the radio resources and/or the fairness among the competing entities. A number of well-established approaches to fairness may be used, including proportional fairness and max-min fairness.

- *Energy-efficient*: The objective in this type of schedulers is to minimize the energy consumption of uplink data transmission. Resource allocation then aims to reduce the transmission power of a device while satisfying the QoS constraints, e.g., keep end-to-end latency within delay tolerance levels.

The LTE uplink scheduler design is non-trivial for smart grid communication where most of the traffic is mainly in the uplink direction and the exchanged messages are generally short, following an event-driven (e.g., protection- and control-related) or periodic traffic activation pattern (e.g., monitoring related, measurement reports). Besides the contention among cellular users and smart grid devices for initial network association, an additional contention round resides in the data transmission phase, where the MAC scheduler needs to perform an efficient resource sharing and allocate radio resources based on different decision criteria. Since the scheduling algorithm is left as a vendor implementation decision, i.e., it is not explicitly standardized by the 3GPP, the problem of LTE scheduling and resource allocation constitutes an intense research area nowadays.

2.2.3 LTE-D2D Communication

LTE network-assisted D2D communication constitutes a recently introduced radio technology that enhances standardized cellular networks to overcome some of the LTE limitations when supporting smart grid services [34]. As an outcome of the continuous evolution of 3GPP-based standards, D2D communication emerges as an enabler of unprecedented decentralized functionalities in the smart grid. As illustrated in Figure 2.6, against the traditional centralized network architecture of cellular networks, D2D communication refers to the direct communication between entities in close proximity of each other (D2D-capable), without the need to route data transmissions through a base station. In this scheme, smart grid devices, e.g., monitoring IEDs conveying mission-critical protection and/or control information, can exchange data utilizing licensed cellular resources over a direct link, allowing for a decentralized and fully automated power system operation.

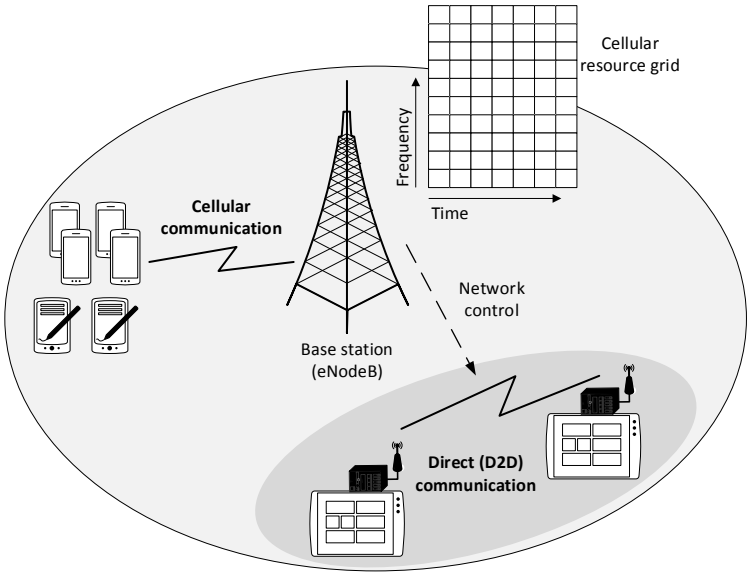

Figure 2.6: LTE network-assisted D2D communication. D2D refers to a radio technology that allows smart grid devices, such as smart meters, circuit breakers and IEDs, to autonomously communicate with each other in a direct manner, bypassing the transmission via a central base station. Network control and resource management among D2D links and cellular users remain under the responsibility of the base station.

The key benefits of LTE-D2D communication as the enabling technology for smart grid operations can be highlighted as follows:

- *Latency and reliability improvements*: Bypassing the core cellular network, time-critical distribution automation functionalities, related to the protection and control of the smart grid, can be performed without the additional delay imposed by the core cellular network. In addition to the immediate end-to-end delay gain achieved by shifting from a two-hop communication model (via the eNodeB) to a single-hop direct communication, a combination of both D2D and infrastructure-based communications can lead to an increased reliability by means of multi-path diversity.
- *Efficient RRM*: The localized nature of the D2D transmissions allows for the reuse of the radio resources while maintaining acceptable interference levels outside a certain spatially-limited area around each transmitting node in the system. Thus, resource sharing with conventional cellular users becomes more efficient [35].
- *Network offload*: By offloading traffic onto direct D2D links, base stations and other LTE network components are relieved of the extensive infrastructure network load, e.g., large volume of metering data in advanced metering infrastructure systems.
- *Energy efficiency*: The shorter communication path among devices compared to the distance between a device and its serving base station, improves energy efficiency and increases device lifetime [36].

Besides the benefits in communication, LTE-D2D enhancement brings fundamental advancements to the current aging distribution grid resulting in a dramatic improvement of the overall power system operation. In particular, LTE-D2D networks allow for a decentralized structure of the power grid with an automated system management that efficiently coordinates the diversified functions, e.g., microgrid distributed management, across the network components [20, 19]. By exchanging information in their local networks, control and real-time status monitoring of all IEDs in the distribution level can be possible, leading to fast detection of faults and reduced system response times, thus, full support of mission-critical functionalities, e.g., substation automation [37]. In addition, bidirectional communication among smart meters and utility centers allows consumers to become aware of the timing and quantity of their personal electricity usage and timely respond to the delivery of electricity pricing information [38].

In the following section, we review recent studies that investigate the challenges for smart grid communication in cellular networks and propose various architectural/protocol improvements. A comprehensive survey of recent works in the field and a classification of the existing approaches is presented, leading to the identification of potential gaps for research contributions.

2.3 State of the Art - Literature Review

The foreseen potential of supporting smart grid applications with cellular technology constitutes the main motivation behind the active research efforts currently ongoing on this area. Technical feasibility studies have been conducted during the recent years to determine the suitability of LTE technology and gain an understanding of the current limitations of the standard. The performance evaluation may even involve experimental validation through field measurement tests. On top of these assessments, architectural and protocol enhancements have been also proposed for evolving the functionality and capabilities of LTE standard to successfully support smart grid use cases. This section provides a classification of the existing works according to their specific approach. Their scope and limitations are thoroughly compared in Table 2.2.

2.3.1 Feasibility Studies

Existing feasibility studies can be classified into two main groups; those based on studying latency[2] and those based on evaluating capacity and scalability of LTE for various smart grid applications.

The stringent latency requirements of delay-critical operations in the power distribution network is the focus in [39], [40] and [41]. Based on conducted field trials, the authors perform a latency and reliability assessment for LTE technology when used for communication among medium-voltage grid entities under various load conditions. Using the IEC-61850 standard as a guideline, the authors argue that LTE can support automatic interactions with a round-trip delay budget of 100ms, achieving small latency deviations compared with other technologies. Reliability levels remain high given that the coverage

[2]Latency in HTC often refers to the *best* or *average* case, whereas for the power grid it is mostly about the *worst* case, since the failure to deliver a single message within its guaranteed delivery time can have a severe impact on the process that is controlled.

Table 2.2: Integration of smart grid communication in cellular networks: State of the art and classification of existing works.

Study/Proposal				Application					Performance Metrics													Validation			Traffic	
Type	Subtype	Focus/Approach	Reference	Smart metering	Distribution automation	Demand-response	Microgrid	Throughput	Latency	Channel utilization	Coverage	Capacity	Blocking probability	Access probability	Collision probability	Packet success/loss rate	Fairness	Energy consumption	Impact on HTC	Experiment/Field trial	Simulation	Theory	Uplink	Downlink
Feasibility study	Latency-based	Latency/reliability analysis for remote control operations	[39]		✓				✓							✓				✓			✓	✓
			[40]		✓				✓		✓					✓				✓			✓	✓
			[41]		✓				✓											✓			✓	✓
		Evaluation of LTE duplexing modes in delay-sensitive operations	[42]	✓	✓				✓	✓											✓		✓	
			[43]	✓	✓				✓	✓											✓	✓	✓	
			[44]		✓				✓		✓					✓					✓		✓	✓
		Impact on HTC when supporting grid traffic	[45]	✓	✓			✓	✓										✓		✓		✓	✓
			[46]			✓		✓	✓							✓			✓		✓		✓	✓
		Analytical traffic modeling for data volume management	[47]	✓		✓			✓			✓							✓		✓	✓	✓	
		Near-simultaneous network entry attempts	[48]	✓					✓					✓	✓			✓			✓	✓	✓	
	Capacity-based	Supported devices for network planning	[49]	✓							✓	✓								✓	✓		Non-specific	
			[50]	✓				✓		✓		✓									✓		✓	✓
		Analytical traffic modeling for data volume management	[51]	✓		✓	✓	✓		✓			✓						✓		✓	✓	Non-specific	
			[47]	✓		✓			✓			✓							✓		✓	✓	✓	
		Random access channel load analysis	[18]	✓	✓				✓			✓		✓	✓				✓	✓	✓		✓	
			[52]	✓				✓	✓							✓			✓		✓		✓	
		Capacity-coverage tradeoff	[53]	✓							✓	✓									✓		✓	✓
LTE enhancements	Random access improvements	Dynamic group paging	[54]	✓						✓				✓	✓						✓		✓	
		Contention-based mechanisms	[55]	✓				✓	✓	✓						✓			✓		✓		✓	
			[56]	✓	✓				✓			✓						✓	✓		✓	✓	✓	
		Access load estimation	[57]	✓	✓				✓					✓							✓	✓	✓	
			[58]	✓					✓							✓					✓	✓	✓	
		Base station assisted cascading-fault detection	[59]		✓				✓												✓		✓	
	Scheduler design & Resource allocation	Weighted round-robin algorithm	[60]	✓	✓		✓		✓											✓	✓		✓	✓
			[61]	✓			✓	✓	✓							✓			✓		✓			✓
		Proportional-fair and round-robin improvements	[62]	✓								✓	✓								✓		✓	
		Static allocation schemes	[63]	✓				✓	✓										✓		✓		✓	
			[64]	✓					✓												✓	✓	✓	
		Adaptive allocation schemes based on queuing modeling	[65]	✓	✓			✓	✓							✓	✓		✓		✓		✓	
			[66]		✓				✓	✓											✓		✓	
		Game theory for bandwidth sharing	[67]	✓				✓	✓								✓				✓		Non-specific	
		Relay-assisted scheduling	[68]	✓					✓										✓		✓		✓	
		Latency distribution	[69]	✓	✓				✓											✓	✓	✓	✓	
	Other	Subframe configuration	[70]	✓				✓	✓												✓		✓	
		Cell coverage planning	[71]	✓					✓		✓					✓				✓	✓		✓	
		Core network provisioning	[72]		✓				✓							✓			✓		✓		✓	
		Multicast technology	[73]			✓		✓	✓							✓		✓			✓			✓
			[74]		✓				✓												✓		✓	✓

is adequate; however, ultra-reliable support of protection messages with virtually-zero latency lies in future LTE developments.

Motivated by the uplink-dominant nature of metering and monitoring traffic, LTE FDD and TDD modes are evaluated in [42] and [43] for delay-sensitive smart grid applications. Through system-level simulations, [42] describes the superiority of FDD over TDD in terms of uplink delay, while TDD achieves a better channel utilization in case of uplink data bursts, due to its flexible channel allocation configuration. In the case of LTE-TDD scheme, the possible uplink/downlink configurations are assessed from latency perspective in [43]. LTE-TDD is also considered in [44] for distribution automation applications with 100ms and 10^{-3} latency and reliability requirements, respectively. However, the authors assume that the random access procedure has already been established;

thus, no additional delay for connection setup is considered. The proposed bandwidth reservation method might also be insufficient in case of intense traffic load conditions.

While the previous works did not quantify the performance degradation of human-type traffic in shared LTE networks, the works in [45] and [46] study the impact of smart grid integration for several application scenarios. The authors argue that, by applying proper LTE-QoS configuration for smart grid traffic, low network latencies and high packet delivery rates can be achieved, while the deterioration of conventional LTE services is not proved significant. However, the smart grid traffic characteristics considered in the simulation setup are associated with large packet interarrival times and modest data rates. These are opposed to the burst traffic patterns of protection-related messages and the increased aggregated data rates in large consumer conglomerations where a massive number of grid entities is considered.

In an effort to accurately characterize the impact of smart grid communication traffic, the authors in [47] develop analytical (periodic and event-based) traffic models based on a queuing system analysis. The average buffer length and queuing delay expressions are analytically derived and the accuracy of the models is validated by considering an LTE simulation scenario. A similar analytical approach for smart grid traffic characterization is proposed in [51]. After validating the derived models, the authors investigate the maximum number of smart grid entities that can be simultaneously supported in a single LTE cell. The impact on conventional LTE voice and data services is also quantified in terms of blocking service probability. In [48], the overloaded RACH performance for LTE is studied considering a surge in initial network entries by a large number of smart meters. In particular, an analytical Markov chain model is proposed for the evaluation of network access and energy consumption, while the feasibility of overload-control mechanisms proposed in the literature is assessed through protocol-level simulations.

Capacity analyses for LTE network dimensioning in the distribution grid are given in [49] and [50]. Focusing on smart metering use cases, the number of supported devices with ensured QoS is determined through simulations. In both studies, a dedicated LTE network is considered; thus, the effect on human-type traffic is not analyzed. The congestion issue when a massive number of smart metering devices initiates network access using the random access procedure is studied in [52]. In particular, the authors discuss the preamble collision problem that occurs due to the limited number of available preambles with respect to the increased access demand. In case the number of preambles available for channel access of metering devices increases, the impact on conventional LTE traffic is quantified in terms of latency and throughput. A random access load analysis is performed in [18] where a smart metering scenario is considered. To overcome network congestion in radio access, an overview of enhanced random access mechanisms are proposed, e.g., ACB schemes, separation/dynamic allocation of random access resources. An analysis of the coverage and capacity of advanced metering systems over a wide area cellular network is presented in [53]. In particular, the authors conduct a coverage analysis predicting the maximum cell size subject to an outage criterion, as well as a capacity analysis that predicts the maximum rate at which a smart meter can send/receive messages over the cellular network. The tradeoff between coverage and capacity is quantified and the authors conclude that the network is coverage-limited rather than capacity-limited for the meter reading use case.

2.3.2 LTE Enhancements for Smart Grid Applications

As introduced in Table 2.2, LTE enhancements can be categorized into two main groups:

- Random access improvements.
- Enhancements in scheduling and resource allocation procedures.

Random Access Techniques

The 3GPP has already raised the need to revisit the radio access design of future cellular systems in order to provide reliable connectivity in applications where the number of devices raises up to tens of thousands per cell. Several methods have been proposed during the recent years to improve the contention-based RACH operation. Most of the available solutions are based on initial proposals compiled by the 3GPP, including separation of random access resources, ACB schemes, and protocol optimizations in the MAC layer [18]. The separation of resources can be achieved either by splitting the available preambles or by allocating different random access slots to the traffic flows [75]. Despite reducing the resource contention among the competing entities, the performance of this mechanism tends to be worse when the traffic load increases. Thus, the benefits of this solution can be attained when applied in conjunction with an additional congestion-avoidance mechanism and resource partition is periodically adapted to the traffic conditions of the system [76].

In recent 3GPP standard releases, the ACB scheme is adopted as an effective overload control mechanism to prevent access failures. Two alternative barring mechanisms have been considered for the ACB-configured devices:

1. The first method is based on dividing the devices into 10 access classes and applying the ON/OFF principle per access class. With this approach, all ACB-configured devices are either barred or not barred from making RACH attempts depending on their access class. System information update is required to end barring for the prohibited device classes or to change the barred classes. In order to allow all ACB devices to access the network at some point of time, the access opportunities need to be circulated between access classes.

2. The second method is based on a probability value and a timer. In case of network overload, the eNodeB broadcasts to the different traffic classes a set of parameters related to ACB, as part of the system information; this includes a barring rate factor and a barring timer for backoff. The devices are then configured to generate a random number between 0 and 1 (Bernoulli trial) prior performing a RACH attempt. If the random number is lower than the barring rate factor, the ACB test is passed and devices may attempt RACH. Otherwise, they have to wait a given amount of time indicated by the backoff timer and draw a new random number before reattempting a new RACH access.

The ACB scheme and its subsequent amendments, e.g., dynamic ACB for adaptive barring and extended ACB for delay prioritization, rely on the assignment of different

barring parameters and backoff periods to disperse the simultaneous access attempts over time and alleviate the congestion [77]. When applied as standalone RACH solutions, they may result in increased access latency that some delay-constrained devices cannot tolerate.

A dynamic algorithm for efficient resource utilization with QoS guarantees in the group-paging[3] mechanism is proposed in [54]. The performance evaluation illustrates significant resource efficiency gains with respect to the static allocation of random access opportunities. However, this work considers a relatively small number of devices with respect to 3GPP specifications [18]. A novel contention-based access scheme based on reduced signaling message exchange is proposed in [56]. Motivated by the characteristics of smart metering traffic, the authors consider a data access scheme utilizing only the shared uplink resources in contrast with the conventional LTE access schemes that utilize the uplink control and the RACH. Their analytical and simulation results demonstrate the improved performance in terms of latency and power consumption even for a large population of attempting devices. A similar approach where the random access procedure is replaced by direct data transmission through the control channel is described in [55]. Despite the improvements in terms of smart meter throughput/latency and the minimal effect on human users, the high packet collision problem remains unsolved.

In an effort to proactively estimate the anticipated network load (alarm reports, periodic measurements), the authors in [57] develop a reliable mechanism that can be easily incorporated in the standard LTE access mechanism. Based on the load estimate, the access opportunities for granting access are determined in a network with dedicated resources for smart grid entities. In [58], a packet aggregation method that mitigates the increased packet collisions in massive smart metering deployments is introduced. However, the reduced packet losses come at the expense of increased access latency, rendering the method insufficient for delay-intolerant services. A mechanism involving cooperative communication with notification messages among peer nodes is developed for a cascading alarm scenario in [59]. The authors propose protocol enhancements in the LTE radio resource layer for rapid fault detection and isolation, to significantly mitigate the access latency with respect to the standard procedure.

Scheduling and Resource Allocation

In the data transmission phase, the scheduler design for efficient RRM constitutes one of the most representative areas of research related to the integration of smart grid use cases in LTE networks. In the literature, several spectrum sharing strategies between smart grid and human-type flows have been proposed. A common approach identified in most works is the traffic prioritization of smart grid services over human-type LTE data transmissions.

A priority-weighted round-robin algorithm is discussed in [60]. Based on the consideration of a queuing model with a non-preemptive discipline, the delay gain is quantified for various types of smart grid traffic in a dedicated LTE network. A similar technique is used in [61], where the authors examine the integration of IEC-61850 Manufacturing

[3]Group paging is proposed to alleviate the random access collision issue. Upon receiving a group paging message from the base station, all devices belonging to the paging group should immediately initiate the random access procedure during a specified time interval.

Messaging Specification (MMS) services, such as smart metering and remote control applications, in shared LTE networks. The downlink performance in network underload conditions is investigated, while the instantaneous communication channel conditions are not taken into account in the scheduling decisions. Enhancements on default round-robin and proportional-fair scheduling algorithms for smart metering use cases are proposed in [62]. In particular, the authors argue that the accommodation of high node densities in a limited coverage area comes at the expense of increased signaling exchange. Therefore, in order to reduce the extensive signaling load, their proposed algorithms exploit the cumulative metering traffic characteristics to adjust the default scheduling granularity.

The previous approaches are based on simple modifications of existing scheduling policies and do not consider the stringent requirements imposed by distribution automation services. Novel resource management strategies based on static allocation schemes are discussed in [63] and [64]. In particular, the authors in [63] propose spectrum reservation (i.e., two consecutive resource block pairs) for guaranteeing smart meter connectivity while in [64], a queue-aware mechanism allocates fixed access grants to devices over periodic time-intervals. Both works aim at the minimization of the required signaling load due to excessive number of devices while guaranteeing QoS for smart metering services; however, they heavily rely on the assumption of periodic traffic modeling for smart grid communication.

The maximum delay tolerance of smart grid messages constitutes the main criterion of the adaptive allocation scheme proposed in [65]. A queuing model is developed for the analysis and the authors illustrate through simulations the superiority of the proposed scheme with respect to the legacy proportional fair scheduler. Similarly, in [66], an LTE scheduler is designed with the main objective of maximizing the percentage of uplink packets that satisfy their individual delay budgets. The authors assume that the eNodeB makes use of the packet age information of each device's queue to prioritize the requests based on the remaining time for scheduling an uplink grant and the pending load in the queue. A two-stage scheduling scheme based on cooperative game theory and multi-criteria decision making is proposed in [67] for different smart grid traffic classes. In particular, the authors first formulate a cooperative bargaining approach to ensure a fair resource sharing among the traffic classes and, at a second level, the resources are allocated according to delay, channel status, queue length, and past average throughput criteria. An uplink scheduling mechanism based on cooperative communications is discussed in [68] and a set of relays is considered to provide the link between the base station and the smart meters. The authors argue that the proposed mechanism outperforms the LTE legacy schemes after computing the percentage of served devices and mobile users with guaranteed QoS requirements. In [69], a novel scheduler is analytically designed based on the latency distribution of phasor measurement messages exchanged in the distribution grid. The scheduler is aimed to maximize the achieved rate of smart grid traffic, however without quantifying the performance degradation of human-type flows.

Other Solutions

There can be found in the literature several LTE enhancements for smart grid traffic integration that cannot be clustered into any specific category since they propose techniques that hold nothing in common with other proposals. The work in [70] pro-

poses a novel frame structure to mitigate heavy uplink metering traffic and achieve better spectrum utilization. The allocated subframes can be flexibly configured to adapt in different traffic loads. Numerical results demonstrate an improvement in terms of delay and throughput without considering possible effects on human-based services.

A semi-analytical approach for cell coverage planning with uplink delay constraints for smart grid applications is proposed in [71], using theoretical outputs from analytical mathematical models combined with real measurements. The authors argue that cell-planning algorithms for future LTE deployments need to incorporate smart grid latency constraints for coverage range computations. Architectural enhancements in the core domain of LTE networks for QoS provisioning of smart grid services are discussed in [72]. Motivated by the strict requirements of distribution automation traffic, the authors employ QoS differentiation mechanisms related with the assignment of dedicated bearers to smart grid traffic types. The simulation results reveal a significant reduction in delay and packet loss rate.

The authors in [73] exploit the LTE multicast technique to design an efficient communication framework between the aggregator and the consumers in demand-response use cases. Multicast technology, already applied for content distribution related to human-oriented services, can provide an efficient point-to-multipoint communication platform for metering information exchange, since demand-response policies are inherently designed for a large set of energy consumers. Through a performance analysis, the authors illustrate the effectiveness of different LTE multicast schemes over the LTE unicast service, in terms of latency, throughput and packet loss. Multicast technique is also employed in [74] where a distributed communication approach for monitoring and control is considered. With the use of a co-simulation platform (i.e., power and communication systems analysis software), the authors highlight the latency gains of a distributed fault management scenario compared to a conventional centralized one.

2.3.3 Resource Management in LTE-D2D Networks

Before LTE-D2D networks successfully support smart grid operations in the distribution grid, there are many research challenges that need to be resolved. A topic with growing research interest nowadays, refers to the efficient RRM in LTE-D2D networks that accommodate both cellular HTC and D2D communication among smart grid devices [78]. The scope and limitations of the existing works in the literature are thoroughly compared in Table 2.3.

Based on the spectrum utilization, D2D can be generally classified in two categories: in-band and out-of-band. In-band refers to D2D utilizing the same spectrum (uplink or downlink resources) used for cellular communications while out-of-band refers to D2D utilizing bands other than cellular band (e.g., 2.4 GHz Industrial, Scientific and Medical (ISM) band). In in-band LTE-D2D networks, D2D links can either share data resources with cellular links (underlay operation) or utilize mutually orthogonal parts of the cellular spectrum (overlay operation). In D2D-underlay, the main challenge refers to the efficient management of intra-cell interference experienced by both cellular and D2D links, whereas in D2D-overlay the main objective resides in the efficient and fair partition of the radio resources to achieve increased spectrum efficiency. The interference caused by D2D to cellular links and vice versa in underlay operation, requires high-complexity resource

Table 2.3: Comparison of proposals for resolving RRM in D2D-enabled cellular networks.

Proposal				Analytical tool							Performance Metrics										Validation		Resources	
Type	Subtype	Approach	Reference	Optimization theory	Game theory	Stochastic geometry	Graph theory	Probability theory	Geometry	Fuzzy logic	Throughput	Coverage probability	Fairness	Transmit power	Interference	Latency	System efficiency	Energy efficiency	Spectrum efficiency	Handover metrics	Simulation	Theory	Uplink	Downlink
In-band	Shared resources	QoS provisioning for D2D/cellular links	[80]	✓							✓										✓		✓	✓
			[81]	✓							✓										✓		✓	✓
			[82]	✓							✓										✓			✓
			[83]	✓				✓			✓	✓									✓		✓	
		Interference-limited areas	[84]					✓	✓		✓		✓								✓		✓	
			[85]						✓		✓				✓						✓			✓
		Power control	[86]					✓	✓		✓				✓	✓					✓	✓	✓	
			[87]	-							✓				✓						✓		✓	
			[88]	-							✓	✓									✓		✓	✓
			[89]	✓		✓		✓			✓	✓									✓	✓	✓	
			[90]	-							✓										✓		✓	✓
			[91]	✓			✓				✓			✓							✓		Non-specific	
			[92]	✓	✓						✓		✓	✓							✓		✓	
		Self-initiated local interference-aware techniques	[93]	-							✓	✓									✓		✓	✓
			[94]	✓							✓										✓		✓	✓
			[95]	✓			✓				✓										✓			✓
			[96]	-							✓										✓		✓	
		Base station-assisted interference coordination	[97]	-							✓										✓		✓	✓
			[98]				✓				✓										✓		Non-specific	
			[99]				✓				✓				✓						✓		✓	
			[100]	✓	✓						✓										✓		✓	
			[101]	✓	✓			✓			✓				✓						✓	✓	✓	
		Time-frequency hopping schemes	[102]	✓		✓		✓			✓	✓									✓	✓		✓
			[103]			✓		✓			✓	✓		✓					✓		✓	✓	✓	
		Auction-based mechanisms	[104]		✓						✓						✓				✓			✓
			[105]		✓						✓		✓				✓				✓			✓
		Power efficiency	[106]	✓										✓							✓			✓
			[107]	✓									✓	✓				✓	✓		✓		✓	
		Sum-rate maximization	[108]	✓			✓				✓		✓								✓		Non-specific	
		Spectral efficiency maximization	[109]			✓		✓			✓	✓							✓		✓	✓	✓	
	Dedicated resources	Fixed allocation schemes	[110]					✓								✓					✓	✓	✓	
			[97]	-							✓										✓		✓	✓
			[56]					✓								✓		✓	✓		✓	✓	✓	
			[111]					✓								✓					✓		✓	
			[112]				✓				✓	✓									✓		✓	
		Carrier sensing	[113]	✓		✓		✓			✓	✓							✓		✓		✓	
		Resource utilization efficiency	[114]	✓				✓											✓		✓		✓	
		Sum-rate maximization	[103]			✓		✓			✓	✓		✓					✓		✓	✓	✓	
			[115]			✓		✓			✓	✓	✓						✓		✓	✓	✓	
		Time-frequency hopping schemes	[102]	✓		✓		✓			✓	✓									✓	✓		✓
			[116]	✓		✓		✓			✓	✓									✓	✓		✓
Out-of-band		Channel sensing	[117]					✓			✓								✓		✓		Non-specific	
		Information-theory ISM side-channels	[118]	-							✓				✓						✓		✓	✓
Integration with short-range technologies		Seamless handover techniques	[119]	-							✓									✓	✓		✓	
			[120]	-																✓	✓		Non-specific	
			[121]	-							✓									✓	✓			✓
			[122]	-							✓	✓						✓		✓	✓		✓	✓
			[123]							✓		✓								✓	✓		Non-specific	
		Cluster-based cooperative schemes	[124]	-														✓			✓			✓
		Offloading mechanisms	[125]	-							✓							✓			✓		✓	✓
			[126]	-							✓					✓			✓		✓			✓

allocation methods, which result in increased computational overhead for the D2D-capable devices [79]. On the other hand, D2D-overlay results in a more controlled interference environment. Finally, the integration of LTE with short-range technologies has been also proposed as a means for achieving enhanced reliability and availability.

Various resource allocation strategies have been proposed in the literature to deal

with interference mitigation. Power control schemes, where D2D pairs dynamically modify their transmission power levels to minimize the interference effects to cellular users, have been studied in [86, 87, 88, 89, 90, 91, 92]. Other works focus on the definition of interference-limited areas for resource sharing, where D2D and cellular links cannot exploit the same frequencies [84, 85]. Local interference-aware mechanisms, driven by the D2D terminals to maximize their performance while guaranteeing the quality of cellular links, have been proposed in [93, 94, 95]. In an effort to avoid the acquisition of channel state information for every potential link and thus reduce the computational complexity of the formulated optimization problems, the authors in [96] propose a location-based resource sharing scheme that instead relies on network planning.

Interference coordination mechanisms with base station assistance have been also considered in the literature [97, 98, 99, 100, 101]. In particular, the works in [100, 101] employ game-theoretic techniques for resource allocation with fictional pricing mechanisms optimized by the base stations and transmitted to the D2D pairs which in turn compete to maximize their individual utility functions. Similar modeling frameworks that rely on auction mechanisms are proposed in [104, 105]. Leveraging stochastic geometry tools, the authors in [102] and [103] present analytical frameworks for the analysis and design of D2D spectrum sharing and make use of time-frequency hopping schemes for interference management and transmit power control. Resource allocation schemes with advanced optimization techniques for QoS provisioning of cellular and D2D links have been studied in [80, 81, 82, 83] and the objective lies in the maximization of the total system throughput. Heuristic power and resource allocation schemes aiming at an enhanced power efficiency with QoS guarantees for cellular and D2D links are proposed in [106, 107], whereas the maximization of spectral efficiency for D2D links is the objective in [109].

In a network with orthogonal spectrum allocation for D2D communication, part of the available cellular resources is subtracted from the general pool and is exclusively used by D2D links, instead of allocating the entire resource grid to both cellular and D2D links. In this case, interference among cellular and D2D links is not the primal concern and the main objective resides in the efficient and fair partition of the cellular resources to achieve increased spectrum efficiency, while satisfying the QoS requirements and traffic demands of the competing entities. The option for dedicated resources for D2D communication has been introduced in [97].

Resource partitioning can be either fixed or dynamically determined. A static allocation scheme based on graph theory is presented in [112], to avoid the interference caused among D2D pairs in a network with orthogonal resources. In [56], a contention-based LTE mechanism is proposed where dedicated resources are utilized for direct data transmission, avoiding the signaling overhead required for network access. A similar method for improving access latency is presented in [111], where the authors propose detailed LTE physical layer enhancements to address the occurring collisions in overload conditions. In [102, 116], the authors investigate the optimal resource partitions between D2D and cellular networks and apply time-frequency hopping schemes to achieve interference randomization. Efficient spectrum sharing strategies that allow a relatively fair and interference-aware partition of cellular resources between cellular users and devices have been also proposed in [103, 115]. In [113], the authors present a distributed mechanism for spectrum allocation using a carrier sensing threshold for self-interference control among D2D communication pairs.

In out-of-band LTE-D2D networks, D2D links utilize unlicensed spectrum in an effort to eliminate interference between D2D and cellular radio connections. The use of other frequency bands, non-overlapping with the cellular spectrum, introduces complexity in coordinating the communication over the two different bands. Out-of-band D2D communication may also suffer from the uncontrolled nature of unlicensed spectrum. Despite its potential gains, out-of-band D2D approaches have received less attention in the literature to date. In [117], the use of the unlicensed ISM band for communication among D2D pairs is proposed. D2D pairs form resource-contention groups depending on their QoS/bandwidth requirements and a group-wise channel sensing technique is then applied. The use of cellular controlled ISM bands to mitigate intra-cell interference management and increase the achieved cellular network capacity has been also studied in [118].

Another hybrid approach encountered in the literature, refers to the integration of LTE with short-range radio technologies, e.g., WiFi or ZigBee, forming the so-called capillary networks [127]. In this heterogeneous network deployment, reliability and availability could be improved by exploiting the transmission diversity with simultaneous radios used for the same purpose. Various seamless handover techniques for optimal network selection among the available ones have been proposed in the literature, mainly aiming at low handover delays [119, 120, 123], QoS preservation [121, 123] and energy efficiency [122]. The authors in [124] present a reliable multicast scheme with cooperative retransmissions in LTE-WiFi networks for reducing both the traffic load and the energy consumption of devices. Offloading mechanisms in LTE-WiFi networks are proposed in [125, 126], along with a performance evaluation of energy consumption and resource utilization efficiency respectively.

2.4 Summary

In this chapter, we provided an overview of the basic phases for uplink communication, i.e., initial network association and actual data transmission, in LTE-based systems. A comprehensive survey and comparison of the existing works related to feasibility studies and LTE enhancements for smart grid services has been presented. The main strengths and weaknesses among the proposed studies/proposals have been identified and one of the basic conclusions that can be drawn is the necessity for radical shifts on the way that cellular systems are currently designed. The peculiar characteristics of smart grid communication challenge the classical design constraints, objectives, and available degrees of freedom of cellular systems and render necessary a reconsideration of the current RAN design principles. In addition, any proposed technical solution for smart grid traffic integration in LTE/LTE-A systems should be evaluated by means of the key performance metrics described in Tables 2.2 and 2.3, which have been pointed out by the different techniques proposed in existing literature.

Some of the key open research areas for turning future cellular networks into a suitable technology for smart grid use cases can be summarized as follows:

1. The development of a tractable analytical framework of the LTE random access procedure to assess the reliability performance of demanding communication services in dense distribution grid deployments.

2. The design of resource sharing strategies for the accommodation of smart grid traffic requirements in shared LTE-based networks without significantly degrading real-time HTC.

3. The development of accurate traffic models that capture the peculiar traffic generation characteristics of smart grid communication.

4. The consideration of well-known industrial communication standards, e.g., IEC-61850 standard defining communication protocols for IEDs, for modeling message exchange in distribution grid automation services.

5. The exploration of D2D communication for the support of mission-critical and reliable information exchange in the smart grid.

In the following chapters, we detail the contributions of the thesis.

Chapter 3

Random Access for Smart Grid Communication

In Chapter 3, we focus on the LTE RACH congestion problem for massive smart grid communication with reliability guarantees. In Section 3.1, a performance assessment of real-time monitoring and metering scenarios reveals the network connectivity limitations due to the signaling overhead. A novel random access mechanism for distribution automation traffic is proposed in Section 3.2 to address the shortcomings of existing 3GPP random access solutions with negligible impact on the background traffic. An analytical model of the RACH procedure is introduced in Section 3.3 which allows us to assess the reliability performance of event-based monitoring traffic under different load conditions and network configurations. In Section 3.4, the relation between the cell size and the availability of orthogonal preambles is investigated. Using the analytical framework of Section 3.3, we propose an interference- and load-aware cell planning mechanism that guarantees reliable support of substation automation traffic. Finally, Section 3.5 is devoted to the study of the state estimation performance in wide-area monitoring systems with imperfect underlying communication in terms of RACH reliability. We provide the details in the following sections.

3.1 Connectivity Limitations for Large-scale Smart Grid Deployments

3.1.1 Introduction

Power distribution networks are often widely distributed to accommodate electrical power feeds to dense cities while monitoring and control systems typically require extensive information exchange among numerous IEDs. Using the existing network infrastructure, cellular technology appears as a key enabler for the support of large-scale metering deployments and wide-area monitoring systems. However, as discussed in Subsection 2.2.1, RACH congestion constitutes a significant challenge in large-scale distribution grid deployments with a high number of communicating entities. As the traffic load and the number of access requests increase, the standard LTE random access mechanism suffers from congestion due to the high probability of collision in the transmission of the available preambles.

In this section, we aim to identify the connectivity limitations that arise when smart grid traffic is supported by the standard LTE access mechanism. To this end, we evaluate the performance of the contention-based random access procedure of LTE/LTE-A systems for real-time monitoring and metering applications. In particular, the impact of smart grid traffic is investigated in terms of access delay and blocking probability under different network configurations and traffic characteristics. Unlike the majority of existing literature where delta traffic or simple Poisson models are used to represent the aggregate smart grid traffic, we leverage the Markov-Modulated Poisson Process (MMPP) framework [128] to capture the bursty behavior of monitoring traffic in event-driven distribution-grid operations. In general, smart grid monitoring traffic exhibits a multimodal probability distribution that cannot be accurately modeled with a simple Poisson process since the exponentially distributed interarrival times may underestimate the inherent traffic burstiness. Extensive simulations of realistic network-overload scenarios demonstrate that the RACH of LTE/LTE-A systems is prone to congestion when a high number of smart grid devices attempt for network access while the bursty nature of monitoring traffic results in even higher performance degradation. The conducted performance assessment offers useful insights regarding the feasibility of the LTE access procedure for distribution grid applications and, in particular, reveals the scalability challenges of LTE when handling massive smart grid traffic.

3.1.2 Smart Grid Communication Scenarios and Traffic Modeling

As the distribution grid evolves towards more complex loads and decentralized generation, distribution planning may need to account for more dynamic and faster changes to the distribution grid through *i*) the extensive installation of IEDs for wide-area monitoring purposes and *ii*) the large-scale smart-metering (i.e., AMI) deployments. In Figure 3.1, two representative communication scenarios in cellular-enabled distribution grids are depicted, where the deployment of an eNodeB offers the required wide-area connectivity. We provide the details in the following.

Wide-area Monitoring Systems

Distribution automation deals with system automatic functionalities that involve communication from numerous IEDs installed along the distribution network [22]. The emergence of DERs results in a growing need for real-time monitoring and quasi-real-time analysis of the grid behavior to enhance the observability and controllability of the distribution network. As illustrated in Figure 3.1, in wide-area monitoring systems spanning long geographical distances, the IEDs -equipped with radio interfaces- transmit monitoring information for situational awareness and supervision of the installed distribution equipment.

Besides the periodic transmission of monitoring information, we consider a scenario where event-driven IED communication is required to detect out-of-step conditions (e.g., excessive/increasing phase angle), issue alarms and initiate control actions to rectify the fault and/or isolate the system. In order to capture the bursty characteristics and varying behavior of IED traffic, we may model each IED traffic generation using a two-state MMPP [129]. The MMPP constitutes a stochastic counting process which is a special case of the Markovian Arrival Process (MAP), initially introduced in [130] and widely used for

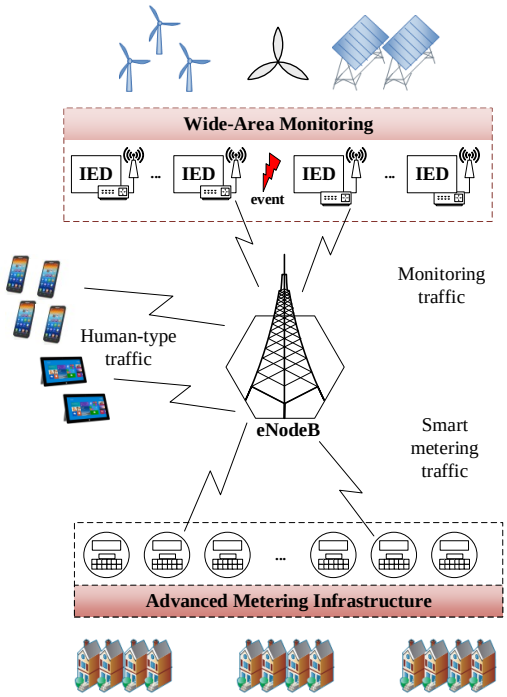

Figure 3.1: LTE networks as the underlying communication technology for advanced distribution grid applications, e.g., distribution automation and advanced metering infrastructure.

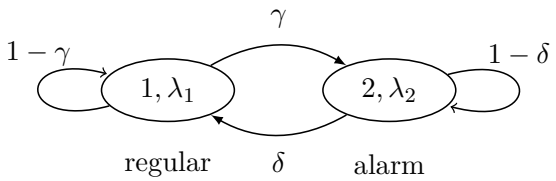

Figure 3.2: The state diagram of an IED traffic generation modeled with an MMPP. A two-state Markov chain describes the transition between the regular and alarm operation of a monitoring IED.

probabilistic analysis of communication network traffic. In particular, the MMPP can be viewed as a superposition of two Poisson processes with an underlying two-state Markov chain modeling the transition between the processes. Thus, the overall arrival rate of an MMPP is modulated by a continuous-time Markov chain. As illustrated in Figure 3.2, the first state corresponds to the regular IED operation, modeled as a Poisson process with rate λ_1; the second state represents the alarm IED operation where the generation of a traffic burst is also modeled as a Poisson process with rate $\lambda_2 > \lambda_1$, to account for the higher arrival intensity of the alarm traffic.

Let P be the state-transition matrix that incorporates the transition probabilities

between the states of the Markov chain. Then,

$$P = \begin{bmatrix} 1-\gamma & \gamma \\ \delta & 1-\delta \end{bmatrix}, \tag{3.1}$$

where γ is associated with the frequency of a burst occurrence and δ is related with the duration of each burst. Let also $\pi = \{\pi_1, \pi_2\}$ be the stationary distribution vector. Then, from the steady-state equations $\pi = \pi P$ and $\pi_1 + \pi_2 = 1$, we derive the stationary distribution π of the chain and the overall arrival rate λ_g of the MMPP as

$$\pi = \left\{ \frac{\delta}{\gamma+\delta}, \frac{\gamma}{\gamma+\delta} \right\} \quad \text{and} \quad \lambda_g = \sum_{i=1}^{2} \lambda_i \pi_i \,, \tag{3.2}$$

respectively.

Advanced Metering Infrastructure Systems

In the case of metering data delivery, a typical AMI system uses smart meters to communicate information between consumers and power utilities for operating and billing purposes. The enhanced coverage offered by LTE/LTE-A networks allows smart-metering deployments to span over vast areas and remote endpoints to be connected into the same management network. As illustrated in Figure 3.1, in this communication scenario, spatially distributed smart meters transmit consumer-meter information from a large number of customer/industrial premises at the utility end for data processing. The AMI systems require infrequent uplink transmissions of small-sized data packets and traffic generation is assumed to follow a Poisson process with an aggregate arrival rate λ_0.

In both communication scenarios, the channel access attempts of numerous distribution grid devices, i.e., IEDs in wide-area monitoring and smart meters in dense AMI deployments, render the standard access mechanism of LTE highly susceptible to congestion due to the limited random access opportunities compared to the increased resource demand. Therefore, RACH scalability constitutes a significant challenge especially for the dynamic environment of the future distribution grid where the number of devices joining the network rapidly evolves, i.e., frequent entry/re-entry [22].

In the following, we evaluate the RACH performance under different network settings and smart grid traffic characteristics.

3.1.3 Performance Evaluation

To evaluate the performance of the LTE random access scheme for monitoring and metering traffic, we consider realistic network-overload scenarios in NS-3 discrete-event simulator where each traffic type is solely present in the system. The presence of a single type of traffic in the simulation setup allows us to individually assess the random access performance and determine the connectivity limitations for each particular scenario. The standard RACH implementation initially developed in [131] is extended with the traffic modules of Subsection 3.1.2 and the integration with LTE radio protocol stack is performed as in [5, 11].

In the simulation setup, numerous IEDs or smart meters generate traffic within a single-cell coverage area and contend for channel access. Starting from a medium-load

Table 3.1: Simulation parameters.

Parameter	**Value**
Preambles for contention-based access	54
RACH configuration index*	{3, 9}
Backoff window size*	20ms
Preamble duration	1ms
Max. allowed preamble transmissions*	10
RAR window size*	5ms
Contention resolution timer*	24ms
Arrival rates λ_0, λ_1, λ_2 (in attempts/ms)	$\{10^{-3}, 2 \cdot 10^{-3}, 0.5\}$
Traffic model transition probabilities γ, δ	{0.5, 0.3}

* Standard values available in [18, 30].

scenario, new devices appear in the system according to a Poisson process with arrival intensities based on the traffic modeling described in Subsection 3.1.2. The MMPP parameters are selected to closely match the traffic behavior of IEC-61850 automation services [11]. As the simultaneous channel attempts progressively drive the system to overload, the RACH performance is evaluated under different network configurations and traffic characteristics when the system operates close to its capacity limits.

Two performance indicators have been used to assess the RACH performance, namely: *i*) average access delay, defined as the time elapsed between the first preamble transmission until the connection response message reception from the eNodeB and *ii*) blocking probability, defined as the probability that a device reaches the maximum number of transmission attempts and is still unable to complete the random access process. Table 3.1 summarizes the basic parameters used in our simulations.

The impact of RACH configuration index (CI) on the average access delay and blocking probability is illustrated in Figure 3.3 for both monitoring (IED) and metering (SM) traffic. In particular, as shown in Figure 3.3a, the average access delay experienced per IED/smart meter increases with increasing monitoring/metering traffic load since contention becomes heavier. A greater value of CI corresponds to a more frequent recurrence of random access opportunities per time frame; i.e., the index CI = 3 corresponds to one random access slot per frame whereas for CI = 9 each frame consists of three random access slots. Thus, when CI is configured to a higher value, we observe that the average access delay is reduced by almost 30% in the high traffic load regime. In addition, as shown in Figure 3.3b, the blocking probability experienced per IED/smart meter also decreases with a greater CI. In particular, we observe an approximate 40% reduction of the blocking probability in the high traffic load regime. In both figures, the average access delay and blocking probability are higher for monitoring traffic compared to the smart metering traffic, due to the bursty traffic nature of IEDs and the higher intensity of the arrival rate. It is important to highlight that the choice of CI value needs to balance the tradeoff between the amount of access opportunities to be scheduled per frame and the amount of resources available for data transmission.

The impact of the number of available preambles for contention-based access on the average access delay and blocking probability is illustrated in Figure 3.4. We consider

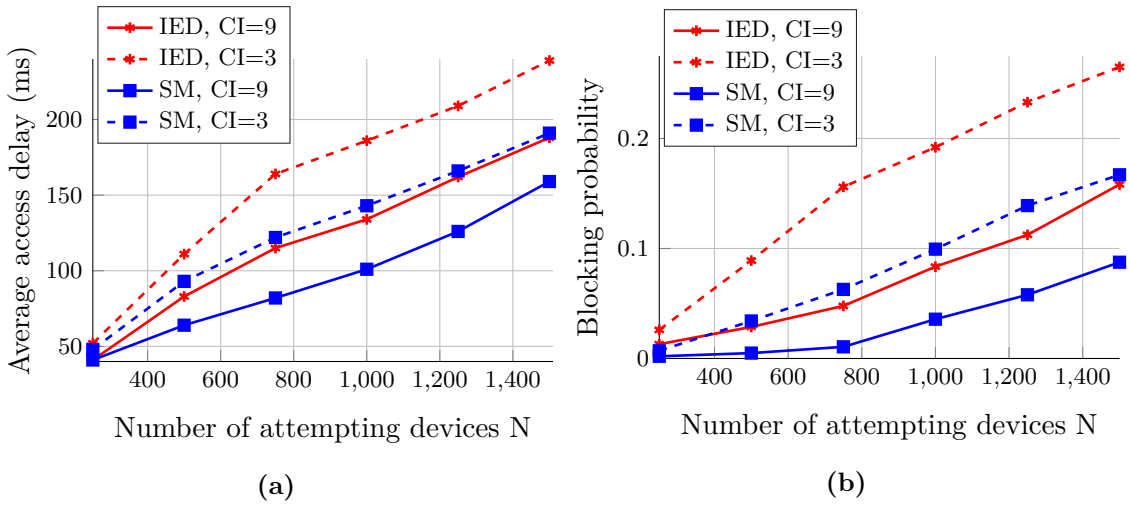

Figure 3.3: Impact of the RACH configuration index (CI) on (a) average access delay and (b) blocking probability for monitoring (IED) and metering (SM) traffic with increasing number of attempting devices.

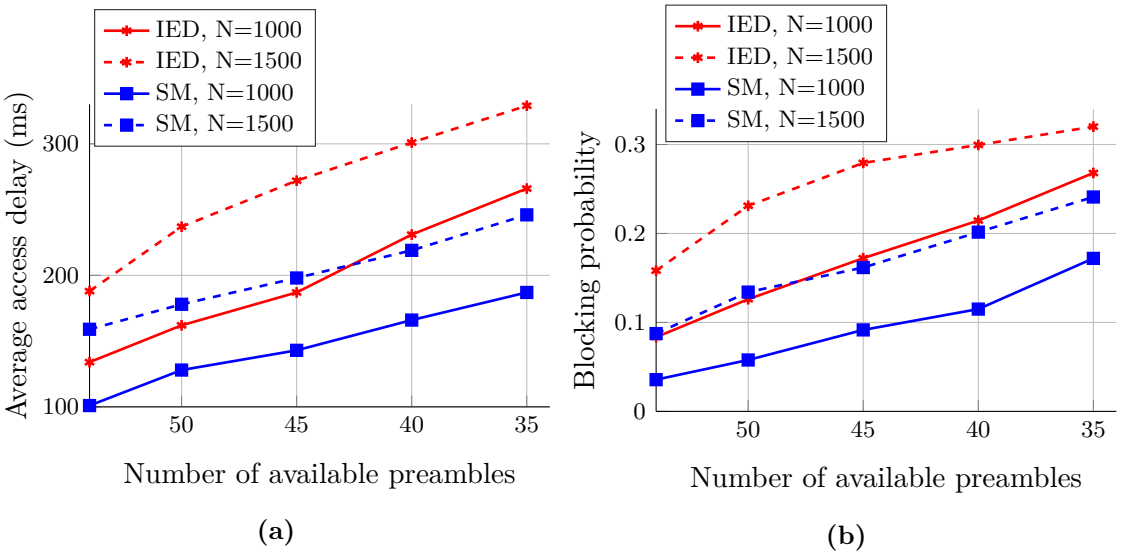

Figure 3.4: Impact of the number of available preambles for contention-based access on (a) average access delay and (b) blocking probability for monitoring (IED) and metering (SM) traffic in network-overload conditions.

both types of smart grid traffic and a high total number of attempting devices. In use cases where the RACH resources are shared with the conventional LTE users, an orthogonal resource partition may be implemented where a dedicated set of preambles is exclusively allocated to smart grid traffic given the targeted performance requirements. In particular, as depicted in Figures 3.4a and 3.4b respectively, the average access delay and blocking probability experienced per IED/smart meter increase as the number of dedicated preambles decreases due to the lack of adequate random access opportuni-

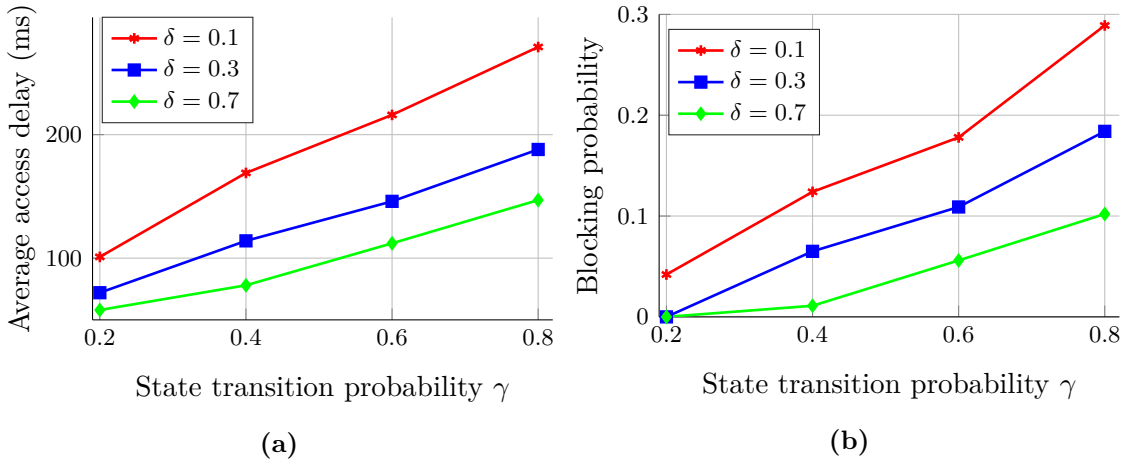

Figure 3.5: Impact of the traffic characteristics γ and δ of the monitoring IEDs on the (a) average access delay and (b) blocking probability in network-overload conditions.

ties. As it can be observed, the performance degradation is higher for the monitoring traffic compared to the smart metering traffic, due to the more aggressive arrival rate of monitoring messages.

In the case of monitoring traffic, the impact of the traffic characteristics γ and δ on the average access delay and blocking probability is depicted in Figure 3.5 for a high number (i.e., 1000) of attempting devices. As defined in Figure 3.2, γ is associated with the frequency of a burst occurrence and δ is related with the burst time duration. In Figure 3.5a, it can be observed that as the frequency of a burst increases, or equivalently γ increases, the average access delay increases due to the higher attempt rate in the alarm state which leads to a surge of channel access attempts. Similarly, due to the heavier contention, the blocking probability in Figure 3.5b increases with increasing γ since it is more possible for an IED to reach the limit of the allowed preamble retransmissions without a successful attempt. In addition, as the length of each burst increases, or equivalently δ decreases, the average access latency and blocking probability increase since the IEDs remain longer in the alarm state and RACH becomes more prone to congestion.

3.1.4 Summary

Our aim in this section of the thesis was to investigate the suitability of the standard LTE/LTE-A systems when applied in large-scale distribution grid communication scenarios and identify the connectivity limitations for the support of a high number of contending devices. To this end, we conducted a performance evaluation of the contention-based random access mechanism in LTE under wide-area monitoring and metering traffic. We investigated the impact of different network configurations and smart grid traffic characteristics on the standard random access procedure of LTE/LTE-A systems. Our feasibility study of realistic network-overload simulation scenarios reveals the signaling bottlenecks of the RACH when a high number of smart grid entities attempt for channel access in a highly-synchronized manner. We have shown that the availability of resources for contention and the smart grid traffic burstiness critically affect the standard LTE per-

formance, rendering in some cases the RACH highly susceptible to congestion due to the uncontrolled connectivity failures. In addition, we have observed that smart grid monitoring traffic results in even higher performance degradation compared to the metering traffic due to its higher arrival intensity.

Radical enhancements are thus required for the efficient accommodation of a high density of smart grid devices in future cellular networks. Motivated by this feasibility study, in the following section, we introduce a novel random access mechanism for the support of IEC-61850 communication services in shared LTE networks.

3.2 Integration of Wide-area IEC-61850 Communication Services

3.2.1 Introduction

The feasibility study conducted in the previous section reveals the LTE scalability challenges introduced by the traffic characteristics of messages exchanged for real-time monitoring, protection and control of the distribution grid. The IEDs associated with advanced distribution automation operations, e.g., fault detection and situational awareness, typically generate sporadic and event-driven traffic which requires time-critical delivery. In addition, a shared LTE network deployment needs to accommodate the HTC generated by the regular LTE subscribers and the access requests from smart grid metering devices conveying power quality measurements. The various traffic classes present in the system generate a harsh contention environment given the scarce radio resources for channel access. Therefore, to achieve reliable communication within the distribution grid, LTE needs to be enhanced with advanced radio access mechanisms adapted to a complex range of network access requirements and smart grid traffic characteristics.

In this section, we devise a novel random access mechanism to enable the integration of mission-critical distribution automation services in public LTE networks. The IEC-61850 standard for power utility automation has been widely used as the state-of-the-art standard for defining the data exchange architecture for the electrical substation automation system in the distribution grid. The standard specifies a set of object-oriented data structures and applications for substation automation that can be mapped to existing communication protocol stacks and services [132]. In what follows, we investigate the performance of the LTE RACH for the support of real-time IEC-61850 automation services in large-scale distribution grid deployments. We present the technical challenges introduced by the data exchange among IEDs in distribution automation operations and discuss the ability of LTE RACH to *i*) handle the traffic surge of simultaneous channel access requests and *ii*) meet the strict latency requirements of mission-critical messages. We focus on a representative application, namely a substation automation scenario, where a cascading power fault affects neighboring segments in the grid and triggers the transmission of notification alarm messages among geographically adjacent IEDs.

The main contribution in this section resides in the design of an efficient access mechanism to ensure the seamless operation of LTE RACH in network overload conditions. We address the shortcomings of existing 3GPP-based random access solutions by proposing a novel mechanism, named Random Access for Distribution Automation (RADA), that consists of an adaptive integration of three individual schemes. In particular, based on

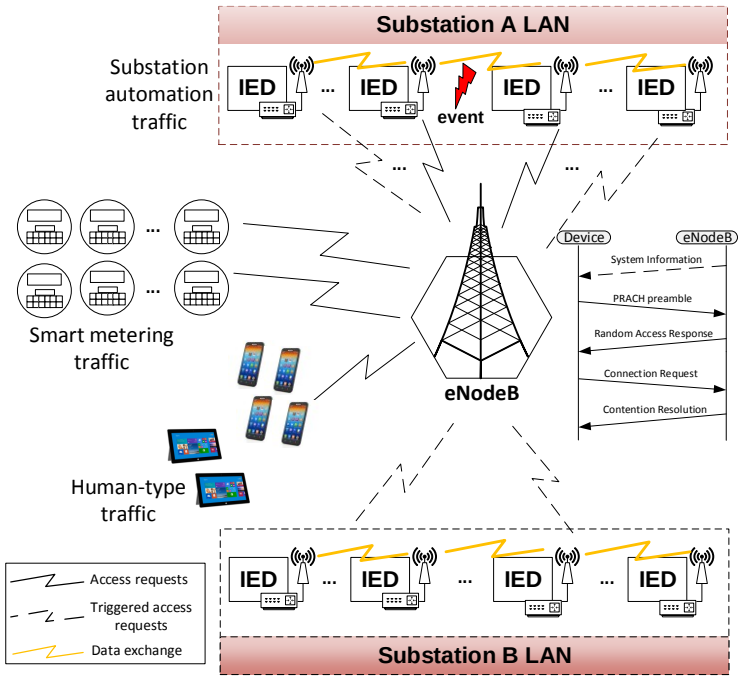

Figure 3.6: Network architecture for the integration of LTE technology in the distribution grid and its system components. The support of substation automation services relies on extensive information exchange among IEDs. Besides the IEDs, regular LTE subscribers and metering devices contend for the shared random access resources, rendering RACH highly prone to network congestion.

the monitoring of the network loading state by the eNodeB, a flexible partition of the available preambles into different traffic classes is applied. In turn, in capacity-overload conditions, a dynamic access barring scheme for delay-tolerant smart metering traffic is employed. RACH congestion is further relieved by a load shedding scheme at the eNodeB that discards unnecessary preamble transmissions from neighboring IEDs. The RADA mechanism rigorously considers the stringent latency constraints imposed by distribution automation traffic while guaranteeing the performance of the contending network entities, e.g., cellular users and smart meters.

3.2.2 LTE for Substation Automation

We consider a substation automation scenario, where communication constitutes a key module for the overall power system operation in the distribution grid. Substation automation systems often involve time-critical message exchange among neighboring IEDs for rapid diagnosis of system faults and initiation of control/isolation actions [132]. Figure 3.6 illustrates the network architecture for a substation automation deployment scenario. We consider a system model that relies on peer-to-peer communications and decision making is distributed among the substations that coordinate through direct communications. In general, this network topology captures use cases where distributed

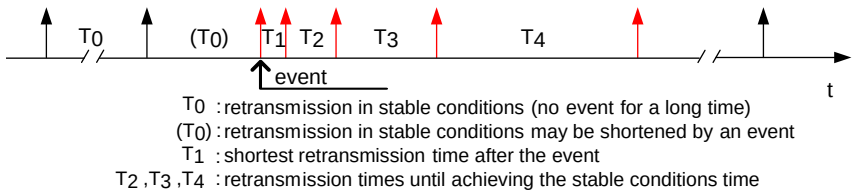

Figure 3.7: GOOSE burst traffic pattern [133]. Under stable conditions, GOOSE messages follow a periodic traffic pattern, but are generated in bursts when an event occurs.

event-driven communication is required. The IEDs, equipped with LTE communication interfaces, reside within the substation LANs and can be seen as controllers that get their input from voltage and current transformers/sensors and provide their output (commands, status data), e.g., to circuit breakers. Via direct control signaling among IEDs attached on the distribution feeders and transformers, real-time situational awareness and supervision of the power equipment is possible [1].

According to the IEC-61850-8-1 specification, Generic Object Oriented Substation Event (GOOSE) messages can be used for fast horizontal communication between IEDs within the same or different[4] substation LANs [133]. The GOOSE messages allow for fast transmission of substation events and, assisted by the ubiquitous LTE coverage, can support inter-substation communication to prevent the extensive propagation of disturbances to the entire power system. As illustrated in Figure 3.7, under stable operating conditions, each IED periodically reports its application states via identical[5] GOOSE messages to neighboring IEDs, as a heart-beat function. In turn, the reception of a GOOSE message sequentially triggers the neighboring IEDs to transmit their own GOOSE messages, conveying the same information in a cascaded and redundant manner. When an event occurs and thus a status change is detected, the retransmission period of GOOSE messages is shortened (burst traffic) to ensure the timeliness of their delivery.

The cascading effect of the fast exchange of GOOSE messages among the neighboring IEDs results in a surge of network access attempts. The congestion problem may deteriorate in future distribution grids, where substation automation services require a dense deployment of IEDs within the substation LANs to improve observability and controllability. In addition, the time-sensitive nature of GOOSE messages renders the standard LTE random access mechanism insufficient for the reliable support of these services [1]. As shown in Figure 3.6, on top of the distribution automation traffic exchanged among IEDs, the shared LTE infrastructure accommodates a wide range of HTC services, e.g., web browsing, voice and video traffic, generated by regular LTE subscribers. Since our system model corresponds to a realistic distribution grid topology, smart metering traffic is also present in the network. In particular, following the IEC-61850 MMS specification, numerous smart meters periodically transmit their power quality measurements to data management systems at the utility end. Smart metering services typically require infrequent uplink transmissions of small-sized data packets and their latency requirements are relatively milder compared to distribution automation functionalities.

[4]The need for wide-area monitoring and control of the distribution grid extends IEC-61850 standard to enable automation services beyond substation premises [133].

[5]Originally based on “best-effort” switched Ethernet in the data link layer, GOOSE reliability is enhanced by transmitting multiple message copies.

Therefore, a significant challenge occurs for the shared LTE RACH on how to efficiently handle the simultaneous network access requests from a high number of smart grid entities present in the system, i.e., IEDs and smart meters, as well as from the HTC users. Due to the cascade effects of GOOSE traffic in the case of a power fault, the high number of neighboring IEDs attempting channel access results in an abrupt increase of the overall traffic load and hence in congestion issues for the standard RACH mechanism. Our objective is to address the implementation challenges so that LTE RACH can reliably support automation services and thus ensure the seamless operation of the power grid, as will be discussed in the following subsection.

3.2.3 Proposed Random Access Mechanism

In this subsection, we introduce RADA, our proposed LTE random access mechanism that enables time-critical IEC-61850 data exchange in distribution automation services. As discussed before, the IEC-61850 standard and its subsequent releases define the communication between IEDs installed within a substation local area network and the corresponding system requirements. The standard was initially defined for local intra-substation automation services using switched Ethernet in the data link layer [25]. The ongoing modernization of the power grid extends the scope of IEC-61850 beyond the substation boundaries to support wide-area monitoring and control services. However, to extend the reach of automation information beyond substation boundaries, IEC-61850 packets would have to be translated to a different wide-area protocol through supporting routing mechanisms. Thus, the set of IEC-61850 services have to be compatible with the LTE radio protocol architecture. Since LTE was not initially designed to support automation tasks, adaptation protocols have to be introduced above the transport layer in the OSI reference model, as illustrated in Figure 3.8.

In an effort to leverage the advantages of various 3GPP RACH amendments when applied as standalone solutions, the RADA mechanism is comprised of an adaptive integration of three individual schemes:

1. A flexible partition of the random access resources by splitting the available preambles in subsets, each of them corresponding to each traffic class present in the system.

2. A dynamic access barring scheme for delaying the access to new arrivals originated from delay-tolerant traffic classes, i.e., MMS smart metering traffic.

3. A load shedding scheme based on the power levels of the received preambles from delay-critical GOOSE traffic generated by neighboring IEDs.

Since the shared LTE network should accommodate a wide range of human-centric and smart grid services, we consider traffic class differentiation via appropriate QoS provisioning, as an essential method for relieving the contention among the competing entities for network access. As discussed in Subsection 2.2.2, QoS provisioning allows for differentiated access handling in shared LTE networks and is achieved through the definition of new QoS traffic classes. In particular, we propose the extension of the standardized QoS-based LTE mechanism with the introduction of additional QoS classes for IEC-61850 GOOSE and MMS services [32]. Based on the latency and reliability requirements, the

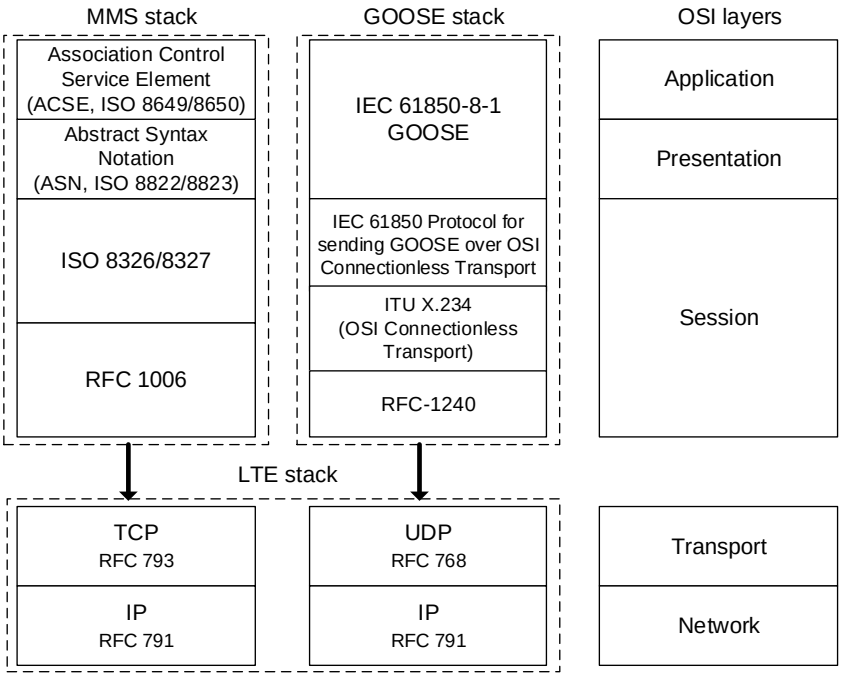

Figure 3.8: The MMS and GOOSE protocol stacks and their association with OSI layers [25, 133]. Adaptation protocols are added to ensure seamless integration with LTE radio protocol stack.

available preambles for contention-based network access are separated in three different subsets, namely: *i*) regular HTC, *ii*) delay-tolerant MMS and *iii*) high priority GOOSE. The competing entities are then restricted to exclusively use the subset of resources according to their class.

The preamble partition is considered to be periodically broadcast by the eNodeB, as part of the master information block message[6] in the physical broadcast channel on downlink [77]. In case of channel access overload, the eNodeB appropriately reassigns the separation of preambles between HTC and GOOSE subsets, to cope with peak congestion levels. This can be achieved via a continuous monitoring of the loading state of the network by the eNodeB, based on a periodic calculation of the average number of preamble retransmissions required to have a successful access request. Although the main goal resides in the support of the stringent performance constraints imposed by GOOSE messages, the preamble partition should be performed in a way that the performance degradation on conventional HTC is kept at a minimum level.

Based on the separation of the random access resources among the different traffic classes, the eNodeB is able to differentiate the origin of the received preambles and apply additional congestion-avoidance mechanisms depending on the traffic class. In particular, a dynamic access baring scheme is applied to MMS devices associated with delay-tolerant smart metering services. Similar to the previous scheme, the eNodeB can determine the congestion level of the RACH by calculating the average number of preamble retrans-

[6]The master information block message includes a limited number of most frequently transmitted system information parameters [77].

Table 3.2: Simulation parameters.

Parameter	Value
Preambles for contention-based access	54
RACH configuration index*	6
Backoff window size*	20ms
Preamble duration	1ms
Maximum preamble retransmissions*	10
RAR window size*	5ms
Contention resolution timer*	48ms
Master information block periodicity*	40ms
Barring rate b_{th}	0.4
Preamble partition {HTC,MMS,GOOSE}	{13,25,16}
Traffic mix {HTC,MMS,GOOSE}	{10%, 55%, 35%}
GOOSE interarrival time* T_0, T_1, $T_N, N \geq 2$	0.5s, 1ms, 2^{N-1}ms

* Standard values available in [18, 30, 133].

missions. In case of high traffic load detection, new access requests from MMS metering traffic are barred and MMS devices perform a random backoff time before scheduling their next preamble transmission. Thus, their access attempts are dispersed over time until channel contention conditions improve. The barring window size is considered to be broadcast by the eNodeB along with the master information block message.

In an effort to alleviate the increased RACH congestion caused by neighboring IEDs when a power fault occurs, a load shedding scheme is applied at the eNodeB based on the power levels of the received preambles associated with GOOSE traffic. As discussed in Subsection 3.2.2, access requests for GOOSE messages conveying identical system fault data, are transmitted in a cascaded and redundant manner by neighboring IEDs to ensure that messages are eventually delivered. However, in cases of RACH capacity overload, we can exploit the spatial proximity of geographically adjacent IEDs to discard the unnecessary preambles with similar received power levels at the eNodeB[7], without adversely affecting the reliability of GOOSE services. Instead, RACH congestion is reduced since the preambles are more frequently available to IEDs and access latency for delay-constrained GOOSE traffic can be substantially improved.

The adaptive integration of the three schemes into the consolidated RADA mechanism aims at the support of the stringent performance constraints imposed by the time-critical GOOSE traffic while keeping the performance of the other competing entities, e.g., cellular users and smart meters, at a guaranteed level. In the following subsection, we evaluate the performance of the RADA mechanism.

3.2.4 Simulation Results

To evaluate the performance of the RADA mechanism, we consider realistic overload scenarios where LTE subscribers generate background HTC within the eNodeB coverage area and contend with the IEDs and MMS meters for the shared channel access. Such

[7]The spatial geographical distance in the deployment of neighboring IEDs ensures that the preambles are not constructively received by the eNodeB [131].

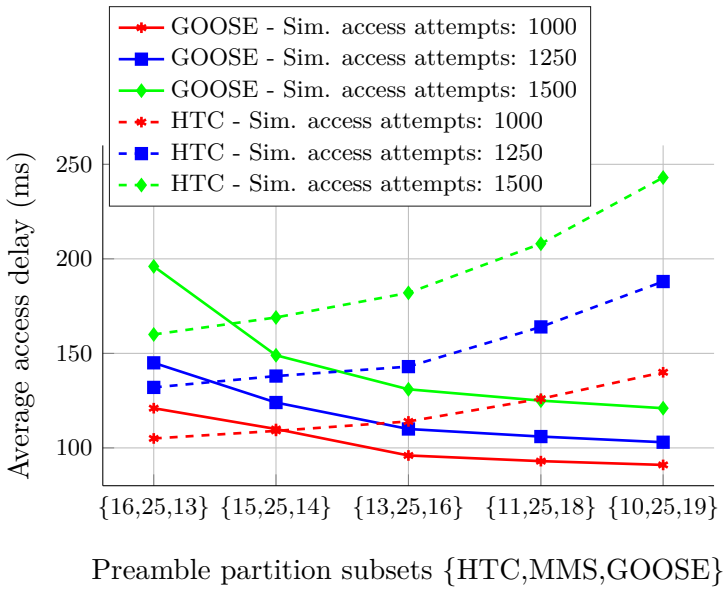

Figure 3.9: Average access delay per IED (GOOSE traffic) and HTC device for different preamble partition subsets of RADA mechanism in traffic overload.

scenarios would arise in practice, if public LTE networks integrated smart grid services that incorporate both distribution automation and metering traffic. Starting from a medium-load scenario, new access requests from all traffic types appear according to a Poisson process with arrival intensities selected so as to drive the system to overload. The traffic mix among HTC, MMS and GOOSE classes, expressed as a percentage of the simultaneous access attempts, is kept at the same level during the simulation runs. The RACH performance is then evaluated when the system operates close to its capacity limits. Table 3.2 summarizes the basic parameters used in our simulations.

Two performance indicators have been used to assess the performance, namely: *i*) average access delay, defined as the time elapsed between the first preamble transmission until the connection response message reception from the eNodeB, and *ii*) blocking probability, defined as the probability that a device reaches the maximum number of transmission attempts and is still unable to complete the access process. All results have been obtained through simulations with NS-3 discrete-event simulator. The RADA mechanism extends the standardized RACH implementation initially developed in [131]. The IEC-61850 GOOSE and MMS traffic modules have been implemented according to IEC-61850-8-1 specification and their integration with LTE radio protocol stack has been performed as in [25, 133]. The existing LTE LENA modules [134] have been properly modified/extended when necessary and the developed random access modules are publicly available in [4].

Optimal operation parameters for RADA mechanism

As discussed in Subsection 3.2.3, the RADA mechanism relies on a dynamic integration of three individual schemes; hence, we first need to determine the parameter values, i.e., preamble partition and MMS access barring rate, that result in an optimal overall system

performance, in cases of traffic overload. To this end, Figure 3.9 illustrates the average access delay experienced per IED and HTC device for different preamble partition subsets {HTC,MMS,GOOSE} of the RADA mechanism when the number of simultaneous access attempts is high. The delay for both traffic types increases with increasing traffic load due to the heavier contention. As expected, by allocating more preambles, originally oriented for HTC, to GOOSE traffic, the access delay for GOOSE messages decreases, whereas the HTC access delay increases due to the lack of adequate access opportunities. The optimal preamble partition $\{13, 25, 16\}$ occurs before HTC performance starts to significantly degrade while GOOSE access delay tends to a common value.

To identify the optimal MMS barring rate for RADA, the blocking probability experienced per MMS metering device is evaluated for different access barring rates in traffic overload conditions. In particular, as shown in Figure 3.10a, the blocking probability decreases with decreasing access barring rate; when the barring rate is set to a more restrictive value, it is more likely that new MMS access requests are spread in time-subsequent attempts due to the backoff window. Although decreasing the barring rate may ease the congestion and improve access success probability, the average access delay for MMS traffic is increased, especially for high number of access attempts as depicted in Figure 3.10b. Based on this tradeoff, the optimal barring rate value $b_{\text{th}} = 0.4$ is determined for MMS devices.

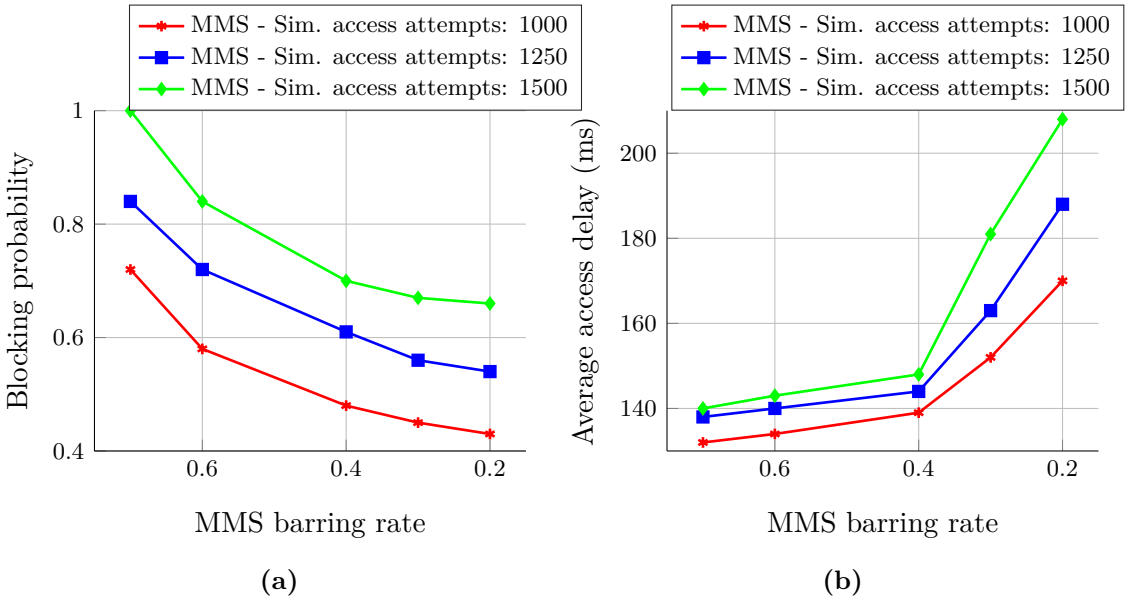

Figure 3.10: (a) Blocking probability and (b) average access delay per MMS metering device for different access barring rates of RADA mechanism in traffic overload.

Comparison with other schemes

After identifying the optimal parameter values for the RADA mechanism in cases of traffic overload, its performance is compared with existing 3GPP RACH solutions for benchmarking purposes [18, 75, 77]. Our goal is to quantify the performance gains yielding from a dynamic integration of congestion-avoidance techniques in a standalone

access solution. In particular, we perform a comparative study among the following schemes:

1. Default random access scheme based on 3GPP standard, with no special handling for different traffic types.
2. Access class barring scheme with barring rate $b_{\text{th}} = 0.4$ applied to MMS traffic.
3. Static preamble partition $\{13, 25, 16\}$ for HTC, MMS and GOOSE traffic, respectively.
4. Our proposed RADA mechanism.

Figure 3.11a illustrates the average access delay experienced per IED for different random access solutions with increasing traffic load. It can be observed that the RADA mechanism outperforms the existing RACH schemes, especially in heavy contention conditions where the average access delay for mission-critical GOOSE messages remains in lower levels. In particular, by means of simulations, a 40-45% reduction on the average access delay can be achieved in the high traffic load regime. It is also worth noting that, even in the case of 1000 simultaneous access attempts, GOOSE average delay remains below 100ms, the upper delay bound for Type-1B data exchange in decentralized distribution automation protection services [135]. This is mainly due to the load shedding scheme applied to preambles from neighboring IEDs, which remain in contention for less time. The superior performance of the RADA is also quantified in terms of blocking probability experienced per IED in Figure 3.11b, where lower figures are attained compared to existing RACH configurations. Even in the high traffic load regime, the largest gains presented reach a 58% reduction on blocking probability.

Naturally, the performance improvement for delay-critical GOOSE traffic causes some performance degradation to HTC traffic. Figure 3.12a illustrates the average access delay experienced per HTC device for the different random access solutions with increasing traffic load. A slight increase in the experienced HTC access delay can be observed for the RADA mechanism. However, the HTC average delay remains less than 200ms in heavy contention conditions; hence it might not be noticeable by end users even for some real-time LTE services. Figure 3.12b depicts the blocking probability experienced per MMS metering device for different random access solutions. Due to the dedicated preambles and the dynamic adaptation of the access barring rate in RADA mechanism, the blocking probability for MMS access requests remains in lower levels compared to other schemes, even in high traffic load conditions.

3.2.5 Summary

The support of advanced monitoring, protection and control operations in the distribution grid requires radical enhancements in the standard LTE RACH procedure to avoid performance degradation due to a high probability of collision in the preamble transmission. The limited random access opportunities compared to the increased resource demand render the standard access mechanism and its potential improvements highly susceptible to congestion for the support of distribution automation services in shared LTE networks. In this section of the thesis, we proposed a novel LTE random access mechanism, named

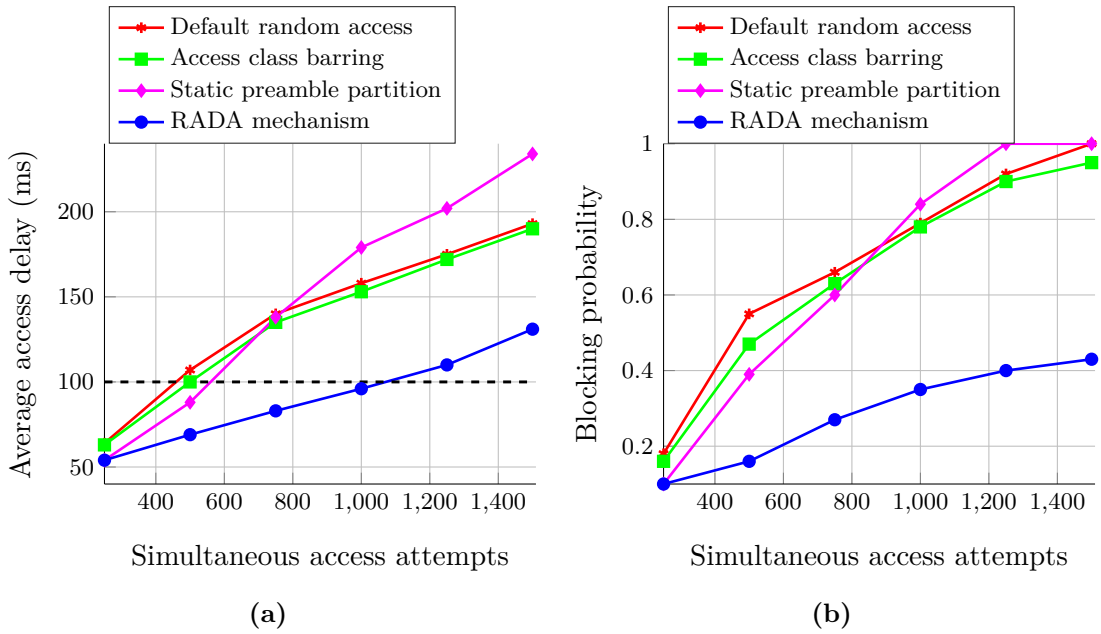

Figure 3.11: (a) Average access delay and (b) blocking probability per IED (GOOSE traffic) for different random access mechanisms with increasing traffic load.

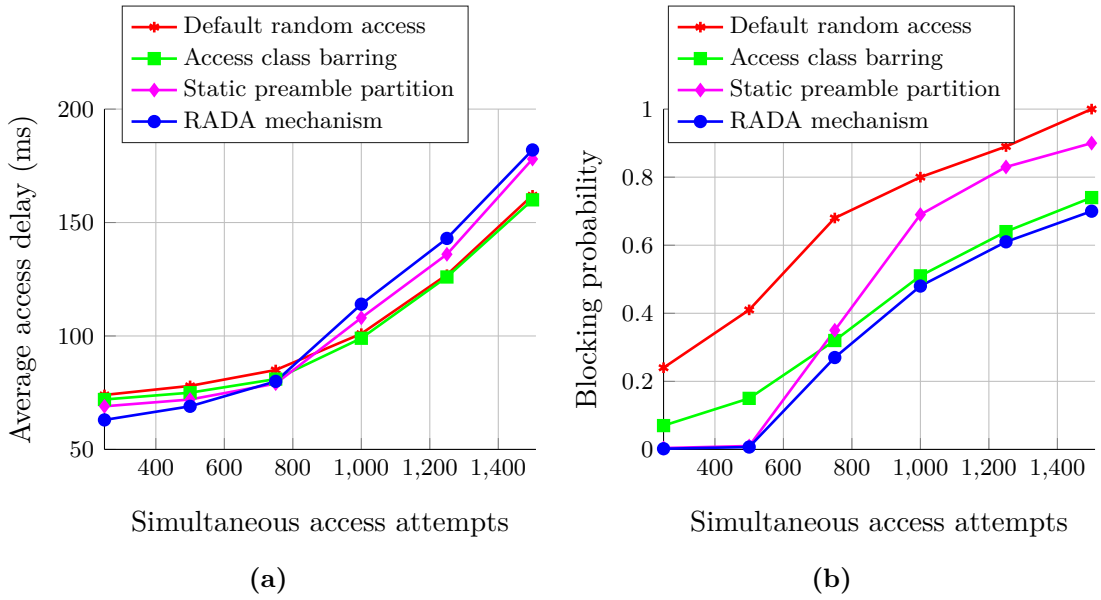

Figure 3.12: (a) Average access delay per HTC device and (b) blocking probability per MMS metering device for different random access mechanisms with increasing traffic load.

RADA, to resolve the contention and efficiently support mission-critical services with minimum impact on background traffic. The RADA mechanism is comprised of an adaptive integration of three congestion-avoidance schemes in an effort to achieve a smooth coexistence of different traffic types present in the system. Our extensive simulations in

a system-level simulator demonstrate the superiority of RADA in terms of access delay and blocking probability compared to the existing 3GPP RACH solutions. Even in the high traffic load regime, our proposed scheme can achieve a 40-45% reduction on the average access delay and a 58% improvement of the blocking probability with respect to the benchmarking schemes. In addition, our proposed scheme can be readily applied to the current LTE-A systems without significant modifications as it is designed based on existing 3GPP RACH amendments.

Since the emerging distribution grid operations are often associated with stringent communication requirements in terms of reliability, in the following section of Chapter 3, we provide a mathematically tractable framework for the reliability analysis of the LTE RACH with smart grid monitoring traffic.

3.3 Reliability Analysis of the Random Access Channel Procedure

3.3.1 Introduction

In this section of the thesis, a performance analysis in terms of reliability is presented for wide-area monitoring systems with underlying cellular connectivity. The LTE random access channel procedure enhanced with an ACB scheme is modeled via a Markov chain taking into account a realistic model of the varying traffic behavior of monitoring devices. Based on the proposed analytical framework, we derive the reliability expression which depends on various RACH and ACB parameters and the monitoring traffic characteristics. With the aid of extensive simulations, we validate the accuracy of our analytical model. A performance evaluation in terms of reliability is also carried out under different network and traffic configurations and several insights can be drawn for the reliable support of monitoring traffic.

As discussed in Subsection 2.3.2, the 3GPP has already raised the need to revisit the radio access design of future cellular networks in order to provide reliable connectivity for massive MTC [18]. Among the various methods proposed to improve the contention-based RACH operation, the 3GPP adopts the ACB scheme as an additional overload control mechanism to prevent access failures [77]. In case of network overload, the eNodeB broadcasts to the different traffic classes a set of parameters related to ACB, as part of the system information; this includes a barring rate factor and a barring timer for backoff. Each device then performs a Bernoulli trial to determine whether it is barred or not, based on the barring rate value. In particular, as illustrated in Figure 3.13, each device draws a uniform random number between 0 and 1 when initiating a connection establishment with the eNodeB and compares it with the current barring rate[8]. Only if the number is lower than the barring rate, the device is able to attempt an access. Otherwise, the access is barred and the device performs a random backoff time uniformly selected over a period determined by the barring timer value, before performing a new trial. The ACB scheme and its subsequent amendments, e.g., *dynamic* ACB [76] for adaptive barring and *extended* ACB [136] for delay prioritization, rely on backoff periods to disperse the

[8]The values of the RACH configuration index and the ACB parameters are broadcast by the eNodeB as part of the system information [30].

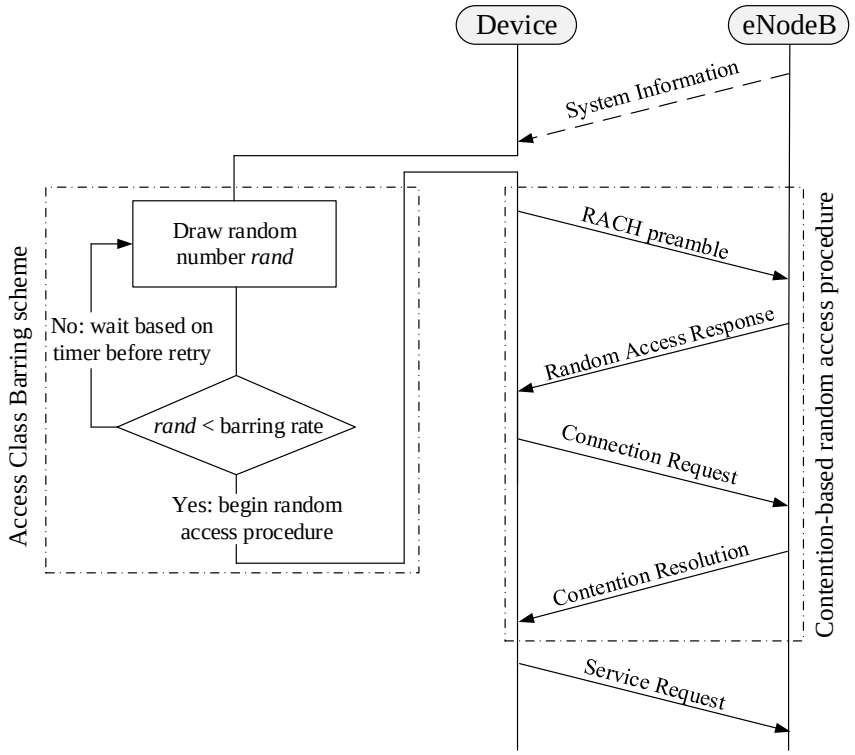

Figure 3.13: Contention-based LTE random access procedure enhanced with an ACB scheme for overload control.

simultaneous access attempts over time and alleviate the network congestion.

Several simulation-based studies [52, 54, 76, 137] and analytical works [57, 138] investigate the performance of the LTE RACH procedure for smart grid traffic. The majority of feasibility studies aim at determining the optimal values of the barring [76, 137], backoff [52] or paging [54] RACH parameters through system-level simulations. In an effort to proactively estimate the anticipated smart grid traffic load (i.e., alarm reports and periodic measurements), the authors in [57] propose a mechanism that determines the channel access opportunities for smart grid entities. A similar approach is followed in [136], where the authors perform an analysis of the extended ACB scheme based on a set of difference equations that characterize the interactions among the arrival process, the backoff and the extended ACB scheme. In both works [57, 136], the 3GPP-based models for uncoordinated and synchronous traffic are adopted. Instead, we hereby assume a reactive approach in dealing with massive monitoring traffic arrivals, where the network loading state is considered to be continuously monitored by the eNodeB with the overload-detection mechanism proposed in Section 3.2. The authors in [138] analytically assess the signaling limitations of the standard RACH procedure for smart grid monitoring traffic. In their analysis, the RACH is not enhanced with the ACB scheme while the adopted traffic modeling approach relies on a simple Poisson process for the aggregated data with periodic reporting frequency. However, this MTC traffic modeling method fails to capture the burstiness and multimodality of the real monitoring traffic distribution [139]. To this end, unlike previous related works, our traffic modeling approach accounts

for the frequency and duration of a burst traffic generation.

In the following, by leveraging tools from Markov chain theory, we introduce a tractable analytical model of the contention-based LTE random access mechanism enhanced with an ACB scheme for the connection establishment of a high number of IEDs. We further use a two-state MMPP traffic model, as introduced in Section 3.1, to capture the varying traffic behavior of monitoring IEDs in power distribution grids. Our developed framework accounts for the features of the random access, barring state, traffic activation, as well as preamble retransmissions, and allows us to derive the analytical expression of the achieved reliability. The accuracy of the proposed analysis is validated with the aid of extensive simulations in NS-3 discrete-event simulator. The performance assessment reveals the impact of the monitoring traffic characteristics and RACH/ACB parameters in the achieved reliability.

3.3.2 Analytical Model

We consider a cellular-enabled power distribution grid where N unsynchronized IEDs reside within a single-cell coverage area and contend in the RACH for network access. In what follows, we study the behavior of a single IED by using a two-dimensional Markov chain model.

Markov Chain Model

Let $\alpha(t)$ and $\beta(t)$ be the stochastic processes corresponding to the random access attempt and the backoff stage at time t, respectively, experienced by an IED contending for channel access. We assume that the stationary probability τ that an IED attempts a random access is constant across all random access slots and independent of other IEDs. This is considered a realistic assumption in the case of a high number of IEDs present in the system. Then, $(\alpha(t), \beta(t))$ constitutes a two-dimensional Markov chain. Let also L be the maximum allowed number of random access attempts, b_{th} be the ACB rate and B, W, the backoff window sizes for barring and random access, respectively.

As indicated in Figure 3.14, for the finite state space of the Markov chain, the following hold:

- The *off* state represents the state when the idle IED is expecting a new packet arrival based on the considered unsaturated traffic model. Let p_{on} denote the traffic generation probability related to the packet activation pattern of the specific smart grid monitoring task.

- The states $(Q_0, \ldots, Q_{B-1})$ model the barring states of the ACB scheme. The probability of entering/returning to a barring state equals to the probability q_0 of the drawn random number being higher than the barring rate b_{th} of the ACB scheme, normalized by the barring backoff window size, B.

- The states $(i, 0)$, $i \in [1, L]$, correspond to the random access states when the IED attempts a preamble transmission. In our model, we assume that an unsuccessful random access attempt may occur only due to preamble collision; thus, the probability of moving from states $(i-1, 0)$ to (i, j), for $i \in [2, L]$, equals to the preamble collision probability, p_c, normalized by the random access backoff window size, W.

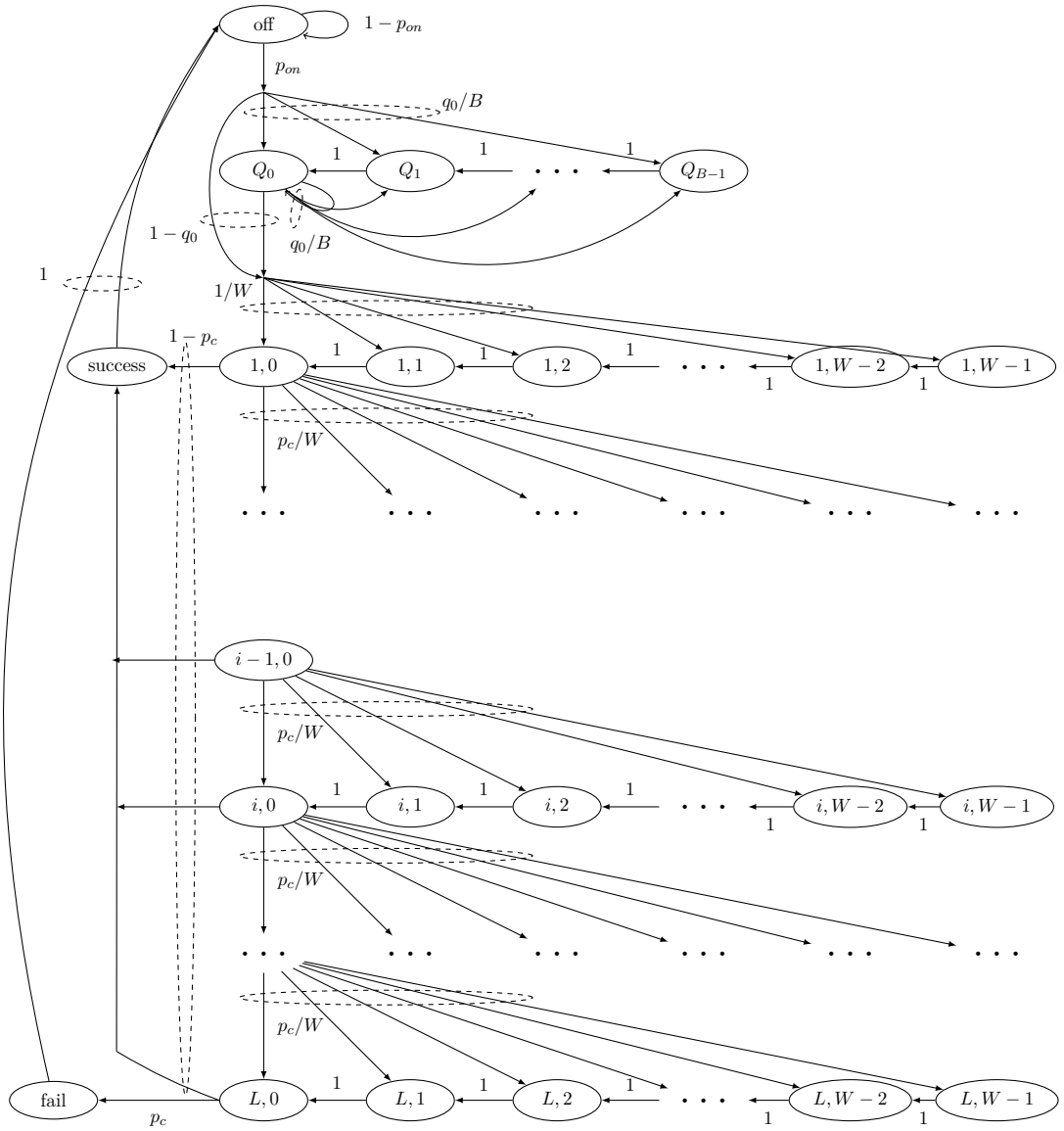

Figure 3.14: Markov chain model for the contention-based LTE random access mechanism enhanced with an ACB scheme.

We leave the consideration of a wireless channel error on an unsuccessful preamble transmission and the capture effect of collided connection request messages for future work.

- The states from $(i,1)$ to $(i,W-1)$, $i \in [2,L]$, represent the backoff states due to an unsuccessful $(i-1,0)$ access attempt. The IED decreases its backoff index by 1 every 1ms and transits from (i,j) to state $(i,j-1)$. A random backoff is also considered upon the initialization of the RACH procedure, i.e., the states $(1,j)$, $j \in [1,W-1]$.
- The *success* and *fail* states model the successful and failed random access attempt,

respectively. A failed random access attempt occurs when the limit of L allowed preamble transmissions is reached without successful attempt.

- The IED always returns to the *off* state after the *success* or *fail* states.

The state transition probabilities associated with the Markov chain of Figure 3.14 can be calculated as follows:

$$\Pr(i,j|i,j+1) = 1,\ 1 \le i \le L,\ 0 \le j \le W-2, \tag{3.3a}$$
$$\Pr(i,j|i-1,0) = \frac{p_c}{W},\ 2 \le i \le L,\ 0 \le j \le W-1, \tag{3.3b}$$
$$\Pr(Q_c|Q_{c+1}) = 1,\ 0 \le c \le B-2, \tag{3.3c}$$
$$\Pr(Q_c|\text{off}) = \frac{q_0}{B}p_{on},\ 0 \le c \le B-1, \tag{3.3d}$$
$$\Pr(Q_c|Q_0) = \frac{q_0}{B},\ 0 \le c \le B-1, \tag{3.3e}$$
$$\Pr(1,j|\text{off}) = \frac{(1-q_0)}{W}p_{on},\ 0 \le j \le W-1, \tag{3.3f}$$
$$\Pr(1,j|Q_0) = \frac{(1-q_0)}{W},\ 0 \le j \le W-1, \tag{3.3g}$$
$$\Pr(\text{fail}|L,0) = p_c, \tag{3.3h}$$
$$\Pr(\text{success}|i,0) = 1-p_c,\ 1 \le i \le L, \tag{3.3i}$$
$$\Pr(\text{off}|\text{success}) = \Pr(\text{off}|\text{fail}) = 1. \tag{3.3j}$$

Eq. (3.3a) indicates the decrease of the backoff index which occurs with probability 1. Eq. (3.3b) represents the probability of collision in the random access and of selecting a backoff state uniformly in the subsequent random access attempt. Eq. (3.3c) shows the transition between the barring states which occurs with probability 1. Eqs. (3.3d) and (3.3e) capture the probabilities of entering and returning to the barring states from the *off* and Q_0 states, respectively. Eqs. (3.3f) and (3.3g) represent the probabilities of moving to state $(1,j)$ from the *off* and Q_0 states, respectively. Eqs. (3.3h) and (3.3i) capture the probabilities of a failed and successful random access, respectively. Finally, Eq. (3.3j) implies that the IED always returns to the *off* state after a successful or failed random access.

Let $(b_{\text{off}}, b_{Q_c}, b_{i,j}, b_{\text{s}}, b_{\text{f}})$, $c \in [0, B-1]$, $i \in [1, L]$, $j \in [0, W-1]$, be the stationary distribution of the Markov chain, where $b_{i,j} = \lim_{t\to\infty} \Pr(\alpha(t) = i, \beta(t) = j)$. From Eqs. (3.3a)–(3.3j), we derive the closed form expression for such distribution chain. In particular, for the stationary probabilities of the barring states we have

$$b_{Q_c} = \frac{q_0}{B}p_{on}b_{\text{off}} + b_{Q_{c+1}} + \frac{q_0}{B}b_{Q_0},\ 0 \le c \le B-2, \tag{3.4}$$
$$b_{Q_B-1} = \frac{q_0}{B}p_{on}b_{\text{off}} + \frac{q_0}{B}b_{Q_0}. \tag{3.5}$$

For the random access and backoff states we obtain

$$b_{1,j} = b_{1,j+1} + \frac{(1-q_0)}{W}\left(b_{Q_0} + p_{on}b_{\text{off}}\right),\ 0 \le j \le W-2, \tag{3.6}$$

$$b_{1,W-1} = \frac{(1-q_0)}{W}\left(b_{Q_0} + p_{on}b_{\text{off}}\right), \tag{3.7}$$

$$b_{i,j} = b_{i,j+1} + b_{i-1,0}\frac{p_c}{W},\ 2 \le i \le L,\ 0 \le j \le W-2, \tag{3.8}$$

$$b_{i,W-1} = b_{i-1,0}\frac{p_c}{W},\ 2 \le i \le L. \tag{3.9}$$

Finally, for the *success* and *fail* states we have

$$b_{\text{s}} = \sum_{i=1}^{M}\left((1-p_c)b_{i,0}\right), \tag{3.10}$$

$$b_{\text{f}} = p_c b_{M,0}. \tag{3.11}$$

Owing to the chain regularities and Eqs. (3.4)–(3.11), the state expressions can be rewritten as

$$b_{Q_0} = \frac{q_0}{1-q_0}p_{on}b_{\text{off}}, \tag{3.12a}$$

$$b_{Q_c} = (B-c)\frac{q_0}{B}\left(p_{on}b_{\text{off}} + b_{Q_0}\right),\ 1 \le c \le B-1, \tag{3.12b}$$

$$b_{1,j} = \frac{W-j}{W}b_{1,0},\ 1 \le j \le W-1, \tag{3.12c}$$

$$b_{1,0} = (1-q_0)\left(b_{Q_0} + p_{on}b_{\text{off}}\right), \tag{3.12d}$$

$$b_{i,j} = \frac{W-j}{W}b_{i,0},\ 2 \le i \le L,\ 1 \le j \le W-1, \tag{3.12e}$$

$$b_{i,0} = b_{i-1,0}p_c = b_{1,0}p_c^{i-1},\ 2 \le i \le L, \tag{3.12f}$$

$$b_{\text{s}} = p_{on}b_{\text{off}}\left(1-p_c^L\right), \tag{3.12g}$$

$$b_{\text{f}} = p_c^L p_{on}b_{\text{off}}. \tag{3.12h}$$

Note that from Eqs. (3.12a)–(3.12h), all states can be expressed as a function of b_{off}. Thus, by applying the expressions for the state stationary probabilities in the normalization condition for the Markov chain,

$$1 = b_{\text{off}} + \sum_{c=0}^{B-1} b_{Q_c} + \sum_{i=1}^{L}\sum_{j=0}^{W-1} b_{i,j} + b_{\text{s}} + b_{\text{f}}, \tag{3.13}$$

we obtain the expression for the stationary probability b_{off},

$$b_{\text{off}} = \left[1 + p_{on}\left(1 + \frac{B+1}{2}\frac{q_0}{1-q_0} + \frac{W+1}{2}\frac{p_c^L - 1}{p_c - 1}\right)\right]^{-1}, \tag{3.14}$$

as a function of the traffic generation probability, p_{on}, the preamble collision probability, p_c, and the probability of barred access, q_0.

In the following, we derive the expression for the traffic generation probability, p_{on}, based on a realistic traffic model selected to match the behavior of a monitoring IED.

Traffic Model

We assume that the IEDs reside within the substation local area networks and can be seen as controllers that get their input from voltage and current transformers/sensors and provide their output (commands, status data), e.g., to circuit breakers, offering monitoring functionalities in the distribution grid. Under stable operating conditions, each IED periodically reports its application states via identical messages as a heart-beat function; however, once an event (e.g., power failure) occurs or a status change is detected, an IED transits from *regular* to *alarm* state while the retransmission period of messages is shortened (burst traffic).

Based on the traffic modeling approach introduced in Subsection 3.1.2, we use a two-state MMPP framework to model each IED traffic activation pattern and derive the expression for the traffic generation probability. Each IED traffic generation can be represented by a two-state Markov chain; the first state models the regular IED operation as a Poisson process with arrival rate λ_1 and the second state represents the alarm IED operation where the generation of a traffic burst is modeled as a Poisson process with a corresponding arrival rate $\lambda_2 > \lambda_1$. The MMPP is characterized by an infinitesimal generator matrix $\mathbf{D}_0$ in case of no arrivals and a diagonal rate matrix $\mathbf{D}_1$ in the case of an arrival. The matrix $\mathbf{D}_0$ is assumed to be stable which implies that it is nonsingular and the sojourn times are finite with probability 1. The elements in $\mathbf{D}_0$ correspond to the state transitions without arrivals and each element in $\mathbf{D}_1$ represents a state transition in the case of an arrival. In particular, the matrices $\mathbf{D}_0$ and $\mathbf{D}_1$ are defined as

$$D_0 = \begin{bmatrix} -\mu_1 & \mu_{1,2} \\ \mu_{2,1} & -\mu_2 \end{bmatrix}, \tag{3.15}$$

$$D_1 = \begin{bmatrix} \lambda_1 & 0 \\ 0 & \lambda_2 \end{bmatrix}, \tag{3.16}$$

respectively, where $\mu_i = \sum_{\substack{j=1 \\ j \neq i}}^{2} \mu_{i,j} + \lambda_i$. The definitions of $\mathbf{D}_0$ and $\mathbf{D}_1$ imply that $\mathbf{D} = \mathbf{D}_0 + \mathbf{D}_1$ is the irreducible infinitesimal generator of the underlying Markov process with stationary probability vector $\boldsymbol{\pi} = \{\pi_1, \pi_2\}^T$, computed using the steady-state equation $\boldsymbol{\pi}\mathbf{D} = \mathbf{0}$ at an arbitrary time instant.

After computing the stationary distribution of the two-state Markov chain, we can derive the expression of the traffic generation probability, p_{on}. Let

$$P_{i,j}(k,t) = \Pr(N_t = k, J_t = j | N_0 = 0, J_0 = i), \tag{3.17}$$

be the entry of a matrix $\mathbf{P}(k,t)$ on the state space $\{(k,i,j);\ k \geq 0,\ 1 \leq i,j \leq 2\}$, where N_t denotes the number of arrivals during the time interval $[0,t)$ and J_t the state of the Markov chain at time t, respectively. The matrices $\mathbf{P}(k,t)$ satisfy the forward Chapman-Kolmogorov equations [130]

$$\frac{d}{dt}\mathbf{P}(0,t) = \mathbf{P}(0,t)\,\mathbf{D}_0, \tag{3.18a}$$

$$\frac{d}{dt}\mathbf{P}(k,t) = \mathbf{P}(k,t)\,\mathbf{D}_0 + \mathbf{P}(k-1,t)\,\mathbf{D}_1,\ \ k = 1,2\ldots, \tag{3.18b}$$

and using the initial condition $\mathbf{P}(0,0)=\mathbf{I}$, $\mathbf{P}(k,t)$ can be determined. Then, p_{on}, defined as the probability to have at least one packet arrival within an LTE subframe of length 1ms, can be calculated as

$$p_{\text{on}} = 1 - \sum_i \sum_j P_{i,j}(0,t), \tag{3.19}$$

where t corresponds to the duration of the LTE subframe (1ms). Let also t_{off} denote the time between two consecutive arrivals in the stationary version of the MMPP. According to the Markov chain model for the contention-based LTE random access, t_{off} corresponds to the duration of the *off* state. Based on the properties of a stationary MAP, if $\mathbf{e}$ represents a unit column vector of length equal to the order of the MMPP, the mean of t_{off}, i.e., the expected holding time of the *off* state, is given by

$$T_{\text{off}} = \frac{1}{\boldsymbol{\pi}\mathbf{D}_1\mathbf{e}}. \tag{3.20}$$

In the following subsection, we derive an analytical expression for the reliability based on the developed Markov chain model.

3.3.3 Reliability Expression

We define reliability, R, as the probability of an IED successfully completing a random access attempt when there are L allowed preamble transmission attempts. Based on the proposed Markov chain model developed in the previous subsection, we derive the expression of reliability as

$$R = \frac{b_{\text{s}}}{b_{\text{s}} + b_{\text{f}}}, \tag{3.21}$$

and using the expressions for b_{s} and b_{f} from Eqs. (3.12g) and (3.12h) respectively, we get

$$R = 1 - p_c^L. \tag{3.22}$$

For the calculation of R we first need to determine the probability τ that an IED attempts a channel access. Assuming that the preamble transmission holds for 1ms, τ is determined as

$$\tau = \frac{\sum_{i=1}^{L} b_{i,0}}{T}, \tag{3.23}$$

where T denotes the expected state holding time for all states and is equal to

$$T = b_{\text{off}}T_{\text{off}} + \sum_{c=0}^{B-1} b_{Q_c} + \sum_{i=1}^{L}\sum_{j=1}^{W-1} b_{i,j} + \sum_{i=1}^{L} b_{i,0}\left(p_cT_1 + (1-p_c)T_2\right) + b_{\text{s}}T_s + b_{\text{f}}T_f. \tag{3.24}$$

In Eq. (3.24), the expected holding time for the *off* state, T_{off}, is given by Eq. (3.20). The expected holding time of each barring and backoff state is assumed to be 1ms. The expected holding time of a random access state $(i,0)$ is obtained as $p_cT_1+(1-p_c)T_2$, where

Algorithm 1 Iterative method to solve non-linear equations.

```
Assume L, B, W, q_0, b_th, p_on, T_off known
Initialize p_c ← 0.9999
Set allowed tolerance ε ← 1e − 3
while p_c > 0 do
  Calculate τ from Eq. (3.23)
  Calculate p'_c from Eq. (3.25)
  if |p'_c − p_c| < ε then                ▷ Convergence test
    break
  else
    p_c ← p_c − 0.0001                    ▷ Update
  end if
end while
```

T_1 and T_2 correspond to the elapsed times from the first access attempt until the end of the contention resolution timer in case of failure, and until the reception of the connection response message in case of success, respectively. Finally, T_f denotes the expected time duration of the *fail* state and T_s corresponds to the average holding time of the *success* state which depends on the adopted resource-scheduling policy of the service request and the message payload of the monitoring IED.

Given that an IED transmits, the preamble collision probability, p_c, from the perspective of the IED, is defined as the probability that at least one of the s IEDs attempting random channel access (from the remaining $N-1$ IEDs) selects the same preamble. Let K be the number of available preambles for contention-based random access, then p_c is given by the conditional probability

$$p_c = \sum_{s=1}^{N-1} \binom{N-1}{s} \tau^s (1-\tau)^{N-1-s} \left(1 - \left(1 - \frac{1}{K}\right)^s\right), \tag{3.25}$$

as a function of τ. It can thus be observed from (3.14)–(3.19) and (3.23)–(3.25), that the reliability expression in (3.22) depends on the monitoring traffic characteristics and the RACH/ACB configuration parameters. Note that for known p_{on} and q_0, the expressions of the probability τ of attempting a random access in (3.23) and the preamble collision probability p_c in (3.25) form a system of non-linear equations that can be solved via an iterative numerical method, as shown in Algorithm 1. Therefore, by plugging the obtained value of p_c in (3.22), the value of R can be calculated.

3.3.4 Model Validation and Performance Evaluation

In this subsection, we validate and evaluate our proposed analytical framework in terms of reliability with the aid of extensive simulations with NS-3 discrete-event simulator. The simulation setup relies on the RACH implementation initially developed in [131] and follows the 3GPP specifications [18]. The existing traffic generation and ACB modules have been properly modified/extended when necessary and the MMPP parameters are selected to closely match the traffic behavior of IEC-61850 GOOSE messages conveying synchrophasor information [11]. A performance evaluation is conducted and we investigate the effect of the traffic characteristics, the barring rate and the number of

Table 3.3: Simulation parameters.

Parameter	Value
Preambles for contention-based access K	54
Number of monitoring IEDs N	1000
RACH configuration index	14
Barring/access backoff window sizes B, W	20ms
Barring rate b_{th}	0.5
Preamble duration	1ms
Max. allowed preamble transmission attempts L	10
RAR window size	5ms
Contention resolution timer	24ms
Master information block periodicity	40ms
Arrival rates λ_1, λ_2 (in attempts/ms)	$\{0.002, 0.5\}$
Time durations T_1, T_2, T_s, T_f (in ms)	$\{32, 16, 20, 1\}$
Traffic model state transition rates $\mu_{1,2}$, $\mu_{2,1}$	$\{0.5, 0.3\}$

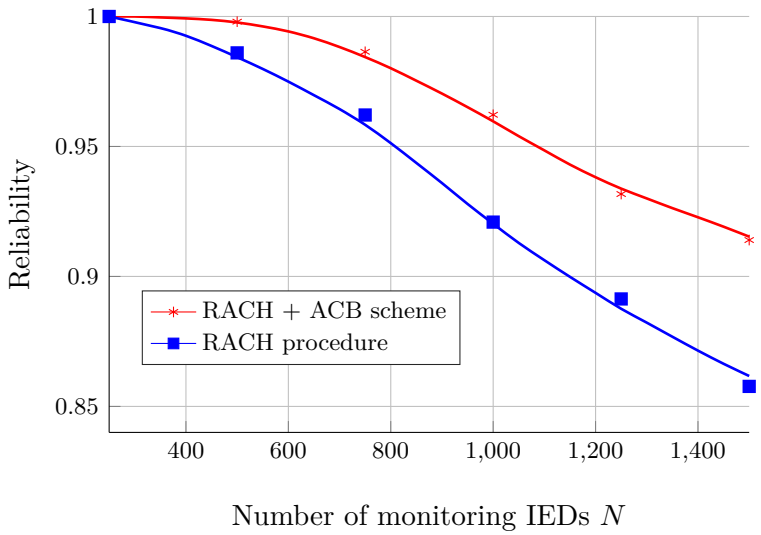

Figure 3.15: Reliability achieved per IED for different number of monitoring IEDs present in the system when RACH procedure is enhanced with the ACB scheme and when ACB is not applied.

available preambles on the achieved reliability. In Figures 3.15–3.18, we illustrate both the analytical results (lines) obtained from the reliability expression in Eq. (3.22) and the simulation results (marks) of the RACH/ACB implementation. It can be observed that the analytical results accurately match the simulation results which validates our proposed analytical model. Table 3.3 summarizes the basic parameters used in our simulations.

Figure 3.15 illustrates the reliability achieved per IED for a different number of monitoring IEDs present in the system, when the ACB scheme is activated, i.e., ($q_0 \neq 0$), and when ACB barring is not applied in the RACH procedure, i.e., ($q_0 = 0$). It can be observed that reliability levels decrease as the number of IEDs increases due to the heavier

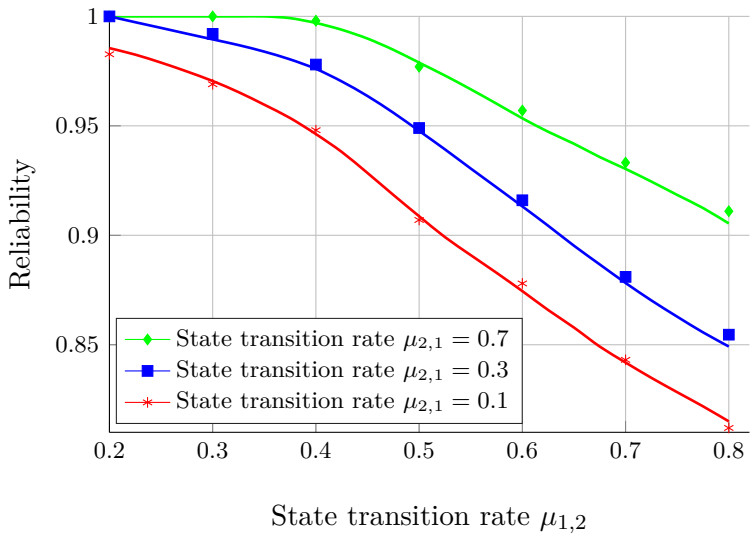

Figure 3.16: Reliability achieved per IED as a function of the traffic characteristics $\mu_{1,2}$ and $\mu_{2,1}$ of the monitoring IEDs when ACB scheme is applied in the RACH.

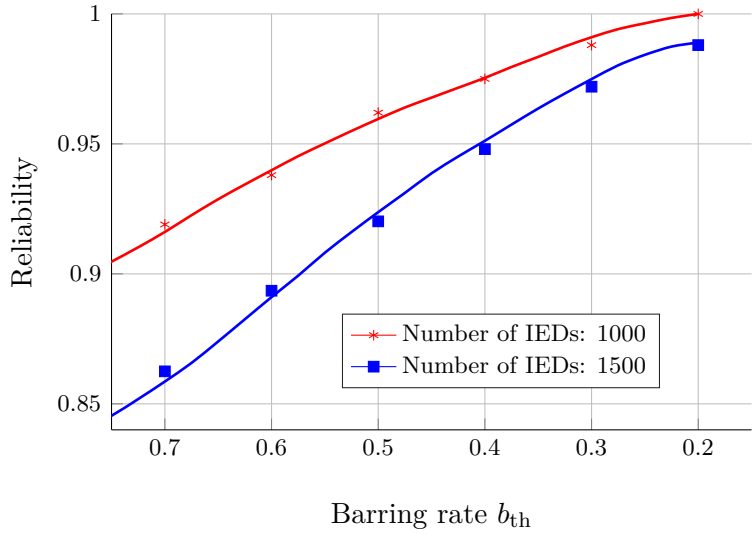

Figure 3.17: Reliability achieved per IED as a function of the barring rate b_{th} of the ACB scheme for a different number of IEDs.

contention; however, a RACH procedure enhanced with the ACB scheme achieves higher reliability even in high traffic regime since IED channel access attempts are dispersed over time. Thus, IEDs remain in contention for less time and preamble collision probability is reduced.

Figure 3.16 shows the reliability achieved per IED as a function of the traffic characteristics (i.e., state transition probabilities $\mu_{1,2}$ and $\mu_{2,1}$) of the monitoring IEDs. As defined in Subsection 3.3.2, $\mu_{1,2}$ represents the transition rate from *regular* to *alarm* state and $\mu_{2,1}$ corresponds to the transition rate from *alarm* to *regular* state. It can be ob-

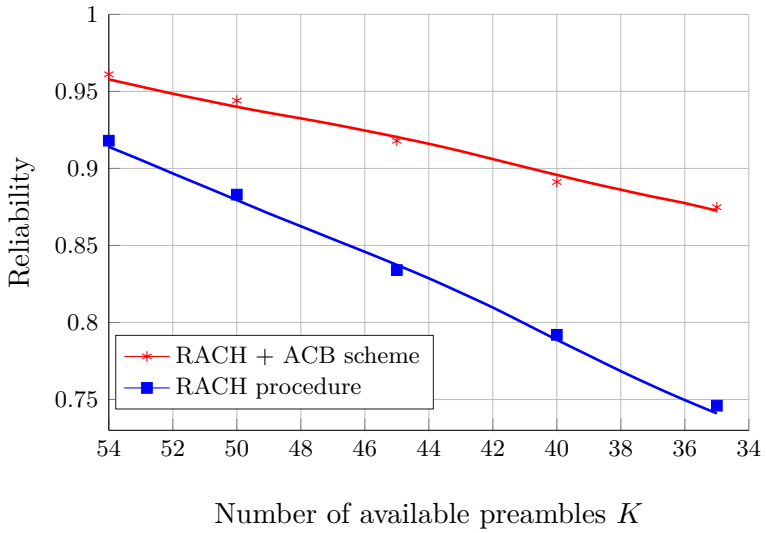

Figure 3.18: Reliability achieved per IED as a function of the number of available preambles K for contention-based access when RACH procedure is enhanced with the ACB scheme and when ACB is not applied.

served that as $\mu_{1,2}$ increases, i.e., the transition to alarm state occurs more frequently, the reliability decreases due to the higher arrival rate in the alarm state which leads to a surge of channel access attempts. In addition, as the length of each traffic burst increases, or equivalently $\mu_{2,1}$ decreases, the reliability decreases since the IEDs remain longer in the alarm state.

Figure 3.17 depicts the reliability achieved per IED as a function of the barring rate b_{th} of the ACB scheme for a different number of IEDs. In particular, the reliability increases with a decreasing access barring rate; when the barring rate is set to a more restrictive value, it is more likely that new IED access requests are spread in time-subsequent attempts due to the barring backoff B. Although decreasing the barring rate may ease the congestion and improve access success probability, the average access delay for IED monitoring traffic is increased, especially for high number of access attempts. We aim to study and quantify the latency-reliability tradeoff for the optimal choice of the barring rate value in future work.

Figure 3.18 illustrates the reliability achieved per IED as a function of the number of available preambles K for contention-based access of the monitoring IEDs. It can be seen that reliability levels decrease as the number of available preambles decreases due to the lack of adequate access opportunities; however, a RACH procedure enhanced with the ACB scheme achieves higher reliability compared to the performance of the pure RACH procedure. In particular, when the number of available preambles reduces from 54 to 34, the reliability levels decrease by at least 20% for the pure RACH whereas in the case of RACH enhanced with ACB, a maximum 9% reliability reduction can be observed. This superior performance is important in use cases where the available preambles for contention-based access are shared with the conventional LTE users in public cellular networks. Similarly to Section 3.2, an interesting tradeoff analysis would determine the optimal number of dedicated preambles for each competing traffic class, given its specific

QoS requirements.

3.3.5 Summary

In this section of Chapter 3, we proposed an analytical framework for reliability analysis of massive monitoring traffic in cellular-enabled distribution grids. Relying on Markov chain theory principles, we modeled the contention-based LTE random access operation enhanced with an ACB scheme for the connection establishment of a high number of IEDs. The ACB scheme is currently adopted by 3GPP as an additional overload control mechanism to prevent access failures. In particular, our tractable analytical model accounts for the features of random access, barring state, traffic activation, as well as preamble retransmissions. In addition, based on the preliminary traffic analysis presented in Section 3.1, we proposed a realistic traffic model that relies on the MMPP stochastic counting process to capture the IED transition from regular to alarm state. We then derived the expression of the traffic generation probability which is used for the calculation of the preamble collision probability. Based on the conducted analysis, we obtained the reliability expression which depends on various RACH and ACB configuration parameters and the monitoring IED traffic characteristics. Our analytical framework was validated through extensive simulations and the impact on the achieved reliability was evaluated under different network and traffic configurations. Since the contention-based random access procedure in recent 3GPP advancements tailored for the IoT, i.e., LTE-M, NB-IoT[9] and NR[10], follows its counterpart in LTE, the rationale of the proposed analytical model can also be applicable for the performance analysis of smart grid monitoring traffic using cellular IoT technologies.

In the following section of Chapter 3, we extend our reliability analysis to a multiple-cell LTE framework where the non-orthogonality between preambles generated from different ZC root sequences needs to be also considered in the reliability assessment.

3.4 Efficient Cell Planning for Reliable Support of Substation Automation Traffic

3.4.1 Introduction

In this section of the thesis, we investigate the relation between the LTE cell size and the number of preambles generated from a single or multiple ZC root sequences and their cyclic shifts. The fact that the number of orthogonal preambles available for contention decreases as the cell radius increases has been rarely considered in existing literature; this relation imposes an additional challenge for the reliable support of smart grid traffic due to the non-orthogonality of preambles originated from different ZC root sequences. We hereby study this impact on the achieved reliability in a substation automation scenario which constitutes a key module for the overall power system operation in the distribution grid, e.g., rapid diagnosis of system faults and initiation of control/isolation actions [133].

[9] Due to the reduced bandwidth in NB-IoT, different preamble design principles are adopted for the NB-IoT physical RACH compared to the legacy LTE physical RACH [140].

[10] Apart from a beam selection process occurring before the preamble transmission, the RACH procedure in NR systems follows almost the same principles as in LTE-based systems.

In related literature, [141] and [142] are the only works where the relation between the cell radius and the availability of orthogonal preambles is considered. However, the effect of the preamble non-orthogonality in the achieved reliability is not analytically studied. In [141], a contention-resolution access mechanism based on a tree-splitting algorithm and a distributed queue is proposed; however, a single macro-cell deployment is considered and the 3GPP-based model for synchronous traffic generation is adopted. A configuration of the ZC root sequences among small cells to enhance the random access performance with massive machine-type traffic is proposed in [142]. However, a static cell-size configuration is considered and the traffic-load conditions are not taken into account. In addition, traffic modeling relies on a simple Poisson arrival process; hence, the spatiotemporal correlation of event-driven machine-type traffic is not accurately captured.

In what follows, we incorporate these considerations in our analytical framework of the LTE RACH procedure developed in Section 3.3 and we derive the expression of the achieved reliability per cell. We further introduce an interference- and load-aware cell planning mechanism that *i)* properly allocates the root sequences among multiple cells to minimize the inter-cell interference and *ii)* regulates the traffic load via a barring parameter to ensure reliable channel access of substation automation traffic. In addition, we present a realistic traffic model that accurately captures the event-driven nature of substation automation traffic. Finally, the performance evaluation of a distribution automation scenario in network-overload conditions reveals the superior performance of our proposed mechanism in terms of RACH reliability against benchmarking network deployment schemes.

3.4.2 Cell Size and Availability of Orthogonal Preambles

We consider an LTE network that accommodates substation automation traffic generated by a high number of IEDs that reside in a geographical area A. We further assume a regular deployment of C_{A} circular cells with radius r_n, $n = 1, \ldots, C_{\mathrm{A}}$, providing coverage to the IEDs. The base stations are considered to be located in the center of the cells. A fixed number of K available preambles is prescribed for each LTE cell and the IEDs randomly choose a preamble to contend in the RACH. The preambles are generated from a single or multiple ZC root sequences and their cyclic shifts. The ZC root sequences satisfy a constant-amplitude zero-autocorrelation property, that guarantees the orthogonality of the preambles generated from the same root [29]. On the other hand, preambles generated from different ZC roots are non-orthogonal inducing interference in the preamble reception. Therefore, orthogonal preambles obtained by a single root sequence should be favored over non-orthogonal preambles. However, additional ZC root sequences need to be used when the required number of preambles cannot be generated by cyclic shifts of a single root sequence.

Each RACH preamble consists of a cyclic prefix and a preamble sequence. The cyclic shift dimensioning is important for the design of the preamble and its value depends on the selected cell size. Let T_{seq} denote the duration of the preamble sequence and N_{ZC} be the length of the ZC root sequence in samples. The minimum length of the cyclic shift duration N_{CS} in terms of number of samples is given by [29]

Table 3.4: Preamble sequence generation parameters in LTE-based networks.

Parameter	**Value**
Preambles K	64
Preamble sequence length T_{seq}	800μs
Zadoff-Chu root sequences N_{RS}	838
Zadoff-Chu sequence length N_{ZC}	839 samples
Maximum delay spread T_{ds}	5.2μs - 16.67μs

$$N_{\text{CS}} = \left\lceil \frac{T_{\text{RTT}} + T_{\text{ds}}}{T_{\text{seq}}} N_{\text{ZC}} \right\rceil, \tag{3.26}$$

where $T_{\text{RTT}} = 2r_n/c$ and T_{ds} denote the maximum round-trip time and the delay spread in a cell of radius r_n, respectively. The maximum number of orthogonal preambles constructed by a single ZC root sequence is then determined by

$$N_p = \left\lfloor \frac{N_{ZC}}{N_{CS}} \right\rfloor, \tag{3.27}$$

whereas the number of ZC root sequences required to produce the K available preambles in a single cell m is

$$N_{s,m} = \left\lceil \frac{K}{N_p} \right\rceil. \tag{3.28}$$

From Eqs. (3.26)–(3.27), it can be observed that the larger the cell radius, the larger the cyclic shift required to generate orthogonal preambles and, consequently, the smaller the number of orthogonal preambles constructed by a single ZC root. Table 3.4 summarizes the default values of the random access parameters in LTE-based networks [29]. Based on this configuration, Figure 3.19 shows that the number of orthogonal preambles N_{p} that can be constructed from a single ZC root sequence decreases as the cell radius becomes larger. A greater number of $N_{s,m}$ is then required to generate the 64 available preambles per cell. In particular, it can be observed that when the cell radius exceeds the 59km, each preamble sequence is generated from a different root sequence. On the contrary, in a cell with radius shorter than 958m, all 64 preamble sequences can be constructed by cyclic shifts of a single root sequence.

The use of different root sequences for the generation of the preambles results in higher interference in the preamble reception due to the orthogonality loss which in turn leads to degraded detection performance at the receiver. Therefore, RACH becomes more prone to congestion in cases where a single macro-cell is used to cover a geographical area with a widespread deployment of IEDs. Instead, as illustrated in Figure 3.19, the deployment of multiple smaller cells would require fewer root sequences and thus would mitigate the intra-cell interference in the preamble reception at the eNodeB due to the higher number of orthogonal preambles.

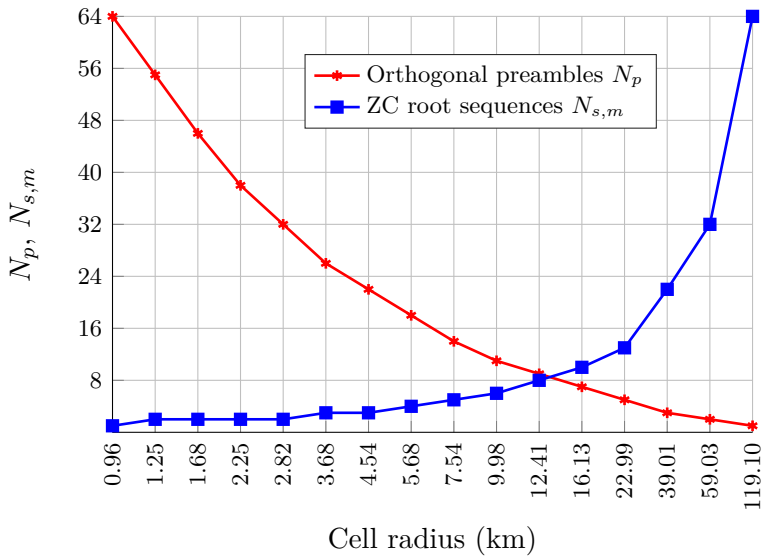

Figure 3.19: Relation among the cell size, the availability of orthogonal preambles per ZC root sequence and the number of ZC root sequences required to generate 64 preambles in a single LTE cell.

Henceforth, we focus on the RACH performance analysis in a reference cell m, where $N_{s,m}$ out of the N_{RS} in total ZC root sequences are allocated for preamble generation of the K preambles. Let $d_{\max}$ denote the maximum preamble-decoding distance which, given T_{seq}, can be estimated by the minimum required preamble-signal power received at the eNodeB to meet a target missed detection and false alarm probability of less than 1% [29]. We define by ν_m the probability that a neighboring cell n resides within the $d_{\max}$ of a preamble used in cell m. That is,

$$\nu_m = \Pr\left(\gamma_{\mathrm{mn}} \leq d_{\max} + r_n\right), \quad n = 1, \ldots C_{\mathrm{A}},\, n \neq m, \tag{3.29}$$

where γ_{mn} denotes the distance between the base stations of the reference cell m and of the neighboring cell n. In the default case where the N_{RS} available ZC root sequences are randomly allocated among the cells for their preamble generation, the probability $p_{\mathrm{seq,m}}$ that at least one of the neighboring cells selects one of the $N_{s,m}$ root sequences of cell m for preamble generation can be expressed as

$$p_{\mathrm{seq,m}} = \sum_{n=1}^{C_{\mathrm{A}}-1} \binom{C_{\mathrm{A}}-1}{n} \nu_m^n (1-\nu_m)^{C_{\mathrm{A}}-1-n} \left(1 - \left(1 - \frac{N_{s,m}}{N_{\mathrm{RS}}}\right)^n\right). \tag{3.30}$$

The probability $p_{\mathrm{seq,m}}$ can be interpreted as an indicator of the level of inter-cell interference experienced in cell m related with the allocation of the N_{RS} root sequences. Figure 3.20 illustrates how $p_{\mathrm{seq,m}}$ evolves with the cell radius in the case of a homogeneous deployment of multiple cells with equal radius r. As the cell radius decreases, or equivalently the number of required cells to cover a geographical area A increases[11], the N_{RS}

[11] In the case of a homogeneous deployment of cells with equal radius r, the required number of cells to provide coverage is $C_{\mathrm{A}} = \left\lceil \frac{A}{\pi r^2} \right\rceil$.

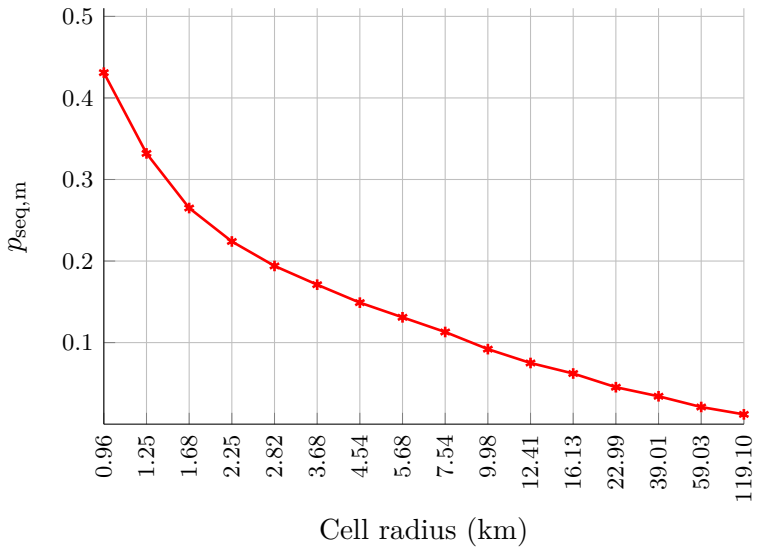

Figure 3.20: Relation between the probability $p_{\text{seq,m}}$ and the cell size for a homogeneous cell deployment. As the cell size decreases, $p_{\text{seq,m}}$ increases reflecting a higher inter-cell interference.

available sequences need to be distributed among a higher density of cells. This naturally leads to an increase in $p_{\text{seq,m}}$ since it becomes more possible for a neighboring cell to be allocated the same ZC root sequence as in the reference cell m.

The discussion presented above reveals an important design tradeoff regarding the relation between the cell radius and the reliability level achieved in each cell. If a single macro-cell is used to cover an area A, then a higher number of ZC root sequences is required to generate the K preambles in the cell. The non-orthogonality between the preambles generated from different roots results in higher probability of collision due to preamble decoding failure. On the other hand, if multiple smaller cells are deployed in A, then less ZC root sequences are required for the generation of the K preambles. However, this comes at the expense of additional installation of base stations and increased inter-cell interference regarding the allocation of roots among the cells. Therefore, an efficient cell planning mechanism is required to properly allocate the ZC root sequences among the different cells and ensure the reliability level achieved in each particular cell.

3.4.3 Cell Planning Mechanism

Reliability Expression

The reliability in the random access procedure is defined as the probability that an IED successfully completes a channel access attempt before exceeding the maximum allowed preamble transmissions. In Section 3.3, we derived an analytical expression for the achieved reliability per cell based on a generalized Markov chain model of the LTE random access. An ACB scheme was further considered as an overload-control mechanism where each IED performs a Bernoulli trial to determine whether it is barred or not, based on a barring rate, b_{th}. The finite state space of the Markov chain includes:

- The *idle* (off) state, where an IED expects a new packet arrival. The traffic generation probability is denoted as p_{on} and its analytical expression is derived in Subsection 3.4.4.
- The *barring* states, where channel access for an IED is barred to relieve RACH congestion. The probability of barred access and the barring backoff window size are denoted by $q_{0,m}$ and B, respectively.
- The *random access* states, where an IED attempts a preamble transmission. The parameter L denotes the maximum allowed number of preamble transmissions.
- The *backoff* states, due to an unsuccessful access attempt. The random access backoff window size is denoted by W and a random backoff is also considered upon the initialization of the RACH procedure.
- The *success* and *fail* states that model the successful and failed random access attempt, respectively.

Let N be the number of IEDs in the cell m. Based on the analysis in Subsection 3.3.3, the reliability, R_m, can be expressed as

$$R_m = 1 - p_{c,m}^L, \tag{3.31}$$

where $p_{c,m}$ denotes the preamble collision probability experienced by an IED in cell m. For the calculation of R_m, we first need to determine the expression for $p_{c,m}$.

Let $K_{z,m}$ denote the number of orthogonal preambles generated by the ZC root sequence z, $z = 1, \ldots, N_{s,m}$, of the reference cell m. As explained in Subsection 3.4.2, if the required number of K preambles in the cell cannot be generated by cyclic shifts of a single root sequence, then additional ZC root sequences should be used. Therefore,

$$K_{z,m} = \begin{cases} N_p, & \text{for } z = 1, \ldots, N_{s,m} - 1, \\ K - (N_{s,m} - 1)\, N_p, & \text{for } z = N_{s,m}\,, \end{cases} \tag{3.32}$$

since less than N_p preambles generated by the last root sequence may be required for the generation of the K available preambles. Given that an IED selects one of the $K_{z,m}$ preambles generated from root sequence z for network access, the $p_{c,m}$ is defined as the probability that at least one of the i devices (from the remaining $N-1$ devices) attempting channel access, selects the same preamble of the orthogonal $K_{z,m}$ preambles or selects a non-orthogonal preamble generated by a ZC root sequence other than z. We assume no capture effect in the collided preambles and that the interference from non-orthogonal preambles constructed by different ZC root sequences results in a preamble-decoding failure at the RACH receiver (i.e., the eNodeB). Then, $p_{c,m}$ is given by

$$p_{c,m} = \sum_{i=1}^{N-1} \binom{N-1}{i} \tau^i (1-\tau)^{N-1-i} \left[\frac{K_{z,m}}{K} \left(1 - \left(1 - \frac{1}{K_{z,m}} \right)^i \right) + \left(1 - \frac{K_{z,m}}{K} \right) \right], \tag{3.33}$$

where τ denotes the probability that an IED is attempting a channel access. By applying the normalization condition of the Markov chain and owing to the chain regularities, the state stationary probabilities can be expressed as a function of the probabilities $p_{c,m}$,

Algorithm 2 Iterative method to solve non-linear equations.

```
Assume L, B, W, q_{0,m}, b_th, p_on, T_off known
Initialize p_{c,m} ← 0.9999
Set allowed tolerance ε ← 1e − 3
while p_{c,m} > 0 do
  Calculate τ from Eq. (3.34)
  Calculate p'_{c,m} from Eq. (3.33)
  if |p'_{c,m} − p_{c,m}| < ε then                ▷ Convergence test
    break
  else
    p_{c,m} ← p_{c,m} − 0.0001                    ▷ Update
  end if
end while
```

p_{on}, q_m and the random access/barring parameters [7]. Then, assuming that a preamble transmission holds for 1ms, τ is given by

$$\tau = \left[\frac{p_{c,m}-1}{p_{c,m}^{L}-1}\left(\frac{T_{\text{off}}}{p_{\text{on}}}+\frac{q_{0,m}}{1-q_{0,m}}\frac{B+1}{2}+p_{c,m}^{L}T_f\right)+p_{c,m}T_1+(1-p_{c,m})\,(T_2+T_s)+\frac{W-1}{2}\right]^{-1}. \quad (3.34)$$

In Eq. (3.34), T_{off} denotes the average holding time of the *idle* state and its analytical expression is derived in Subsection 3.4.4. The T_f and T_s represent the expected time durations of the *fail* and *success* states, respectively. The expected time durations T_1 and T_2 correspond to the elapsed times from the first access attempt until the end of the contention resolution timer in case of access failure, and until the reception of the connection response message in case of successful access, respectively. It is worth noting that for given random access/barring parameters $(L, B, W, q_{0,m}, b_{\text{th}})$ and known IED traffic characteristics $(p_{\text{on}}, T_{\text{off}})$, the expressions of the preamble collision probability $p_{c,m}$ in Eq. (3.33) and the probability τ of attempting a random access in Eq. (3.34) form a system of non-linear equations that can be solved via an iterative numerical method, as shown in Algorithm 2. Therefore, by plugging the obtained value of $p_{c,m}$ in Eq. (3.31), the value of R_m can be calculated.

Since the expression of R_m is not in closed-form, finding the optimal cell radius r_m that maximizes the achieved reliability is mathematically intractable. Therefore, we propose a heuristic interference- and traffic load-aware mechanism that determines the cell sizes in a generic heterogeneous cell deployment for the reliable support of event-driven IED. We provide the details in the following.

Proposed Cell Planning and ZC Root Sequence Allocation

We assume that the mobile network operator is aware of the number of cells C_{A} required to provide full coverage in a geographical area A and specifies a range of supported radii $[r_{\min}, r_{\max}]$ for a heterogeneous cell deployment. Initially, a random radius is uniformly selected for each cell. Our proposed cell planning mechanism employs a spatial ZC root sequence allocation scheme where the ZC root sequences selected by each cell are spatially-separated and can only be reused by cells located at a distance larger than the preamble-decoding distance $d_{\max}$. In this way, the allocation of the same root sequences in neighboring cells is avoided and the resulting inter-cell interference decreases since the

Algorithm 3 Cell planning and ZC root sequence allocation.

1: Assume $L, B, W, q_{0,m}, b_{\text{th}}, p_{\text{on}}, T_{\text{off}}, R_{\text{th}}$ known
2: Initialize $l \leftarrow 0$ iteration index
3: Pick cell m with max. number of neighbors and set $r_m^{(0)} \leftarrow r_{\max}$
4: Determine $N_{s,m}^{(0)}$ from Eqs. (3.26)–(3.28)
5: Reuse $N_{s,m}^{(0)}$ only beyond $d_{\max}$ ▷ Interference-aware
6: Calculate $p_{c,m}^{(0)}$ and $\tau^{(0)}$ using Algorithm 2
7: Calculate $R_m^{(0)}$ from Eq. (3.31)
8: **while** $R_m^{(l)} < R_{\text{th}}$ **do** ▷ Main iteration
9: $l \leftarrow l + 1$
10: Decrease $r_m^{(l)}$
11: Repeat steps 4-7 and update $N_{s,m}^{(l)}, p_{c,m}^{(l)}, \tau^{(l)}, R_m^{(l)}$
12: **if** $R_m^{(l)} < R_m^{(l-1)}$ || $r_m^{(l)} < r_{\min}$ **then**
13: Set $r_m^{(l)} \leftarrow r_m^{(l-1)}$
14: Update $N_{s,m}^{(l)}$
15: **do**
16: Set $b_{\text{th}} \leftarrow b_{\text{th}} - 0.01$ ▷ Traffic load-aware
17: Update $p_{c,m}^{(l)}$ and $\tau^{(l)}$ using Algorithm 2
18: Calculate $R_m^{(l)}$ from Eq. (3.31)
19: **while** $R_m^{(l)} < R_{\text{th}}$
20: **end if**
21: **end while**
22: Repeat for neighboring cell with max. number of neighbors

power falloff with the distance is exploited. In addition, the mechanism dynamically modifies the ACB rate, b_{th}, to relieve congestion and prevent access failures. The steps of the mechanism are presented in Algorithm 3.

Starting from the cell m with the higher number of neighboring cells, the maximum available radius $r_{\max}$ is selected. Using Eqs. (3.26)–(3.28), $N_{s,m}$ is calculated and the minimum reuse distance of the selected ZC root sequences is determined by $d_{\max}$. Based on the iterative method described in Algorithm 2, the preamble collision probability $p_{c,m}$ is obtained and the value of R_m can thus be calculated using Eq. (3.31). The mechanism keeps decreasing the cell radius and appropriately updates the ZC root sequence selection until the achieved reliability surpasses a predefined threshold R_{th} that depends on the particular distribution automation application. In case the updated reliability value is lower than in the previous iteration due to increased inter-cell interference or the minimum available radius is reached, a traffic-aware scheme is employed where the ACB rate, b_{th}, is set to a more restrictive value in order to disperse the access attempts in time. In this way, the congestion is reduced and preamble collision probability decreases resulting in an improved reliability value. The dynamic configuration of the b_{th} ends when R_{th} is satisfied. The value of b_{th} is assumed to be periodically broadcast by the eNodeB to the IEDs of each cell, as part of the system information block message in the physical downlink broadcast channel. Once the cell radius and the root allocation for the cell m is completed, all the relevant parameters are updated and the mechanism iteratively proceeds to the neighboring cell with the higher number of neighbors until all cells are processed.

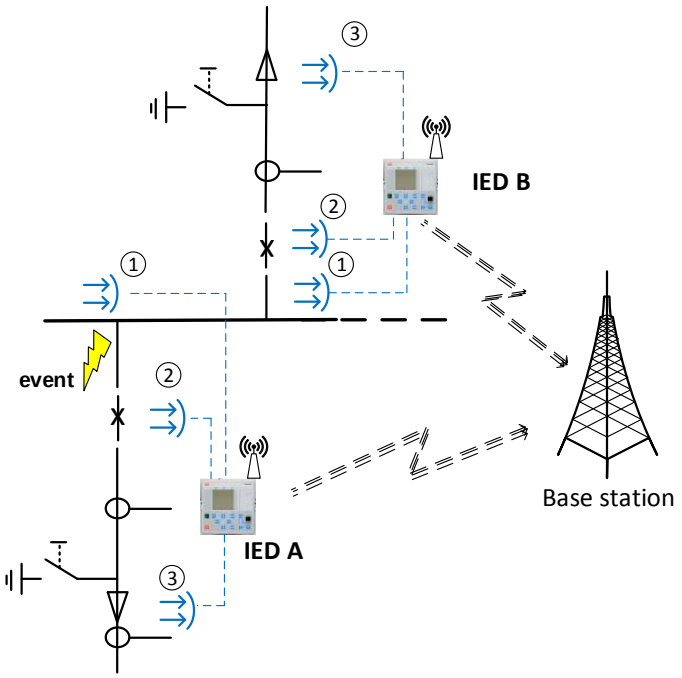

Figure 3.21: Network model for a cellular-enabled substation automation system where arc-fault detection is performed. Each IED is equipped with sensors for detecting possible arc faults appearing in the busbar, circuit-breaker feeder and cable termination compartments. Traffic is generated in bursts and sequentially triggers the transmission of alarm messages in neighboring IEDs.

In the following subsection, we derive the analytical expression for the traffic generation probability, p_{on}, based on a realistic traffic model selected to capture the spatiotemporal correlation of IED communication in certain substation automation scenarios. The value of p_{on} is required for the calculation of the reliability, as shown in Algorithms 2 and 3.

3.4.4 Traffic Model

Power grids are often vulnerable to cascade component failures which can lead to the isolation of a large number of grid segments causing consumer interruptions or even the collapse of the entire power system. In substation automation scenarios characterized by a cascade of component outages, the IED communication often involves the transmission of highly space- and time-correlated messages. The network architecture of such a substation automation system is illustrated in Figure 3.21. As shown in the figure, in the case of an arc-fault detection in substation automation systems [1], a cascading power fault affects neighboring segments in the grid and triggers the transmission of notification alarm messages among geographically-adjacent protection devices. To model this traffic behavior, similar to the monitoring traffic analysis detailed in Subsection 3.3.2, we assume that the arrivals in each IED are governed by two application phases; a *regular* phase when

no event occurs and an *event* phase where the interarrival time is shortened to ensure a timely message-delivery in case of an event (burst).

Let $\mathcal{S}_i$ be the set of sensors that an IED i is equipped with and let $\mathcal{U}_i$ be the set of its neighboring devices. Let also $\alpha_{i,s}[t]$ be a binary parameter that indicates whether sensor s of an IED i captures a local event at time t. Then, the spatiotemporal correlation in the arrival stream of an IED i can be captured with the aid of the parameter $\beta_i[t]$,

$$\beta_i[t] = \begin{cases} 1, & \text{if } \sum_{s\in\mathcal{S}_i} \alpha_{i,s}[t] > 0\,, \\ 1, & \text{if } \sum_{j\in\mathcal{U}_i} \sum_{s\in\mathcal{S}_j} \alpha_{j,s}[t] > 0\,, \\ 0, & \text{otherwise,} \end{cases} \tag{3.35}$$

where an arrival in an IED i may be triggered due to a detection of a local event either by one of its own sensors or by one of the sensors of its neighboring IEDs.

In order to capture the interdependent and non-exponential interarrival times of an IED, we leverage a two-state MAP framework to properly characterize the traffic stream. The MAP constitutes a stochastic counting process that is able to represent time correlation in the arrival streams and provide analytical tractability. The essential difference with the MMPP[12], which constitutes a subclass of the MAP used in Subsection 3.3.2, is whether or not the IED application phase is potentially changed just after an arrival. Recall that $\mathbf{D}_1$ in Eq. (3.16) is a diagonal matrix, i.e., all inter-state transitions are accompanied by no arrivals, and all arrivals are assumed to be caused only by self-state transitions. On the other hand, MAP provides a more generic framework where an arrival may result in a state change which is the case of local cascade failures in substation automation systems.

The arrival rate of the MAP is governed by a continuous-time Markov chain [143]. The states of the Markov chain correspond to the IED application phases and a transition between states generates an arrival with a given probability. To account for the spatial and temporal correlation in the arrival stream of an IED i, the convex combination of the infinitesimal generator matrices, $\mathbf{D}_0$ and $\mathbf{D}_1$, in the regular and event phase is considered with the aid of the parameter $\beta_i[t]$, as in [144]. Therefore, MAP is characterized by the rate matrices $\{\mathbf{D}_0', \mathbf{D}_1'\}$ where

$$\mathbf{D}_0' = (1 - \beta_{\mathrm{i}}[t])\,\mathbf{D}_{0,\text{ regular}} + \beta_{\mathrm{i}}[t]\,\mathbf{D}_{0,\text{ event}}, \tag{3.36a}$$

$$\mathbf{D}_1' = (1 - \beta_{\mathrm{i}}[t])\,\mathbf{D}_{1,\text{ regular}} + \beta_{\mathrm{i}}[t]\,\mathbf{D}_{1,\text{ event}}. \tag{3.36b}$$

Following the same procedure as in Subsection 3.3.2, for the calculation of the traffic generation probability, p_{on}, let

$$P_{i,j}(k,t) = \Pr(N_t = k, J_t = j | N_0 = 0, J_0 = i)\,, \tag{3.37}$$

be the entry of a matrix $\mathbf{P}(k,t)$, where N_t denotes the number of arrivals during the time interval $[0,t)$ and J_t the phase of the Markov process at time t, respectively. The matrices

[12] Although the MMPP model allows higher precision than aggregated traffic models used in related work, it uses a Poisson process for source modeling that significantly reduces the flexibility of the model.

$\mathbf{P}(k,t)$ satisfy the forward Chapman-Kolmogorov equations [130]

$$\frac{d}{dt}\mathbf{P}(0,t) = \mathbf{P}(0,t)\,\mathbf{D}_0', \tag{3.38a}$$

$$\frac{d}{dt}\mathbf{P}(k,t) = \mathbf{P}(k,t)\,\mathbf{D}_0' + \mathbf{P}(k-1,t)\,\mathbf{D}_1',\ k = 1,\ldots, \tag{3.38b}$$

and using the initial condition $\mathbf{P}(0,0)$=$\mathbf{I}$, $\mathbf{P}(k,t)$ can be determined. Then, p_{on} is calculated as

$$p_{\text{on}} = 1 - \sum_i \sum_j P_{i,j}(0,t)\,, \tag{3.39}$$

where t corresponds to the duration of the LTE subframe (1ms). For the calculation of the average holding time of the *idle* state, T_{off} in Eq. (3.34), we follow a similar procedure as in Subsection 3.3.2. If $\boldsymbol{\pi}$ denotes the stationary probability vector, then from the analysis of the time-stationary MAP, it holds $T_{\text{off}} = [\boldsymbol{\pi}\mathbf{D}_1\mathbf{e}]^{-1}$, where $\mathbf{e}$ represents a unit column vector.

In the following subsection, a performance assessment of our proposed mechanism is presented in terms of achieved reliability.

3.4.5 Numerical Results

To evaluate the performance of our proposed cell planning and ZC root sequence allocation mechanism, we consider a realistic scenario of power distribution automation where a high number of IEDs are uniformly deployed within a geographical area A. The IEDs are equipped with communication interfaces and generate event-based multicast traffic based on their input from voltage and current transformers/sensors. The random dropping model is used for the location of the IED transmitters whereas the location of a neighboring IED receiver is distributed according to a uniform distribution in a circular area around its associated IED transmitter. The MAP framework is used to capture the spatiotemporal correlation of the event-driven IED traffic and the well-studied expectation-maximization statistical framework [130] has been used for parameter $\{\mathbf{D}_0', \mathbf{D}_1'\}$ fitting, based on the arrival traces of power automation traffic captured by a discrete-event simulator that implements the IEC-61850 GOOSE protocol [5, 133]. The expectation-maximization algorithm constitutes an iterative method for the maximum-likelihood estimation of the MAP parameters and is particularly useful for stochastic models that involve many parameters [143].

Table 3.5 summarizes the basic parameters used in our simulations. A regular cell deployment is considered to provide coverage and the unsynchronized IEDs are assumed to contend for RACH access after a cascading power failure that affects the area A. An ACB scheme enhances the standard RACH procedure as an additional overload-control mechanism. Starting from a low-load scenario, new access requests generated by IEDs affected by the cascading events, appear progressively in the system until it is driven to overload. The contention-based RACH/ACB performance is then evaluated in terms of reliability when the system operates close to its capacity limits. In particular, a comparative evaluation study of the achieved reliability R_m is performed among the following network deployment options:

Table 3.5: Simulation parameters.

Parameter	**Value**
Preambles for contention-based access K	64
Coverage area A	100km×100km
Range of cell radii $[r_{\min}, r_{\max}]$	[100m, 100km]
Transmit power	24dBm
Thermal noise power	-114dBm
Required preamble signal energy to noise ratio	18dB
Channel model	Suburban
Path loss coefficient	3.5
RACH configuration index	14
Barring/access backoff window sizes B, W	20ms
Default barring rate b_{th}	0.5
Reliability threshold R_{th}	0.6
Preamble duration	1ms
Max. allowed preamble transmission attempts L	10
RAR window size	5ms
Contention resolution timer	24ms
Master information block periodicity	40ms
Time durations T_1, T_2, T_s, T_f (in ms)	{32, 16, 20, 1}

1. A single macro-cell deployment is used to provide coverage to the IEDs.

2. A default (traffic-unaware) heterogeneous deployment of multiple smaller cells with radii uniformly selected from the range $[r_{\min}, r_{\max}]$ and ZC root sequences randomly chosen among a set of N_{RS} available roots in total.

3. A heterogeneous cell deployment based on our proposed mechanism where each cell radius is properly determined from $[r_{\min}, r_{\max}]$ to provide reliability guarantees for the IED traffic, according to the interference-aware ZC root sequence allocation and the load-aware barring rate configuration, as described in Algorithm 3.

Figure 3.22 illustrates the achieved reliability R_m per IED of a random cell m with increasing network traffic load. It can be observed that in the case of a single macro-cell deployment, the reliability level rapidly decreases with increasing traffic load, as the intra-cell interference becomes higher due to the orthogonality loss of the received preambles generated by different ZC root sequences. On the other hand, for a default heterogeneous deployment of multiple smaller cells, the intra-cell interference is reduced due to the larger number of orthogonal preambles which leads to better preamble detection performance; however, since no reliability provisioning is considered for the cell size and the ZC root sequence allocation, this improvement comes at the expense of increased inter-cell interference, especially when the number of cells required to provide coverage increases, as shown in Figure 3.22. Therefore, the reliability gains for the default approaches remain limited. Instead, in the case when our proposed mechanism is applied, reliability remains in higher levels even in the high traffic load regime. In particular, it can be observed that our proposed scheme significantly outperforms the reliability attained with a single

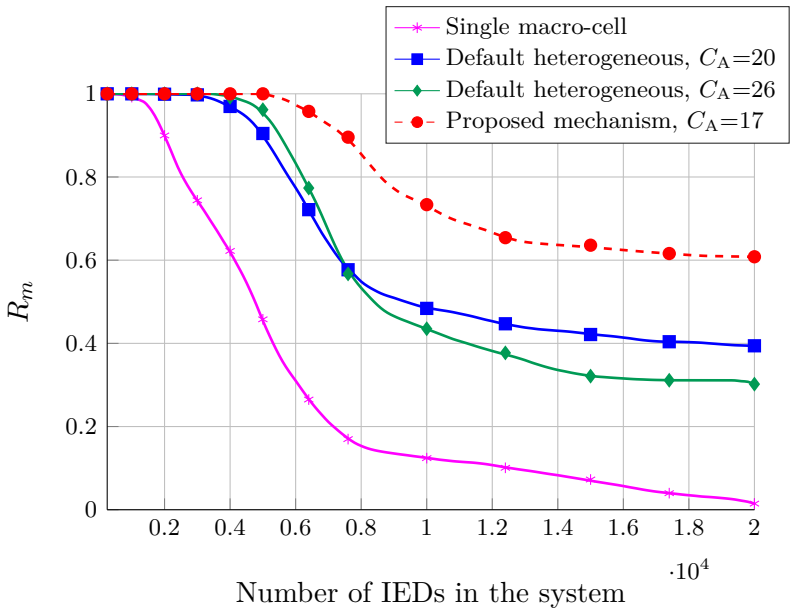

Figure 3.22: Reliability achieved per IED for different cell-network deployments and ZC root sequence allocation schemes.

macro-cell, and achieves reliability gains by almost a factor of 1.5-2 with respect to the default heterogeneous deployments. The proper selection of the cell sizes and the spatial separation of the available ZC root sequences reduces the inter-cell interference since the allocation of the same roots among neighboring cells becomes less probable. In addition, the dynamic configuration of the ACB rate b_{th} provides reliability guarantees and relieves network congestion in high traffic load conditions. It is also important to point out that, with our proposed cell planning mechanism, a lower number of deployed cells is required to achieve the same reliability level as in the default cell-configuration case, which eventually leads to lower installation costs for the network operator.

3.4.6 Summary

The relation between the LTE cell radius and the number of available orthogonal preambles reveals an important limitation for cells with large radius due to the non-orthogonality of preambles generated by multiple ZC root sequences. On the other hand, root sequence allocation needs to be properly performed among smaller cells to minimize inter-cell interference in the preamble reception. According to these limitations, in this section of the thesis, we introduced an interference- and load-aware cell planning mechanism to provide reliable channel access for a high density of IEDs. Our proposed scheme aims to minimize the inter-cell interference through a proper allocation of the ZC roots among neighboring cells while regulating the substation automation traffic via an adaptive ACB mechanism. In addition, a realistic traffic model was proposed to accurately capture the spatiotemporal correlation of event-driven IED traffic in substation automation scenarios. The numerical evaluation of our mechanism demonstrates its superiority in terms of reliability with respect to benchmarking deployment schemes and useful insights can

be drawn for the network planning of such cellular systems.

In the final section of Chapter 3, we leverage the performed analysis to quantify the impact of the LTE RACH reliability on the accuracy of the power system state estimation in wide-area monitoring systems.

3.5 Impact of Random Access Channel Reliability on Power System State Estimation

3.5.1 Introduction

With the envisioned large-scale integration of DERs into the power system, the demand for timely and reliable network quality monitoring, control, and fault analysis is rapidly growing. In this context, power system state estimation defined as the determination of the system state variables, i.e., voltage magnitude and angles, at all the buses of the power network from a set of remotely-acquired measurements, becomes a cornerstone for the monitoring of the power grid. In particular, state estimation constitutes a key function in supervisory control and planning of power grids as it contributes to a quasi-real-time analysis of the grid behavior [3]. The increasing use of PMUs, capable of providing synchronized measurements, is expected to enhance the state estimation accuracy and improve the situational awareness of the power system. PMU devices are normally installed at sensitive locations of the grid, e.g., buses and feeders, and their main functionality is to gather data in real-time and communicate them to a local phasor data concentrator. The PMU data consist of the local measured amplitude and phase angles of voltage and current waveforms sampled at the same time instant using Global Positioning System (GPS) signaling. In addition, based on the measured amplitudes and phase angles, a PMU can estimate the frequency and its change rate and include this information in the transmitted data.

In order to exploit the PMUs as inputs for an efficient state estimation solution, a reliable and scalable underlying communication technology is required to support reliable PMU data exchange in different parts of the grid in future wide-area monitoring systems. However, the effect of communication constraints on power system state estimation has not been thoroughly addressed in existing literature. In this section of Chapter 3, we investigate the impact of the LTE RACH reliability on the PMU information acquisition in cellular-enabled monitoring systems and, consequently, on the state estimation accuracy. As the emerging monitoring systems are expected to expand over large geographical areas, a shared LTE network needs to accommodate the channel access attempts originated from a large number of measurement devices ranging from PMUs to massive-scale smart meter infrastructure. The concurrent transmission attempts originated from a large number of devices results in a high probability of collision in the transmission of the preambles due to the limited random access opportunities compared to the increased resource demand. Besides the scalability problem, as detailed in Section 3.4, the radius of an LTE cell is related to the number of orthogonal preambles available for contention in RACH. This imposes an additional challenge for the reliable PMU data exchange in wide-area monitoring deployments since the non-orthogonality between preambles generated from different root sequences results in decoding failures at the base station [8].

Unlike the majority of existing literature where communication constraints are either

absent [145], [146] or limitedly considered [147] in power system functionalities, we hereby present a numerical study on the impact of communication reliability deficiencies on state estimation quality. In particular, we evaluate the effect of the achieved LTE RACH reliability levels on the transmitted PMU measurements and, consequently, on the accuracy of the state estimation algorithm under different traffic and network configurations. To this end, we consider two representative network deployment scenarios, namely *i*) a shared LTE network, where PMUs contend for the shared channel access resources along with a high number of smart metering devices present in the system, and *ii*) a dedicated LTE network, where the selected range of an LTE cell that provides coverage solely to PMUs, determines the availability of the orthogonal random access preambles. In both cases, we demonstrate that the state estimation accuracy critically depends on the achieved RACH reliability levels for PMU communication. Therefore, useful design insights can be drawn for state estimation schemes when the problem of estimation is coupled with the reliability challenges in information acquisition.

3.5.2 State Estimation System Model

We consider a power system which spans over a specific geographical area. This electrical network is supervised by a control center which has the responsibility to perform control and protection actions based on the monitoring of the network state. The latter hinges on the reliable data acquisition from remote endpoints that are assumed to record the system footprint at a specific time instant. We assume that the power system is composed of N_{B} buses represented by the graph $\mathcal{G} = (\mathcal{V}_{\mathrm{B}}, \mathcal{E}_{\mathrm{B}})$, where $\mathcal{V}_{\mathrm{B}}$ denotes the set of buses with cardinality $|\mathcal{V}_{\mathrm{B}}| = N_{\mathrm{B}}$; and $\mathcal{E}_{\mathrm{B}}$ stands for the set of edges that describes their interconnections (branches), with cardinality $|\mathcal{E}_{\mathrm{B}}|$. The complex current injections at the buses, i.e., $\mathbf{i} = [I_1, \ldots, I_{N_{\mathrm{B}}}]^T$, satisfy $\mathbf{i} = \mathbf{Yv}$, where $\mathbf{Y} \in \mathbb{C}^{N_{\mathrm{B}} \times N_{\mathrm{B}}}$is the nodal admittance matrix [145] and $\mathbf{v} = [V_1, \ldots, V_{N_{\mathrm{B}}}]^T \in \mathbb{C}^{N_{\mathrm{B}}}$ stands for the complex voltages of measurements at selected buses and branches. Power system state estimation aims to determine the complex voltages at all the buses of the system from a number of measured variables in selected buses and branches, as illustrated in Figure 3.23. In what follows, we define the Cartesian representation of the system state, as $\mathbf{x} = [\Re\{V_1\}, \Im\{V_1\}, \ldots, \Re\{V_{N_{\mathrm{B}}}\}, \Im\{V_{N_{\mathrm{B}}}\}]^T \in \mathbb{R}^{2N_{\mathrm{B}}}$. Hence, the measurement model can be defined as

$$\mathbf{z} = \mathbf{h}(\mathbf{x}) + \mathbf{e}\,, \tag{3.40}$$

where $\mathbf{z} \in \mathbb{R}^M$ stands for the corresponding measurement vector, $\mathbf{h}(\mathbf{x})$ denotes a nonlinear function of $\mathbf{z}$ on $\mathbf{x}$ in compliance with the AC power flow model and $\mathbf{e} \in \mathbb{R}^M$ stands for zero-mean Gaussian noise with known covariance matrix $\mathbf{R_e}$. It is worth noting that, typically, we have $M >> 2N_{\mathrm{B}}$. According to Eq. (3.40), the conventional state estimator is given by the solution to the following non-convex optimization problem

$$\hat{\mathbf{x}} = \arg\min_{\{\mathbf{x}\}} \frac{1}{2} \left\| \mathbf{z} - \mathbf{h}(\mathbf{x}) \right\|_2^2 . \tag{3.41}$$

Traditionally, problem (3.41) is solved via gradient-based schemes [148]. Other efficient solutions based on convex relaxations [149, 150] and graphical models have been also

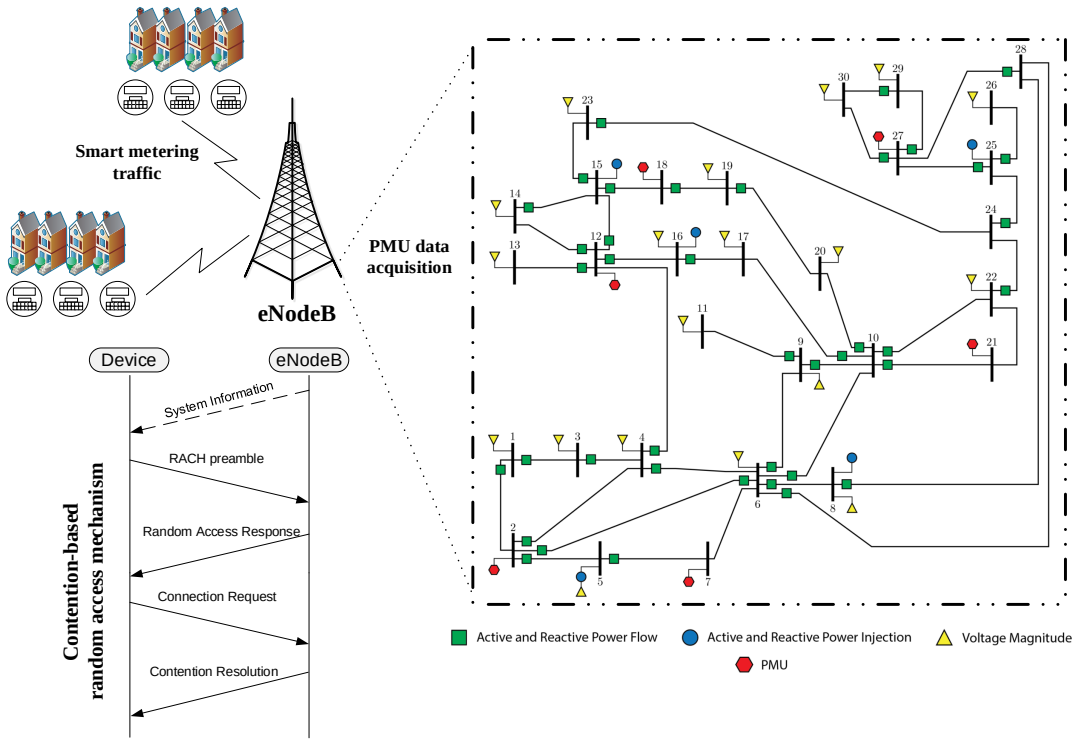

Figure 3.23: The IEEE 30 bus test case including possible measurement devices in specific buses and branches. Cellular communication via the installation of LTE base stations is provided where the PMUs may contend for the shared channel access resources with smart metering devices.

proposed during the latest years [151]. As discussed before, a crucial element in order to improve the monitoring quality of the system is the phasor technology. The deployment of the PMUs, providing linear measurement functions, can significantly improve the accuracy of the state estimation via precise and synchronized measurements. In this case, the following linear model holds

$$\mathbf{z} = \mathbf{H}\mathbf{x} + \mathbf{w}\,, \tag{3.42}$$

and, hence, state estimation becomes a convex (least-squares) optimization problem

$$\hat{\mathbf{x}} = \arg\min_{\{\mathbf{x}\}} \frac{1}{2} \|\mathbf{z} - \mathbf{H}\mathbf{x}\|_2^2\,, \tag{3.43}$$

where $\mathbf{H} \in \mathbb{R}^{M \times 2N_{\mathrm{B}}}$ stands for the corresponding measurement matrix, and $\mathbf{w}$ denotes zero-mean Gaussian noise with known covariance matrix $\mathbf{R}_{\mathbf{w}}$. When $\mathbf{H}$ is full-rank, i.e., observability via PMUs is achieved [148], the least-squares problem has the unique solution $\hat{\mathbf{x}} = (\mathbf{H}^T\mathbf{H})^{-1}\mathbf{H}^T\mathbf{z}$.

However, problem (3.43) refers to the ideal case where $\mathbf{z}$ includes a full measurement set corrupted only with *i.i.d.* Gaussian noise with low standard deviation. In a more realistic scenario, the efficient and timely PMU data transmission relies on the reliability of

the respective communication technology that each power utility leverages. The convergence to a correct state estimate highly depends on link failures commonly encountered in communication networks. However, the time-synchronized nature of PMU access attempts along with the massive presence of smart meters in a shared LTE network, renders the LTE RACH mechanism highly susceptible to congestion and may compromise the required reliability levels for accurate state estimation. Based on the reliability framework for the contention-based RACH procedure developed in Sections 3.3 and 3.4, we incorporate the imperfect PMU data exchange in LTE-based systems as a consideration for the accuracy of the transmitted measurements. In particular, we use the expression of the preamble collision probability in Eq. (3.33) to determine the achieved reliability per PMU as a function of *i*) the number of contending devices in the system and *ii*) the number of orthogonal preambles per ZC root sequence which in turn depends on the selected cell coverage range.

In the following subsection, we quantify the impact of the achieved reliability levels per contending PMU on the accuracy of a state estimation algorithm in LTE-based wide-area monitoring systems.

3.5.3 Numerical Results

In order to study how RACH reliability affects the state estimation performance, we consider realistic network scenarios where PMUs, equipped with LTE communication interfaces, reside within the coverage of a single LTE cell. The PMUs provide direct measurements of voltage and current phasors collected over multiple substation local area networks to provide situational awareness of the power system state. A simple periodic traffic model has been used to generate the time-synchronized RACH attempts of the PMUs. Table 3.6 summarizes the basic network parameters used in our simulations.

The state estimation performance has been assessed via computer simulations, solving the optimization problem in (3.43). We have considered both the IEEE 30 and 118 bus test cases where we have guaranteed system observability with PMUs according to the number and location of devices proposed in [152]. We conduct Monte Carlo experiments to build some statistics of our state estimation algorithm performance. In particular, 500 random measurement sets have been generated and the values have been corrupted with additive white Gaussian noise of standard deviation $\sigma = 10^{-4}$. The estimation accuracy is given in terms of normalized[13] error, i.e., $\|\hat{\mathbf{x}} - \mathbf{x}\|_2 / 2N_{\mathrm{B}}$, where $\hat{\mathbf{x}}$ denotes the estimated power system state and $\mathbf{x}$ the actual one, averaged over realizations. For power flow simulations we have used Matpower [153].

In order to independently quantify the impact of the *i*) the number of contending devices in an LTE cell and *ii*) the selected cell coverage range on the achieved state estimation accuracy, we consider the following scenarios:

1. *Shared* LTE network, where a large number of smart metering devices generate background traffic within the coverage area of the base station and compete with the PMUs for the available RACH preambles. Such scenarios would arise in practice, if public LTE infrastructure was shared by smart metering deployments and grid

[13]Notice that the error is normalized to the number of elements in the state vector and, hence, it is independent of the number of buses in the electrical network.

Table 3.6: Simulation parameters.

Parameter	Value
Preambles for contention-based access K	64
Transmit power	24dBm
Thermal noise power	-114dBm
Required preamble signal energy to noise ratio	18dB
Channel model	Suburban
Path loss coefficient	3.5
RACH configuration index	14
Barring/access backoff window sizes B, W	20ms
Barring rate factor	0.5
Preamble duration	1ms
Max. allowed preamble transmission attempts L	10
Contention resolution timer	24ms
Time durations T_1, T_2, T_s, T_f (in ms)	{32, 16, 20, 1}

monitoring equipment. Given a cell coverage range, we quantify the degradation of the achieved reliability and state estimation accuracy when an increasing number of smart meters is generating channel access requests.

2. *Dedicated* LTE network, where only PMU traffic is accommodated in the system. This scenario corresponds to the use case when a utility-dedicated communications infrastructure is deployed by the mobile network operator. In this case, our interest is focused on how the state estimation accuracy performance evolves for different cell coverage range. As discussed in Subsection 3.4.3 and shown in Eq. (3.31), the cell radius is related with the number of orthogonal preambles and, in turn, affects the achieved reliability per PMU.

In both scenarios, whenever a RACH attempt for a synchrophasor measurement fails, after exceeding the maximum number of retransmissions, it is replaced by a pseudo-measurement with higher standard deviation, i.e., $\sigma = 10^{-1}$ or $\sigma = 5 \cdot 10^{-1}$, in the measurement vector $\mathbf{z}$.

Shared LTE network

Figure 3.24 illustrates the reliability per PMU with increasing number of smart meters coexisting as background traffic in the shared LTE network. In particular, starting from a medium-load scenario, new access requests from smart meters appear progressively in the system until it is driven to overload. The contention-based RACH performance is then evaluated in terms of reliability when the system operates close to its capacity limits. It can be observed that as the number of contending smart meters increases, the reliability experienced per PMU decreases due to the heavier contention in RACH. It is also noted that reliability performance further deteriorates when a higher number of PMUs is considered.

Based on the reliability levels attained with increasing smart metering traffic load and PMUs, we evaluate the error performance of the state estimation algorithm in Figure 3.25.

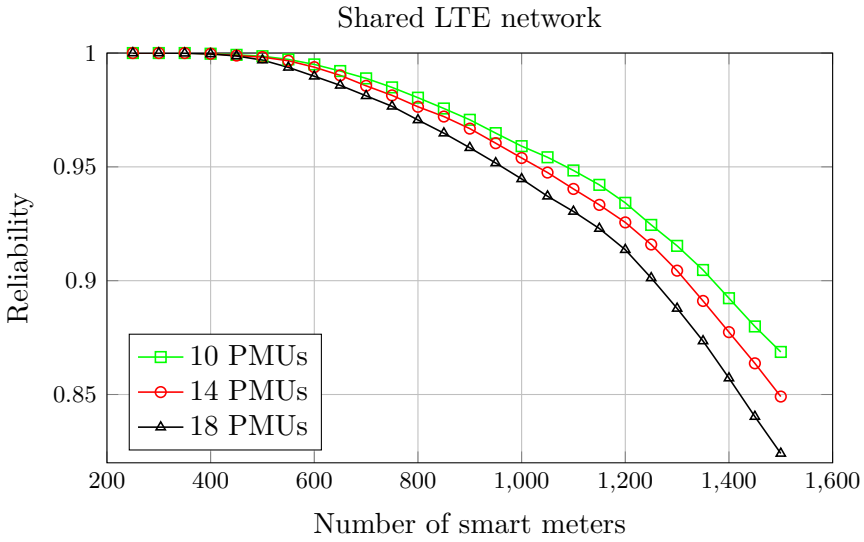

Figure 3.24: Reliability experienced per PMU with increasing number of smart meters generating background traffic.

In particular, as the figure reveals, the lower PMU reliability figures achieved due to the increasing number of smart meters, leads the state estimation algorithm to performance degradation. However, it can be observed that the state estimation accuracy improves when a higher number of PMU devices is considered. Although increasing the PMUs leads to heavier contention and slightly-degraded reliability, as shown in Figure 3.24, the benefits in estimation accuracy are higher when the number of PMUs increases. The additional PMUs not only help reduce the state estimation uncertainty but also desensitize the estimation error to the effect of the lower communication reliability caused by the increased background traffic. Moreover, as expected, the choice of the standard deviation value for the pseudo-measurements has significant impact on the state estimation performance.

Dedicated LTE network

The reliability per PMU with increasing cell coverage range is illustrated in Figure 3.26. As the cell radius increases, the number of available orthogonal preambles decreases and thus more ZC root sequences are required to generate the total number of 64 random access preambles. In turn, this results in a degradation of the reliability performance due to the orthogonality loss for preambles generated from different roots. In addition, as shown in Table 3.7, when the cell coverage increases, the minimum number of PMUs required to provide full observability of each power subsystem increases, resulting in a degradation of the achieved reliability since additional contending devices are requesting network access.

Based on the reliability levels achieved with increasing cell coverage range, we evaluate the error performance of the state estimation algorithm in Figure 3.26. In particular, five different power systems have been considered for assessment where each cell coverage rage corresponds to a respective subsystem of the IEEE 118 bus test case. For instance, as

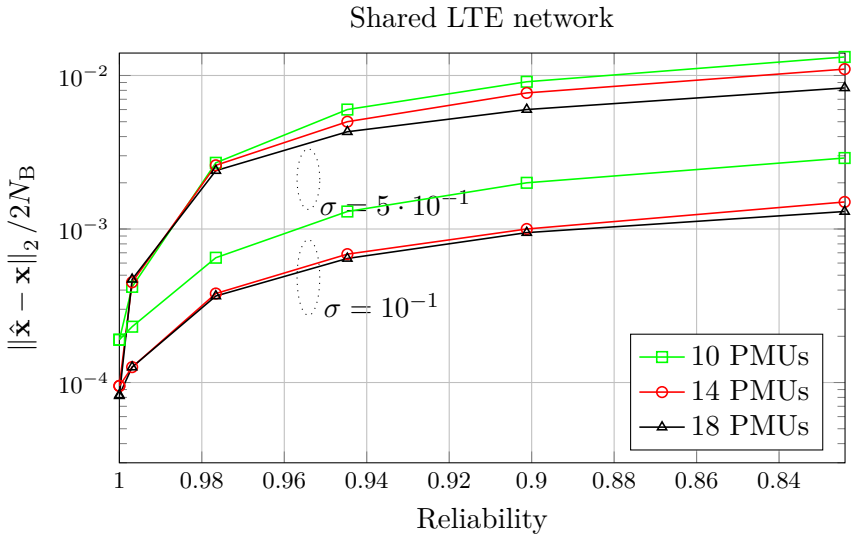

Figure 3.25: Normalized error associated to the estimated state vector with respect to reliability achieved for varying smart metering traffic load.

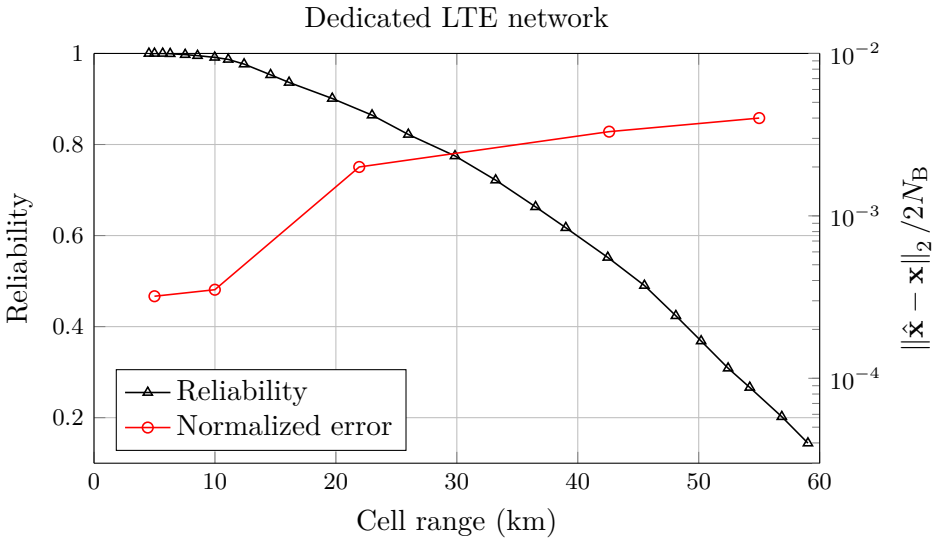

Figure 3.26: Reliability experienced per PMU (y-axis on the left) and normalized error associated to the estimated state vector (y-axis on the right) for varying cell coverage range.

illustrated in Table 3.7, the first coverage range under concern corresponds to a 15-bus subsystem of the original network while the last one represents the whole system. Consequently, each case-subsystem includes a higher number of buses and accordingly PMUs. The red curve in Figure 3.26 depicts that the estimation error increases with increasing cell radius. In stark contrast with the previous scenario, it is worth noting that the respective increased number of PMUs included in the larger coverage, does not improve the state estimation accuracy. As indicated in Figure 3.26, the PMU reliability severely

Table 3.7: Reliability and state estimation performance for varying cell coverage range.

Subsystem of interest	No. of buses in subsystem	Cell range (km)	Orthogonal preambles	PMUs	Reliability	Normalized error
1	15	4.54	22	9	1	3.2×10^{-4}
2	41	9.98	11	24	0.9914	3.51×10^{-4}
3	72	22.99	5	30	0.8645	2×10^{-3}
4	98	45.51	3	39	0.4903	3.3×10^{-3}
5	118	59.03	2	48	0.1441	4×10^{-3}

degrades with the increasing cell radius, leading to a state estimation performance degradation that cannot be counterbalanced by the higher number of available synchronized measurements. It can thus be inferred that network planning and cell size dimensioning need to be carefully configured by the operator in order to exploit the accuracy gains of PMUs' installation.

3.5.4 Summary

The utilization of PMUs in the monitoring, protection and control of power systems has become increasingly important in recent years. As such, the communication reliability for these critical measurements nodes becomes a significant issue. In the final section of Chapter 3, the impact of the RACH reliability on the state estimation performance in LTE-based monitoring systems was investigated. Unlike existing literature where the reliability limitations imposed by the underlying communication technology are decoupled from the state estimation problem, we demonstrated how the number of contending devices and the cell coverage range critically affect the state estimation accuracy in LTE-based monitoring systems. The numerical evaluation of realistic network scenarios that involve acquisition of PMU information using LTE systems reveals that reliability constraints introduce significant state estimation accuracy limitations. The consideration of imperfect communication can thus provide useful insights for the design of reliability-aware power system state estimators for wide-area monitoring systems.

Future work aims to enhance the presented study by considering the optimal PMU placement problem under communication reliability constraints. In particular, we aim to determine the minimum number of PMUs along with their optimal locations while ensuring *i*) full observability of the power system and *ii*) acceptable reliability levels due to the varying wireless channel conditions. In addition, a potential extension of the present feasibility study would consider a multi-area state estimation scenario where a multiple-cell LTE heterogeneous network deployment would provide the required coverage.

Chapter 4

Resource Scheduling for Smart Grid and Human-Type Traffic

Chapter 4 deals with the RRM problem for the seamless integration of smart grid data transmissions in shared LTE-based networks. In Section 4.1, a novel scheduler is introduced for the support of IEC-61850 automation services with stringent communication requirements. Radio resources are allocated in a way that keeps the degradation of cellular users at a minimum level while achieving low latency performance for real-time distribution automation services. Section 4.2 investigates the benefits of a dynamic switch to direct D2D transmission for event-based IED communication in substation automation scenarios. A joint mode selection and resource allocation mechanism is developed, resulting in higher data rates with respect to the conventional cellular transmission in overload conditions. The orthogonal resource partition between cellular and D2D links is performed in a way that prevents the underutilization of the scarce cellular spectrum. We provide the details in the following.

4.1 Scheduler Design for IEC-61850 Communication Services

4.1.1 Introduction

In this section of Chapter 4, we develop an adaptive LTE data scheduling and resource allocation scheme for the integration of IEC-61850 MMS and GOOSE communication services associated with substation automation operations. Since standard LTE cannot meet the stringent latency requirements of such services, a new LTE QoS class is introduced along with a new scheduling policy that prioritizes automation traffic with respect to background human-centric traffic. We focus on two representative grid automation services, namely *i*) centralized client-server scenarios, where IEDs periodically report measurements to a remote controller, according to IEC-61850 MMS protocol, and *ii*) distributed event-driven peer-to-peer communications among IEDs, according to IEC-61850 GOOSE protocol. The achievable latency and throughput performance is evaluated on a radio system simulator platform. Simulations of realistic overload scenarios demonstrate that properly designed LTE schedulers can successfully meet the performance requirements of

IEC-61850 services with almost negligible impact on background traffic.

A variety of communication technologies have been proposed for data transmission in distribution automation services. In [21], the applicability of WiFi for intra-substation communication is studied. However, its relatively short range is not adequate for inter-substation communication between IEDs located in remote areas. Existing LTE implementations have difficulties to meet the energy automation requirements in data transmission mainly due to the limited number of different services and QoS levels that they support [31]. We address this issue by prioritizing energy data flows over conventional LTE traffic in network-overload scenarios. In this context, the role of scheduler is significant to resolve the contention. In static allocation schemes [110], no resource contention is taking place; however, such schemes are rendered inefficient in terms of spectrum utilization. The scheduling of the data transmission in LTE needs to dynamically consider the demanding latency and throughput requirements that smart grid data transmission imposes. The downlink performance of LTE round-robin scheduler in network-underload was investigated in [61] for IEC-61850 MMS services. Instead, here we propose a channel-aware adaptive scheduling scheme to address the most challenging uplink scenario, where the physical resources allocated to each service class must be contiguous in frequency and hence traffic overload naturally arises due to the scarcity of uplink resources [30]. In [69], an LTE scheduler is analytically designed to maximize the control traffic rate. Instead, we propose an adaptive scheduling scheme that dynamically allocates contiguous uplink resources and prioritizes smart grid traffic to guarantee its strict latency and throughput requirements. In addition, we quantify the minimum impact of grid traffic prioritization on the performance of human-centric and real-time LTE services.

4.1.2 Automation Scenarios and Requirements

Two representative grid automation scenarios involving IED data exchange are depicted in Figure 4.1. The solid arrows correspond to a centralized architecture where MMS traffic is exchanged between the IEDs and the control center. The IEDs are equipped with LTE radio interfaces for communication with the eNodeB and belong to the same substation LAN. A connection-oriented communication is established, where the backward-compatible IEC-61850 methods with MMS over TCP/IP are used [133]. Focusing on event reporting use cases, we consider a scenario where LTE RACH procedure has been successfully completed and real-time power quality measurements are periodically sent to a remote controller to monitor system state. In turn, this information is used to detect out-of-step conditions (e.g., excessive/increasing phase angle), issue alarms and initiate control actions to rectify the fault and/or isolate the system.

An envisaged architecture that could enable localized control interactions is depicted with dashed arrows in Figure 4.1. We consider a distributed automation scenario that relies on peer-to-peer communications. In particular, we propose a system model where there is no centralized decision logic that coordinates the substations based on information collected from the entire grid. Instead, the decision making is built into the substations in a distributed way and direct communication among them is established, so that delays can be kept to a minimum. This network topology captures use cases where distributed event-driven communication is required. This is the case of a scheme that coordinates the control actions of decentralized generation with distributed networked

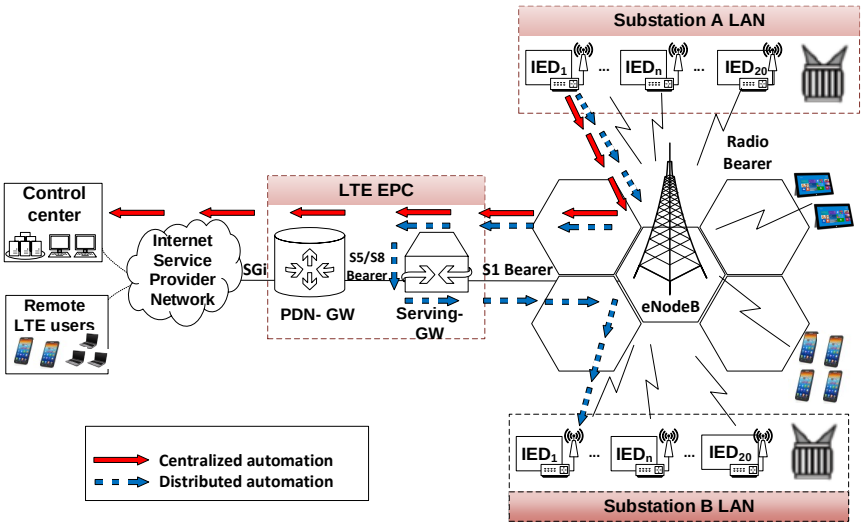

Figure 4.1: Centralized/distributed architecture for energy automation services in the distribution grid. A regular LTE cellular deployment with a hexagonal grid is considered, where smart grid communication is based on IEC-61850 MMS (solid arrows) and GOOSE messages (dashed arrows) respectively. The Packet Data Network Gateway (PDN-GW) acts as interconnection point between the LTE Evolved Packet Core (EPC) network and the external IP networks [11].

controllers, such as tap changers and capacitor banks, to minimize the operational cost of the grid. The required communication may take place either through the eNodeB, as depicted in Figure 4.1, or via the D2D paradigm. Establishing a peer-to-peer network over LTE facilitates time-critical GOOSE messages to be exchanged between neighboring IEDs that belong to the same or different substation LANs. GOOSE services provide fast transmission of substation events, such as protection commands/alarms, and enable localized decision-making. The IEC-61850-90-5 technical report describes a standardized mechanism to route IEC-61850-8-1 GOOSE packets over UDP/IP by forwarding them as inter-substation traffic, exchanged among different geographic locations. Since the use of UDP transport protocol does not guarantee message/data delivery, once an event occurs, a specific retransmission scheme of identical GOOSE messages is applied, as detailed in Section 3.2 (Figure 3.7). Thus, with high probability, given that the network is intact, any GOOSE message will be eventually received by the intended IED.

Table 4.1: Performance requirements of IEC-61850 automation traffic [154].

	Min throughput	Max delay
Centralized automation using MMS	2 kbit/s	100 ms
Distributed automation using GOOSE	70 kbit/s	50 ms

Table 4.1 summarizes the performance requirements for centralized and distributed grid topologies, as these have been identified by the EIT research activity LTE for Smart Energy [154]. Our objective is to address the implementation challenges so that LTE

meets these requirements, as discussed next.

4.1.3 LTE Scheduling for Automation Services

In this subsection, we propose a novel LTE scheduling policy that enables IEC-61850 communication services. Similar to our approach in Section 3.2, adaptation protocols have to be introduced above the transport layer in the OSI reference model to render IEC-61850 compatible with the LTE radio protocol architecture and extend the reach of automation information beyond substation boundaries. In addition, as shown in Table 4.2, we propose the extension of the standardized QoS-based LTE mechanism (i.e., Table 2.1) with the introduction of an additional QoS class of highest priority for IEC-61850 MMS and GOOSE services, based on the performance requirements mentioned in Table 4.1. QoS provisioning is achieved through the establishment of dedicated bearers to be exclusively used by IEC-61850 traffic. Notice that the definition of a new QCI is necessary to ensure QoS-differentiation between automation and other types of traffic. Otherwise, automation services would have to compete with mobile applications that belong to the same class. This QoS-differentiation mechanism ensures different packet-forwarding treatment (i.e., scheduling and queue management, resource allocation) of grid automation and conventional traffic. Based on QCI value, the LTE scheduler could schedule traffic flows so as to achieve the corresponding QoS targets.

Table 4.2: Extended LTE QoS characteristics.

QCI	Resource type	Priority	Packet delay budget (ms)	Packet loss rate	Example services
10	GBR	Highest	100, 50	10^{-6}	IEC communication services (MMS, GOOSE)

Figure 4.2 illustrates the proposed uplink scheduling framework. Consider F traffic classes, where a smaller class index $i = 1, \ldots, F$, corresponds to higher priority traffic, as presented in Table 2.1. We model class-i arrivals as a Poisson process of arrival rate λ_i and their payload size as an exponential random variable with mean b_i bytes. As discussed in Chapter 2, the available bandwidth in LTE-based systems can be seen as a time-frequency grid of physical resource blocks. Two time-consecutive resource blocks form an resource block pair which constitutes the minimum scheduling unit that can be allocated to a traffic class in every TTI. We denote by $\mathcal{N}_{\mathrm{RB}}$ the set of available resource block pairs for data transmission in every TTI. Uplink resource allocation needs to conform to the contiguity constraint, i.e., adjacent resource block pairs have to be allocated to each performance class [30].

Let x_i^n be the decision variable that indicates whether resource block pair $n \in \mathcal{N}_{\mathrm{RB}}$ is assigned to class i and let $\mathbf{x}_i = \{x_i^n : n \in \mathcal{N}_{\mathrm{RB}}\}$ denote the corresponding allocation vector. Then, for the service rate of class i, R_i, according to Shannon-Hartley theorem, we have

$$R_i\left(\mathbf{x}_i\right) = \sum_{n \in \mathcal{N}_{\mathrm{RB}}} x_i^n \frac{V}{|\mathcal{N}_{\mathrm{RB}}|} \log_2\left(1 + \mathrm{SINR}_{i,n}\right), \tag{4.1}$$

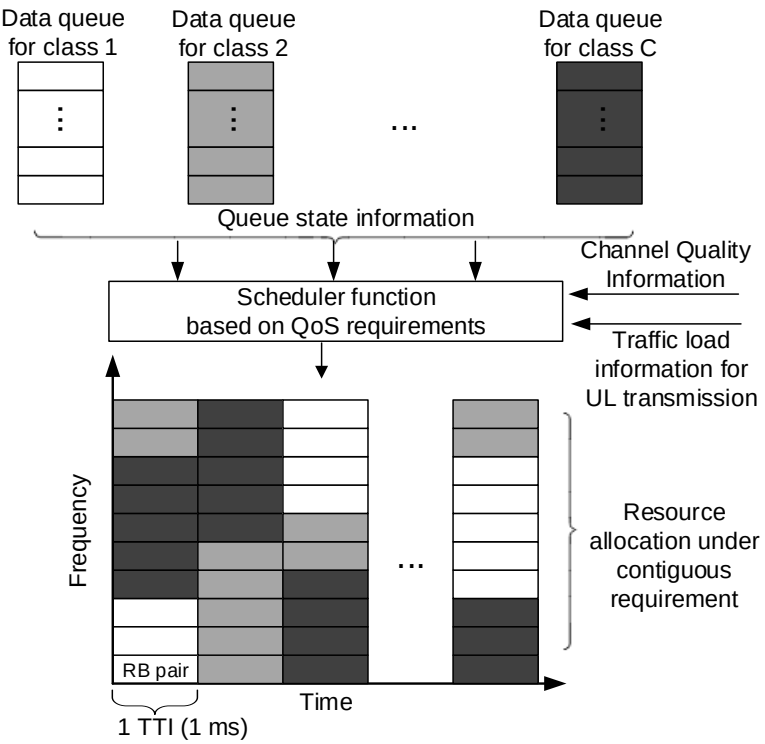

Figure 4.2: Generic view of the LTE uplink scheduler. In each TTI, multiple adjacent resource block pairs can be assigned to a number of performance classes.

where V denotes the total available system bandwidth and $\mathrm{SINR}_{i,n}$ is the average signal to interference and noise ratio for the resource block pair n for class i. The latter information is generally available through reporting mechanisms (channel quality and traffic load information) provided by LTE standard [30]. Based on the above, the service time of class i, S_i, follows an exponential distribution with a mean value of $s_i = b_i/R_i$. Thus, we may model the system as F M/M/1 queues, where each queue holds the traffic of the respective class, and the resulting average delay $T_i(\mathbf{x}_i)$ is given by [155]

$$T_i(\mathbf{x}_i) = \frac{\lambda_i b_i^2}{R_i(\mathbf{x}_i)\left(R_i(\mathbf{x}_i) - \lambda_i b_i\right)} + \frac{b_i}{R_i(\mathbf{x}_i)}. \tag{4.2}$$

As illustrated in Figure 4.1, the delay of the core LTE network domain, T_{core}, has to be taken into consideration; hence, the actual average end-to-end latency for message delivery becomes

$$T_{i,\mathrm{total}}(\mathbf{x}_i) = T_{\mathrm{core}} + T_i(\mathbf{x}_i). \tag{4.3}$$

Our objective lies on the maximization of overall system throughput subject to the resource contiguity, throughput and delay constraints. If n_i^a and n_i^b denote the first and last resource block allocated to user i, uplink scheduling can be formulated as the following

optimization problem:

$$\max_{\mathbf{x}} \quad \sum_{i=1}^{F} \sum_{n=n_i^a}^{n_i^b} R_i\left(\mathbf{x}_i\right) \tag{4.4a}$$

$$\text{s.t.} \quad \sum_{i=1}^{F} x_i^n \leq 1\,, \;\; \forall n \in \mathcal{N}_{\mathrm{RB}}\,, \quad x_i^n \in \{0,1\}\,, \tag{4.4b}$$

$$\sum_{n=n_i^a}^{n_i^b} x_i^n = n_i^b - n_i^a + 1\,, \;\; \forall i\,, \tag{4.4c}$$

$$R_i(\mathbf{x}_i) \geq R_{i,\min}\,, \quad \forall i\,, \tag{4.4d}$$

$$T_{i,\mathrm{total}}(\mathbf{x}_i) \leq \tau_i\,, \quad \forall i\,. \tag{4.4e}$$

Constraint (4.4b) ensures that each resource block pair is allocated to at most one traffic class. Constraint (4.4c) reflects the resource block pair contiguity constraint of LTE uplink [31]. Constraint (4.4d) implies that the throughput lower bound, $R_{i,\min}$ has to be met for each class i. Constraint (4.4e) captures the requirement that the overall transfer time for class i should be at most τ_i. Solving problem (4.4) is particularly challenging. First, the decision variables x_i^n are binary constrained. Second, the presence of the decision variables in the denominator of the performance constraints results in a nonlinear problem [156]. Third, the contiguous resource block pair allocation constraint renders the problem NP-hard [31].

Due to mathematical intractability of problem (4.4), we propose an adaptive heuristic scheduling scheme, as described in Algorithm 4. The heuristic algorithm is executed on a per-TTI basis following a QoS-, queue- and channel-aware policy. At each TTI, the scheduler calculates the SINR values based on the buffer status report and channel quality information. Prioritization is performed by assigning resource block pairs in sequential order from the higher-priority to lower-priority classes. In particular, starting from the highest priority class, the initial number of resource block pairs to be allocated for class i is set to 1. The proposed heuristic scheduler then estimates the achieved throughput R_i and the response time T_i. If R_i and the overall transfer time $T_{i,\mathrm{total}}$ do not meet the respective requirements $R_{i,\min}$ and τ_i, an additional, neighboring resource block pair is allocated. The scheduler keeps increasing the number of allocated resource block pairs which results in an increase of R_i and a corresponding decrease of T_i until the requirements of the throughput and latency are both met. Iteratively, the scheduler proceeds by processing the lower priority traffic flows. Finally, once the allocation is completed, the system updates all the relevant parameters. Note that at each TTI, the proposed scheduler dynamically assigns resources to meet the QoS requirements and prevent spectrum underutilization.

In the following subsection, we assess the performance of our proposed heuristic scheduler and quantify the impact of smart grid prioritization on the background LTE real-time traffic.

4.1.4 Numerical Results

To evaluate the performance of the proposed LTE scheduler, we consider realistic overload scenarios where LTE subscribers generate background traffic within the eNodeB

Algorithm 4 LTE scheduling and resource allocation scheme.

$N_{\mathrm{RB}} \leftarrow$ set of available resource block pairs
$I_{\mathrm{A}} \leftarrow$ set of assigned resource block pairs
$U_{\mathrm{A}} \leftarrow$ set of unassigned resource block pairs
$x_i \leftarrow$ number of resource block pair assigned to class-i data flow
RB $\leftarrow$ resource block pair index
▷ Initialization
$I_{\mathrm{A}} \leftarrow \emptyset$; $U_{\mathrm{A}} \leftarrow N_{\mathrm{RB}}$; RB $\leftarrow 0$; $x_i \leftarrow 0 \quad \forall i$
for $n \leftarrow 1$ to $|N_{\mathrm{RB}}|$ **do**
  for $i \leftarrow 1$ to F **do**
    Calculate SINR value for each traffic class and resource block pair
  end for
end for
▷ Main iteration
for $i \leftarrow 1$ to F **do**
  RB $\leftarrow 1$
  while $|I_{\mathrm{A}}| < |N_{\mathrm{RB}}|$ **do**
    Calculate T_i , R_i
    if $(T_{i,\mathrm{total}} \leq \tau_i \;\; \&\& \;\; R_i \geq R_{i,\mathrm{min}})$ **then**
      if $|I_{\mathrm{A}} \cup \{x_i\}| < |N|$ **then**
        $x_i \leftarrow$ RB (Assign RB block pairs to class-i)
        $I_{\mathrm{A}} \leftarrow I_{\mathrm{A}} \cup \{x_i\}$
        $U_{\mathrm{A}} \leftarrow U_{\mathrm{A}} \setminus \{x_i\}$
      else
        $x_i \leftarrow |U_{\mathrm{A}}|$
        Resume allocation in next TTI
      end if
    else
      RB $\leftarrow$ RB $+ 1$
    end if
  end while
end for

coverage area and compete with the IEDs for the available resources. Such scenarios would arise in practice, if public LTE infrastructure was shared by smart grid and conventional traffic. Similar to Section 3.2, we simulate the full LTE protocol stack and we consider traffic generated by typical mobile applications, e.g., web browsing (HTTP), Voice-over-IP (VoIP), video streaming and file transfer (FTP). Starting from a medium-load scenario, new users appear in the system according to a Poisson process with the arrival intensities selected so as to drive the system to overload. Network performance is then evaluated as the system operates close to its capacity limits. Regarding MMS and GOOSE traffic, we consider traffic patterns that follow IEC-61850 specifications, as described in Subsection 4.1.2.

Table 4.3 summarizes the basic parameters used in our simulations. For benchmarking purposes, each experiment is conducted both with the proposed scheme that prioritizes smart grid control traffic and the native LTE scheduler. In particular,

- The dashed curves correspond to simulations where both background LTE and smart grid flows are mapped to the same default bearer and resource allocation is

Table 4.3: Simulation settings overview.

Parameter	**Value**
System bandwidth	5MHz
Number of subcarriers per resource block	12
Resource block bandwidth	180kHz
Transmission time interval	1ms
Transmission mode	MIMO 2x2
{User, eNodeB} transmission power	{24, 43}dBm
{User, eNodeB} noise figure	{9, 5}dB
IEDs in a substation LAN	20
Channel model	Suburban
User distribution	Uniform
Average {EPC, Internet} delay	{10, 10}ms

Table 4.4: Simulation parameters for the centralized scenario.

	Traffic Type				
	Web	VoIP	Video	FTP	MMS
Initial number of active users/IEDs	3	3	1	2	2
Arrival intensity	2.0	3.0	0.75	4.0	1.0
Number of active devices in overload	27	34	15	25	20

performed with the proportional-fair scheduling policy. This setting captures the default network configuration with no special handling of smart grid with respect to other LTE traffic.

- The solid curves depict the performance of our proposed scheme where a dedicated bearer is established for the control traffic flow with QoS requirements specified in Table 4.1. Smart grid control traffic is prioritized over conventional LTE which is mapped to the default bearer.

In what follows, a comparative study of the two approaches is performed in terms of latency and throughput, aiming to verify whether the performance requirements for each scenario are met with the proposed QoS-differentiation scheduling scheme.

Centralized automation scenario

Table 4.4 provides the details of the simulated centralized (client-server) scenario. We assume that remote control traffic between the IEDs and the control center follows a periodic data transmission pattern with constant interarrival times of 6ms and a payload of 150 bytes [154]. In overload conditions, all IEDs that belong to the same substation LAN are considered active and send data to the control center.

Figure 4.3a presents the CDF of delay that MMS messages experience, measured at the control center. It can be observed that the proposed scheduler outperforms the con-

ventional LTE scheme. In particular, our scheduler guarantees that even in overload only 0.5% of the messages experience delay slightly above the maximum acceptable threshold of 100ms whereas the corresponding percentage for the native LTE scheduler is 21.8%. Figure 4.3b illustrates the CDF of throughput for MMS automation traffic. When the proposed priority-scheduling approach is applied, the throughput measured at the control center satisfies the requirement of 2 kbit/s per connection. On the other hand, with the default network configuration, 4% of the MMS traffic throughput remains below the threshold.

Naturally, this improvement causes some performance degradation to the background human-type traffic. Since user Quality of Experience (QoE) should not be sacrificed, we quantify the impact of smart grid traffic prioritization on delay-sensitive applications. Figure 4.4 depicts the CDF of the delay for real-time voice and video services in presence of MMS traffic. As a result of MMS traffic prioritization, a slight increase in the delay of the voice frames (up to 20ms) can be observed. However, this level of degradation would not be noticeable by the end users. Typically, delays of up to 150ms have marginal impact on the call quality and thus can be considered acceptable for VoIP services [157]. It can also be seen that video streaming delay increases by up to 0.5sec with respect to the default LTE scheme. The performance degradation is higher compared to the case of voice services; however, since 95% of video frames are delivered with a delay of less than 0.6sec, QoE can be considered acceptable.

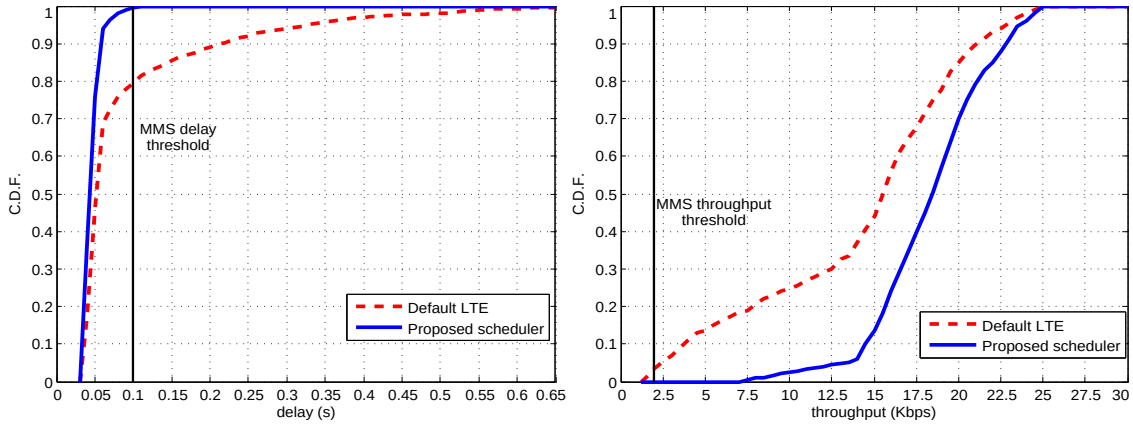

(a) **(b)**

Figure 4.3: CDF of (a) delay and (b) throughput for MMS traffic.

Distributed automation scenario

In the peer-to-peer scenario, under stable operating conditions, each IED periodically reports its state via GOOSE messages to other IEDs within the same or different substation LANs. Once an event is detected, the retransmission period is shortened which results to a GOOSE burst. The generation of a GOOSE traffic burst can be modeled as a Poisson process. Table 4.5 summarizes the characteristics of GOOSE traffic in both stable and burst operation modes, according to Figure 3.7. We assume also that in overload all IEDs belonging to the two substation LANs identify the event and eventually switch to

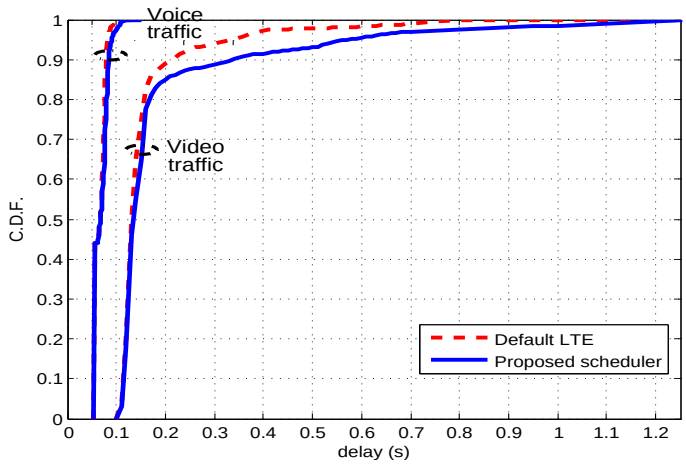

Figure 4.4: CDF of background voice and video delay in presence of MMS traffic.

Table 4.5: GOOSE traffic characteristics.

Parameter	**Value**
Payload	250 bytes
Retransmission $\{T_0, T_1\}$	$\{0.5\text{sec}, 1\text{ms}\}$
Retransmission T_N	$T_N = 2^{N-1}T_1\,,\ \text{for}\ N \geq 2$

burst mode. The details of the simulated scenario are described in Table 4.6. Note that due to the increased traffic load for GOOSE services, overload is reached with a lower number of background LTE users.

Figure 4.5a depicts the CDF of delay for GOOSE messages, measured at the receiving IED. It can be observed that the proposed priority-scheduling scheme outperforms the default one. Despite the intense traffic conditions imposed by the GOOSE bursts, 77.6% of the messages experience delays below the maximum allowed threshold of 50ms, whereas less than 2% require more than 60ms. The corresponding values under the default LTE scheme are 66.4% and 10%. Figure 4.5b shows the CDF of throughput for GOOSE traffic for both simulation sets, measured at the receiving IED. By applying the proposed priority-scheduling policy, the achieved throughput improves significantly. In particular, only 4.8% of the throughput is below the threshold of 70 kbit/s whereas the corresponding percentage in the default scheme is 18%.

Figure 4.6 illustrates the impact of GOOSE traffic prioritization on the performance of background real-time voice and video services. Compared to the first scenario, the impact on voice applications is higher mainly due to the stringent QoS requirements and the bursty nature of GOOSE traffic. Voice users would experience a delay increase of up to 30ms with respect to the default scheme. However, the resulting delay level can be considered acceptable since it remains significantly lower than the 150ms threshold and thus would not lead to dropped calls. For video users, the respective delay increases up to 0.85sec. The overall delay levels are now higher with respect to Figure 4.4, reaching up to 2.6sec. Moreover, 77% of video frames are now transmitted with less than 0.6sec delay. Thus, the video quality can still be considered acceptable; however, the perfor-

Table 4.6: Simulation parameters for the distributed scenario.

	Traffic Type				
	Web	VoIP	Video	FTP	GOOSE
Initial number of active users/IEDs	3	3	1	2	2
Arrival intensity	0.75	1.0	0.75	2.0	0.8
Number of active devices in overload	25	18	29	10	40

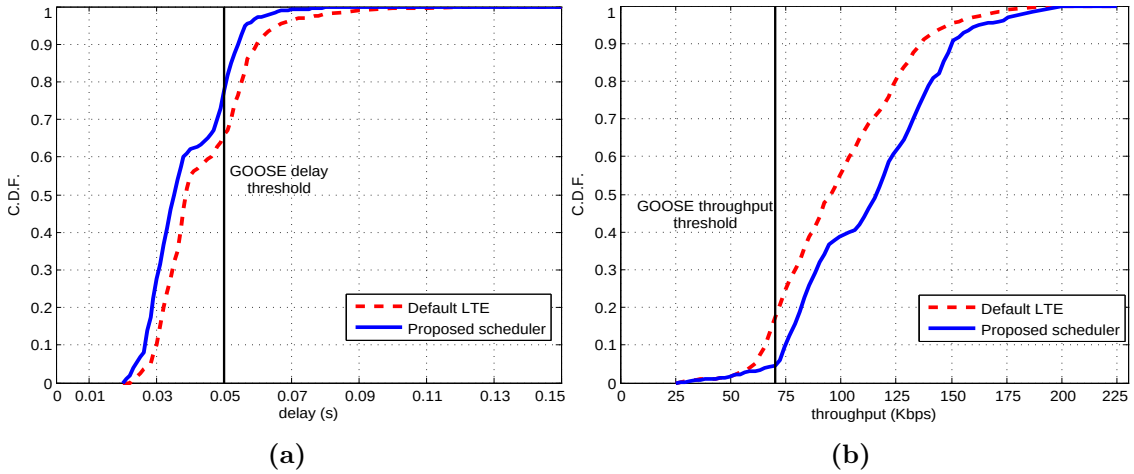

Figure 4.5: CDF of (a) delay and (b) throughput for GOOSE traffic.

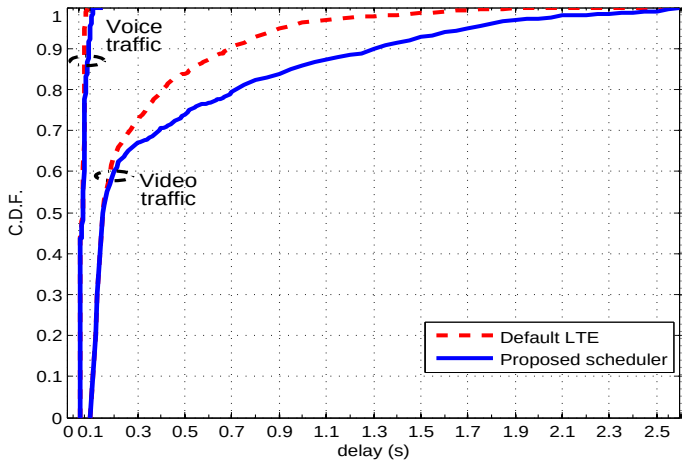

Figure 4.6: CDF of background voice and video delay in presence of GOOSE traffic.

mance deterioration may lead to some unsatisfied video users. Note that here all types of background traffic are considered equivalent and hence are handled identically. However, QoS differentiation can be extended to background traffic so as to reduce the impact of smart grid traffic prioritization on delay-sensitive services.

4.1.5 Summary

In this section of Chapter 4, we demonstrated how data transmission based on IEC-61850 standard can be implemented over LTE to extend energy automation services beyond the substation boundaries. Since such time-critical applications are not adequately supported by current LTE/LTE-A implementations, we devised a novel LTE scheduling policy that prioritizes automation traffic. Resource allocation decisions take into account the stringent latency and throughput requirements of smart grid traffic and conform to the SC-FDMA contiguity constraint of LTE uplink. Our extensive simulations in a system-level simulator indicate that our proposed scheduler enables public LTE infrastructure to efficiently support automation services with minimum impact on background LTE traffic. In particular, the performance requirements for IEC-6180 MMS services (centralized automation) can be fully satisfied whereas a significant improvement for IEC-6180 GOOSE services (distributed automation) can be observed with respect to the default LTE scheduler.

In the following section of Chapter 4, we investigate the benefits of direct D2D communication among IEDs as a means of enhancing the performance of distributed automation services in LTE-based systems.

4.2 Transmission Mode Selection for Substation Automation Traffic

4.2.1 Introduction

In this section of Chapter 4, we propose D2D communication over dedicated cellular resources, i.e., D2D-overlay mode, as a key enabling technology for reliable information exchange in power distribution grids. As discussed in Subsection 2.2.3, bypassing the cellular infrastructure, D2D mode can yield a dramatic latency reduction which is of utmost importance especially for time-critical protection and control applications in the distribution grid, e.g., substation automation and outage management. In addition, D2D-overlay transmission mode results in a more controlled interference environment since D2D and cellular links utilize orthogonal parts of the cellular spectrum. Motivated by the stringent requirements of substation automation traffic, we jointly address two fundamental issues: *i*) the seamless transition from cellular (i.e., communication via the base station) to D2D-overlay mode for smart grid entities upon detection of a surge of channel access attempts and *ii*) the efficient orthogonal resource partition for cellular and D2D links. An analytical framework capturing the event-driven nature of substation automation traffic and both phases of uplink communication is introduced and the joint problem of mode selection and resource allocation (MSRA) is formulated as a sum-rate maximization problem. A dynamic heuristic MSRA mechanism is then proposed that adaptively allocates uplink resources for D2D links to prevent spectrum underutilization and guarantees a minimum rate requirement for cellular users. The performance of our proposed scheme is evaluated through extensive simulations under different performance criteria and numerical results demonstrate the rate gains of a dynamic switch between D2D-overlay and conventional cellular mode for substation automation traffic.

Mode selection, i.e., the process of determining whether a D2D-capable pair should ex-

change data in cellular or D2D mode, has recently become a topic of considerable interest. However, the majority of the available literature is focused on distance-based mode selection schemes and the channel access loading state is not considered for switching between direct and conventional cellular communication [79]. While in D2D-underlay several works deal with the mode selection problem in an effort to achieve improved spectrum/power efficiency [158, 159], the focus in D2D-overlay has been mainly in the self-interference mitigation among D2D pairs [102, 113, 115]. Mode selection and spectrum partition techniques proposed in the literature so far, do not consider the sporadic activity patterns of mission-critical smart grid message exchange; hence, they are rendered insufficient for event-driven distribution grid operations where congestion may arise in a short period of time. Instead, here we propose a dynamic MSRA mechanism that adapts to the system traffic conditions, monitored during the initial network association phase. Motivated by the stringent requirements of mission-critical smart grid messages, we summarize our main contributions as follows:

1. Based on a realistic traffic model that accurately captures the event-driven nature of substation automation traffic, we present a unified analytical framework that accounts for both uplink communication phases, i.e., random access and data resource allocation, and we formulate the joint MSRA problem as a sum-rate maximization problem with a performance constraint for protecting the cellular users.

2. We introduce a load- and interference-aware MSRA mechanism for substation automation traffic in cellular-enabled distribution grids. Our proposed scheme captures use cases where event-driven D2D communication is required to achieve high transmission rates and relies on a dynamic orthogonal partition of the uplink spectrum; a part dedicated to D2D-overlay communication while the rest of the resources are allocated to regular cellular communication. Numerical results demonstrate that substation automation traffic can substantially benefit from a carefully-designed MSRA mechanism.

4.2.2 Substation Automation Scenario and Traffic Model

Substation automation systems often involve message-exchange among neighboring IEDs for real-time situational awareness and supervision of the power equipment, e.g., rapid diagnosis of system faults and initiation of control/isolation actions [133]. We consider a cellular-enabled substation automation system with an underlying LTE network providing connectivity to a number of IEDs, as illustrated in Figure 4.7. On top of a wide range of human-oriented services generated by synchronized mobile terminals (i.e., UEs) always connected in cellular mode, the shared cellular infrastructure accommodates the substation automation traffic exchanged among D2D-capable[14] IEDs.

As depicted in Figure 4.7, an arc-fault detection scheme is implemented in a substation LAN. Each IED is equipped with three arc sensors and transits from idle to connected state when a state change is captured by one of its sensors. In particular, when IED A detects an arc in the busbar compartment via sensor 1, it transmits a substation-event message to notify its neighboring devices within the substation, e.g., to IED B, and

[14] We assume that the D2D-capable pairs are already peer-discovered.

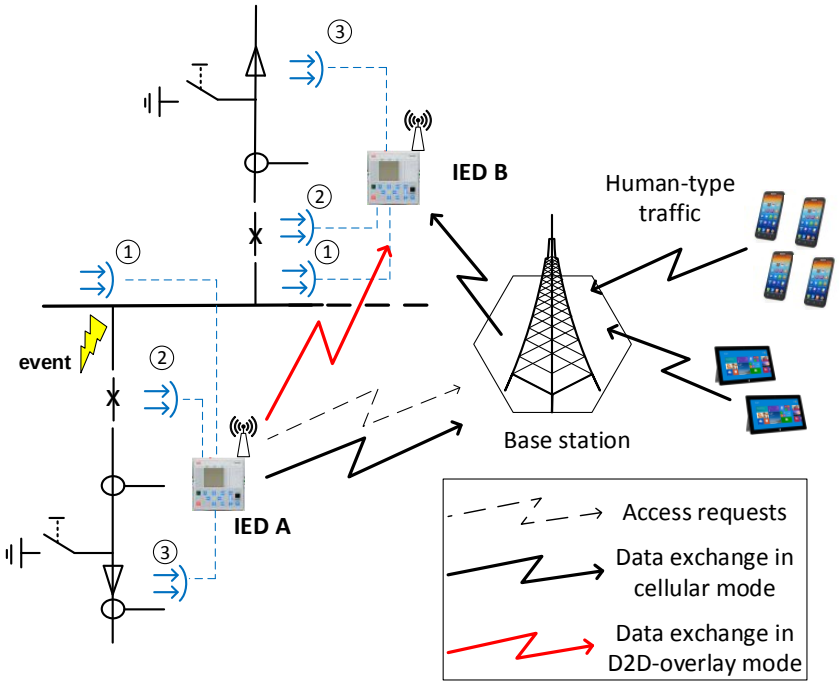

Figure 4.7: Network model for a cellular-enabled substation automation system where arc-fault detection is performed. The hybrid architecture in the radio access domain is characterized by the coexistence of cellular links that communicate via the base station and autonomous D2D-overlay links for IED mission-critical message exchange.

issues a trip command to the corresponding circuit breaker. In turn, the reception of a substation-event message sequentially triggers the neighboring IEDs to transmit their own substation-event messages to allow for a fast distribution of the fault information within the substation. Due to the near-simultaneous channel access requests from neighboring IEDs, an abrupt increase in the network load of the contention-based RACH procedure can be detected [5]. While the channel access requests are transmitted to the base station, the subsequent transmission of the substation-event message may now switch from cellular to D2D-overlay mode, to ensure the timeliness of the message delivery and achieve reduced system response times. To model this IED traffic behavior, we leverage the two-state MAP framework that was introduced in Subsection 3.4.4 for substation automation traffic. In particular, due to the spatiotemporal correlation in the arrival traffic stream (cascade effect), the interdependent packet interarrival times of an IED can be accurately captured by the MAP stochastic counting process and the traffic generation probability p_{on} can be calculated using Eq. (3.39).

Due to the event-driven nature of substation automation messages, the seamless transmission mode selection for IEDs constitutes a significant challenge. In addition, an efficient spectrum partition for cellular and D2D-overlay links is required while satisfying the performance requirements of the coexisting cellular UEs. In the following subsection, we

present an efficient mechanism for the MSRA problem of D2D-capable IEDs transmitting substation-event messages in cellular-enabled power distribution grids.

4.2.3 The Mode Selection and Resource Allocation Problem

System Model and Analytical Framework

Let us consider the uplink of a single-cell cellular network with total system bandwidth V that accommodates the traffic generated in a cellular-enabled substation automation system, as the one described in Subsection 4.2.2. According to 3GPP, the available bandwidth can be seen as a time-frequency grid of physical resource blocks pairs for the initial network association and data transmission phases. The network entities present in the system consist of cellular UEs and D2D-capable IEDs which can transmit and receive data across a set of links, i.e., pairs of distinct nodes. Let $\mathcal{C}$ be the set of communication links between cellular UEs and $\mathcal{D}$ the set of communication links between D2D-capable IEDs with cardinalities C and D, respectively. We assume that the cellular UEs are always synchronized and connected in cellular mode; thus, they are not contending in the RACH for initial network association. On the other hand, the IEDs are triggered to generate traffic with probability p_{on} after an substation event and thus are considered unsynchronized. Therefore, the IEDs need to contend in the RACH by randomly selecting one of the available preambles for transmission over the random access resources [5].

Given that an IED of a link $i \in \mathcal{D}$ attempts channel access, the preamble collision probability, p_c, from the perspective of the IED, is defined as the probability that an IED of at least one of the remaining j links, $j \in \mathcal{D} \setminus \{i\}$, attempts channel access and selects the same preamble. Let K be the number of available orthogonal preambles for the contention-based random access, then p_c is given by

$$p_c = \sum_{j=1}^{D-1} \binom{D-1}{j} \tau^j (1-\tau)^{D-1-j} \left(1 - \left(1 - \frac{1}{K}\right)^j\right), \tag{4.5}$$

where τ denotes the probability that an IED attempts a channel access. Based on the generalized Markov chain model of the LTE random access procedure developed in Section 3.3, τ can be expressed as a function of the probabilities p_c, p_{on}, and the various random access parameters, as

$$\tau = \left[\frac{p_c - 1}{p_c^L - 1}\left(\frac{T_{\text{off}}}{p_{\text{on}}} + p_c^L T_f\right) + p_c T_1 + (1-p_c)(T_2 + T_s) + \frac{W-1}{2}\right]^{-1}. \tag{4.6}$$

In Eq. (4.6), the parameter L denotes the maximum allowed preamble transmissions, W is the random access backoff window size and T_{off} denotes the average holding time of the IED in idle state. The T_s, T_f represent the expected time durations of the success and fail states that model the successful and failed random access attempt, respectively. The expected time durations T_1 and T_2 correspond to the elapsed times from the first access attempt until the end of the contention resolution timer in case of access failure, and until the reception of the connection response message in case of successful access, respectively [7].

Let $\mathcal{N}_{\text{RB}}$ be the set of resource block pairs available for data transmission and N_{RB} the corresponding cardinality. Henceforth, we focus on the performance analysis of a typical

transmitter-receiver link i belonging to any of the UE or IED sets. We denote by $x_{i,m}^n$ the decision variable that indicates whether resource block pair $n \in \mathcal{N}_{\text{RB}}$ is assigned to link i in mode m, where index $m = \{c, d\}$ denotes the cellular and D2D-overlay mode, respectively. Due to the orthogonal resource partition, the available resource block pairs for links in cellular mode and D2D-overlay mode are $N_c = (1 - \theta)N_{\text{RB}}$ and $N_d = \theta N_{\text{RB}}$ respectively, where θ represents the fraction of resource block pairs allocated to D2D-overlay transmissions. Let $\mathcal{N}_c$ and $\mathcal{N}_d$ be the corresponding resource sets for the two modes, respectively. Then, the fraction θ can be expressed as

$$\theta = \frac{\sum_{i \in \mathcal{D}} \sum_{n \in \mathcal{N}_d} x_{i,d}^n}{N_{\text{RB}}}. \tag{4.7}$$

Let also $\mathbf{x}_i = \{x_{i,m}^n : n \in \mathcal{N}_m, m = \{c, d\}\}$ denote the corresponding allocation vector. Then, according to the Shannon-Hartley theorem, the maximum achievable rate for link i in mode m is

$$R_{i,m}(\mathbf{x}_i) = \sum_{n \in \mathcal{N}_m} x_{i,m}^n \frac{V}{N_{\text{RB}}} \log_2 \left(1 + \text{SINR}_{i,m}^n\right), \tag{4.8}$$

where $\text{SINR}_{i,m}^n$ represents the signal to interference and noise ratio perceived at the receiver of link i in mode m when transmitting in resource block pair n and is given by

$$\text{SINR}_{i,m}^n = \frac{g_{ii,m}^n P_{i,m}}{\sigma^2 + I_{i,m}^n}, \tag{4.9}$$

where $P_{i,m}$ is the transmission power for link i in mode m, $g_{ii,m}^n = \left|h_{ii,m}^n\right|^2$ the power gain (the channel gain h captures the effects of path loss and Rayleigh small-scale fading) from the transmitter of link i in mode m and resource block pair n, and σ^2 the noise power at the receiver of link i. The interference, $I_{i,m}^n$, experienced at the receiver of link i, is

$$I_{i,m}^n = \sum_{j \neq i} g_{ji,m}^n P_{j,m}, \tag{4.10}$$

where $g_{ji,m}^n = \left|h_{ji,m}^n\right|^2$ denotes the power gain between the transmitter of link j and the receiver of link i in mode m for resource block pair n. For links transmitting in cellular mode, the N_c resource block pairs are allocated orthogonally based on the legacy uplink SC-FDMA scheme of 3GPP-based standards; thus, $I_{i,c}^n = 0$, $\forall i$, $n \in \mathcal{N}_c$.

As discussed in Subsection 4.2.2, in the case of a substation event, neighboring IEDs attempt near-simultaneous channel access resulting in a traffic surge of access requests. The limited number of random access opportunities (up to 64 preambles in LTE) compared to the increased resource demand results in an increased probability of collision in the transmission of the preambles. Based on a continuous monitoring of the preamble collision probability, p_c, by the base station, the D2D-capable IEDs may be signaled to switch from cellular to D2D-overlay mode to transmit substation-event information. However, mode selection should also consider the interference level among the D2D-overlay links due to the resource sharing of their N_d resource block pairs. Therefore, to account for both, the

mode selection probabilities for each link $i \in \mathcal{D}$, are given by

$$\Pr(m = d) = \Pr\left(p_c > p_{c,\text{th}}\right) \cdot \Pr\left(\sum_{\substack{j \in \mathcal{D} \\ j \neq i}} x_{j,d}^n I_{i,d}^n \leq I_{\text{th}}^n\right), \tag{4.11}$$

and $\Pr(m = c) = 1 - \Pr(m = d)$, where $p_{c,\text{th}}$ denotes the threshold value for the preamble collision probability and I_{th}^n is the interference tolerance level for resource block pair n. Note that both $p_{c,\text{th}}$ and I_{th}^n can be optimized to maximize the overall system achievable rate. We assume $p_{c,\text{th}}$ and I_{th}^n as predefined parameters that depend on the reliability of the supported substation automation application and we leave their joint optimization within the MSRA problem for future work. According to the adopted system model, cellular UEs always transmit in cellular mode whereas D2D-capable IEDs may dynamically switch between the cellular and D2D-overlay mode according to the mode selection policy. Therefore, for the average achievable rate of a link i, it holds

$$R_i\left(\mathbf{x}_i\right) = \begin{cases} R_{i,c}\left(\mathbf{x}_i\right), & \text{if } i \in \mathcal{C}, \\ \Pr(m = c) R_{i,c}\left(\mathbf{x}_i\right) + \Pr(m = d) R_{i,d}\left(\mathbf{x}_i\right), & \text{if } i \in \mathcal{D}. \end{cases} \tag{4.12}$$

Problem Formulation

Our goal is to jointly consider the mode selection of D2D-capable IEDs and the orthogonal resource assignment of cellular and IED links, while maximizing the achievable sum-rate for all the links present in the system. Specifically, if $n_{i,c}^a$ and $n_{i,c}^b$ denote the first and last resource block pair allocated to link i in cellular mode, the MSRA problem can be formulated as

$$\max_{\mathbf{x}_i} \quad \sum_{i \in \mathcal{C} \cup \mathcal{D}} \sum_{n \in \mathcal{N}_{\text{RB}}} R_i\left(\mathbf{x}_i\right) \tag{4.13a}$$

$$\text{s.t.} \quad \sum_i x_{i,m}^n \leq 1, \ \ \forall n \in \mathcal{N}_c, \ \ m = c, \tag{4.13b}$$

$$\sum_m x_{i,m}^n \leq 1, \ \ \forall i \in \mathcal{D}, \ \ \forall n \in \mathcal{N}_{\text{RB}}, \tag{4.13c}$$

$$\sum_i x_{i,m}^n = 0, \ \ \forall i \in \mathcal{C}, \ \ \forall n \in \mathcal{N}_c, \ \ m = d, \tag{4.13d}$$

$$\sum_{n=n_{i,m}^a}^{n_{i,m}^b} x_{i,m}^n = n_{i,m}^b - n_{i,m}^a + 1, \ \ m = c, \tag{4.13e}$$

$$\sum_{i \in \mathcal{D}} \sum_{n \in \mathcal{N}_d} x_{i,m}^n \leq N_{\text{RB}}, \ \ m = d, \tag{4.13f}$$

$$R_i(\mathbf{x}_i) \geq R_{i,\min}, \quad \forall i \in \mathcal{C}, \tag{4.13g}$$

$$x_{i,m}^n \in \{0, 1\}. \tag{4.13h}$$

Constraint (4.13b) ensures that each resource block pair $n \in \mathcal{N}_c$ is allocated to at most one link in cellular mode. Constraint (4.13c) implies that each link among IEDs can

be either in cellular or D2D-overlay mode whereas cellular UEs operate always in cellular mode according to constraint (4.13d). Constraint (4.13e) captures the uplink resource contiguity constraint due to the SC-FDMA scheme for the links in cellular mode [11]. Constraint (4.13f) implies that the fraction θ of resources allocated to D2D-overlay must be at most equal to one, according to Eq. (4.7). Performance-protection constraint (4.13g) indicates that the minimum rate requirement, $R_{i,\min}$, has to be met for each link $i \in \mathcal{C}$ associated with a GBR of human-type services.

Due to the coupled variables p_c and τ in Eqs. (4.5) and (4.6) respectively, the expression of $R_i(\mathbf{x}_i)$ in Eq. (4.12) is not in closed-form; thus, solving problem (4.13) is mathematically intractable. In addition, the decision variables $x_{i,m}^n$ are binary constrained and their presence in the performance constraint (4.13g) results in a nonlinear problem [156]. Finally, the contiguous allocation constraint (4.13e) for links in cellular mode renders the problem NP-hard [11]. While transmission scheduling for the links in cellular mode can be adequately addressed using our priority-aware resource allocation algorithm proposed in Subsection 4.1.3, the joint consideration of D2D-capable IEDs requires an efficient mechanism for a dynamic selection of the transmission mode and allocation of data resources with performance guarantees. We provide the details in the following.

Solution Approach

Due to the mathematical intractability of solving efficiently problem (4.13), we propose a dynamic heuristic MSRA scheme for the D2D-capable IEDs that employs a traffic load- and interference-aware discipline. We assume that the base station has full knowledge of the channel gains between all transmitters and receivers within the cell; this constitutes a realistic assumption based on the static or slow-moving nodes in the network deployment of Figure 4.7. Besides the known channel state information, the proposed scheme relies on a continuous monitoring of the network loading state by the base station during the contention-based RACH procedure of the unsynchronized IEDs. The steps of the MSRA mechanism are presented in Algorithm 5.

Initially, we assume that all D2D-capable IEDs are in cellular mode and are scheduled for transmission with the cellular UEs following the contiguous resource allocation algorithm proposed in [11]. For each link $i \in \mathcal{D}$, the preamble collision probability is first calculated using an iterative numerical method, since the expressions of p_c in Eq. (4.5) and τ in Eq. (4.6) form a system of non-linear equations. Then, upon detection of higher levels of p_c than the predefined threshold, $p_{c,\text{th}}$, the link i is signaled to switch from cellular to D2D-overlay mode. Resource allocation for link i is then performed by adaptively assigning adjacent resource block pairs until the interference at the receiver of link i for each resource block pair gets lower than the allowed tolerance level, I_{th}^n. While the base station keeps increasing the number of allocated resource block pairs for each IED link, if the minimum rate requirement for the cellular UEs is violated, the IED link switches back from D2D-overlay to cellular mode and is scheduled for transmission with the cellular UEs, following the contiguous allocation Algorithm 4 proposed in Subsection 4.1.3. Iteratively, mode selection and resource allocation proceeds by processing all the D2D-capable IEDs and once allocation is performed, the system updates all the relevant parameters. It is noted that, in every iteration, the proposed scheme dynamically assigns adjacent uplink data resources aiming to allocate the minimum possible for each D2D-overlay IED link

Algorithm 5 MSRA mechanism for D2D-capable IEDs.

Assume $L, W, p_{\text{on}}, T_{\text{off}}$ known
$\mathcal{S}_c$: set of UE or IED links in cellular mode
$\mathcal{S}_d$: set of IED links in D2D-overlay mode
i: index for IED links
k: index for UE links
▷ Initialization
$\mathcal{S}_c = \{\mathcal{C}, \mathcal{D}\}$; $\mathcal{S}_d = \varnothing$; n=1
for $\forall i \in \mathcal{D}$ **do**
  Initialize $p_c \leftarrow 0.9999$ ▷ Calculation of p_c
  Set allowed tolerance $\epsilon \leftarrow 1e-3$
  while $p_c > 0$ **do**
    Calculate τ from Eq. (4.6)
    Calculate p'_c from Eq. (4.5)
    if $|p'_c - p_c| < \epsilon$ **then** ▷ Convergence test
      break
    else
      $p_c \leftarrow p_c - 0.0001$ ▷ Update
    end if
  end while
  if $p_c > p_{c,\text{th}}$ **then** ▷ Traffic-aware
    $\mathcal{S}_c \leftarrow \mathcal{S}_c \setminus \{i\}$
    $\mathcal{S}_d \leftarrow \mathcal{S}_d \cup \{i\}$
    $x^1_{i,d} \leftarrow 1$
    while $\sum_{\substack{j \in \mathcal{D} \\ j \neq i}} x^n_{j,d} I^n_{i,d} > I^n_{\text{th}}, \forall n$ **do** ▷ Interference-aware
      $n \leftarrow n + 1$
      $x^n_{i,d} \leftarrow 1$
      $x^n_{k,c} \leftarrow 0, \forall k \in \mathcal{C}$
      Calculate $I^n_{i,d}$ from Eq. (4.10)
      Update R_i, $i \in \mathcal{D}$ and R_k, $k \in \mathcal{C}$ from Eq. (4.12)
      if $R_k < R_{k,\min}$, $k \in \mathcal{C}$ **then** ▷ UEs protection
        $\mathcal{S}_c \leftarrow \mathcal{S}_c \cup \{i\}$
        $\mathcal{S}_d \leftarrow \mathcal{S}_d \setminus \{i\}$
        break
      end if
    end while
  end if
end for
Calculate θ from Eq. (4.7)

and thus minimize the impact on the background traffic generated by cellular UEs.

In the following subsection, we evaluate the performance of our proposed MSRA scheme under various performance metrics and we quantify the throughput gains for IEDs due to the seamless transition between cellular and D2D-overlay mode.

4.2.4 Numerical Results

Our aim in this subsection is twofold: *i*) to assess and evaluate the performance of our proposed MSRA scheme through extensive simulations and *ii*) to derive useful insights for

Table 4.7: Simulation parameters.

Parameter	Value
System bandwidth	10MHz
Resource block bandwidth	180kHz
Cell radius	1km
IEDs in a substation LAN, cellular UEs	{20, 20}
Transmit power in {cellular, D2D-overlay} mode	{24, 16}dBm
Thermal noise power	-114dBm
Channel model	Suburban
Path-loss coefficient	3.5
User distribution	Uniform
Distance between D2D-capable IEDs	50m-100m
Preambles for contention-based access K	54
RACH configuration index	6
Backoff window size W	20ms
Preamble duration	1ms
Max. allowed preamble transmission attempts L	10
RAR window size	5ms
Contention resolution timer	24ms
Master information block periodicity	40ms
Payload for IED, UE	{250, 500}bytes
Min. rate requirement for UEs, $R_{i,\min}$	12Kbps

the transmission mode of IEDs conveying substation-event messages in cellular networks.

Simulation Setup

The numerical results are obtained by simulating the uplink of a single-cell network where synchronized cellular UEs are randomly (uniformly) dropped within the cell coverage area and generate background traffic. The random dropping model is also used for the location of the IED transmitters whereas the location of each IED receiver is distributed according to a uniform distribution in a circular area around its associated IED transmitter. We perform independent Monte Carlo experiments, each with a random network topology, to build statistics over the performance measures of interest when employing our MSRA mechanism. The MAP framework is used to capture the spatiotemporal correlation of the event-driven IED traffic and the well-studied expectation-maximization statistical framework [130] has been used for parameter $\{\mathbf{D}_0', \mathbf{D}_1'\}$ fitting based on the arrival traces of substation automation traffic captured by a discrete-event simulator that implements the IEC-61850 GOOSE protocol [5, 133].

Table 4.7 summarizes the basic parameters used in our simulations. The unsynchronized IEDs are assumed to contend for RACH access after a substation event and are dynamically signaled to transmit either in cellular or D2D-overlay mode according to the MSRA mechanism described in Subsection 4.2.3. Starting from a medium-load scenario, new channel access requests from IEDs appear progressively in the system until it is driven

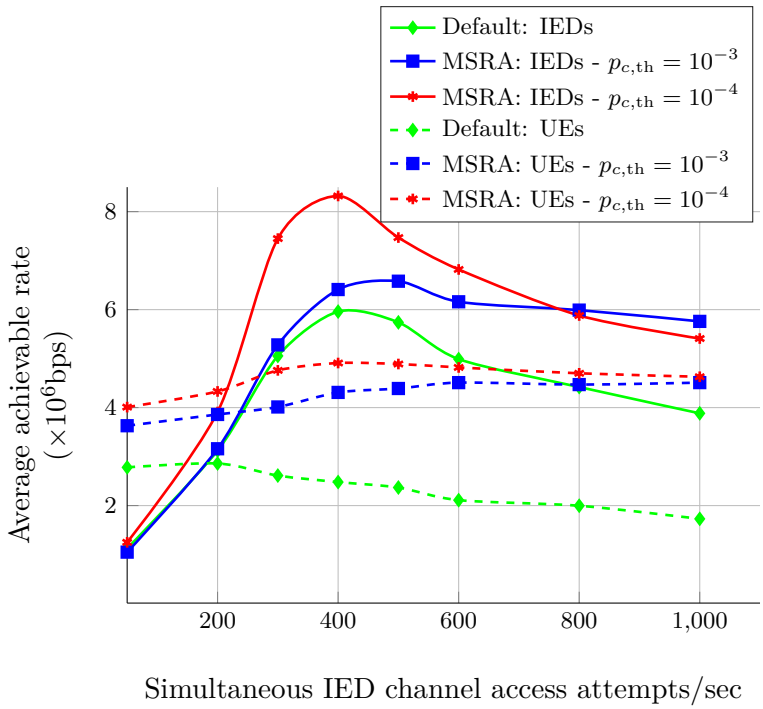

Figure 4.8: Average achievable rates for cellular UEs and D2D-capable IEDs in the default transmission case and with the proposed MSRA scheme for different preamble collision probability thresholds given $I^n_{\text{th}} = 0$dB and increasing IED traffic load.

to overload. The performance of the MSRA mechanism is then evaluated in terms of the average achievable rate when the system operates close to its capacity limits. In addition, we conduct a comparative evaluation of the MSRA scheme with the default case where IED transmission occurs solely in cellular mode via the base station and the priority-aware scheduler of [11] is used as a benchmark for the allocation of resources between the UE and IED links.

Performance Evaluation

The average achievable rates for cellular UEs and D2D-capable IEDs for different $p_{c,\text{th}}$ with increasing IED traffic load are illustrated in Figure 4.8. It can be observed that, compared to the default case when IED transmission occurs solely in cellular mode, our proposed MSRA mechanism achieves significant rate gains for both IEDs and UEs. By dynamically switching to D2D-overlay mode, the IEDs can exploit the shorter communication path to transmit their data in higher rates and drastically reduce the end-to-end latency. It is worth noting that the average rate gains can be leveraged even in heavy traffic load conditions where the IED achievable rate notably reaches approximately 1.5 times higher values. In addition, we observe that when our MSRA scheme is employed, the average rate of cellular UEs slightly increases with increasing IED rate, since IEDs switch to D2D-overlay mode more often, thus reducing the waiting time for the cellular UEs in the scheduling queue for cellular mode. The average rate of IEDs initially increases since the threshold $p_{c,\text{th}}$ gets violated and an increasing number of D2D-capable

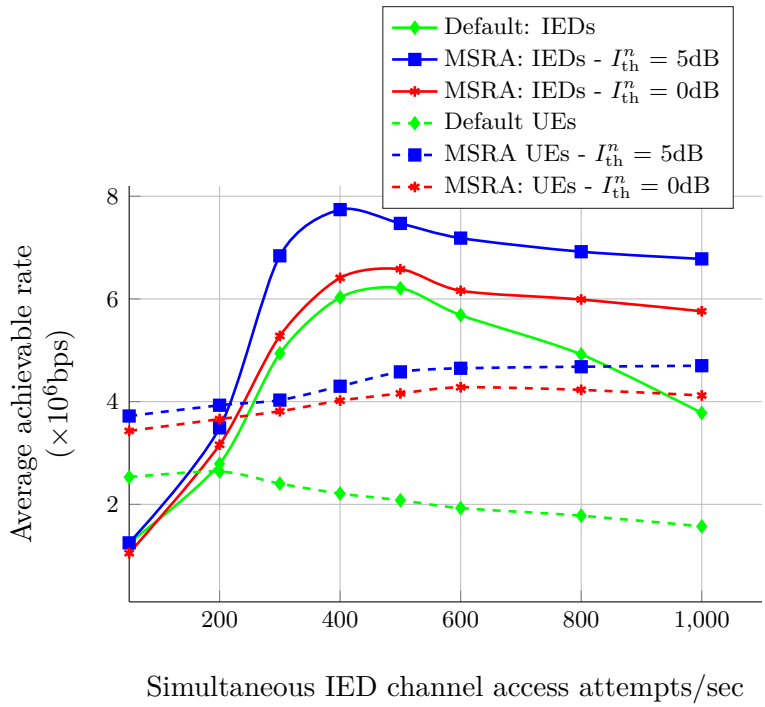

Figure 4.9: Average achievable rates for cellular UEs and D2D-capable IEDs in the default transmission case and with the proposed MSRA scheme for different interference tolerance levels given $p_{c,\text{th}} = 10^{-3}$ and increasing IED traffic load.

IEDs choose the D2D-overlay mode; however, it can be seen that the rate then starts decreasing due to the increased interference among the D2D links. This can be intuitively justified by the fact that the average rate of D2D-capable IEDs is determined by the rates for both cellular and D2D-overlay modes, as shown in Eq. (4.12). We further observe that a tighter $p_{c,\text{th}}$ initially results in higher average rates for both network entities, since more and more IED links switch to D2D-overlay; however, the higher D2D interference causes a quicker performance degradation for IEDs.

The effect of I^n_{th} in the average achievable rates of cellular UEs and D2D-capable IEDs with increasing IED traffic load is illustrated in Figure 4.9. Once again, it can be seen that our proposed MSRA mechanism outperforms the default scheme in terms of the rate performance of both IEDs and UEs, especially in the high traffic load regime where rate increases by a factor of 1.5-2.5. In particular, we observe that for the MSRA scheme the average rates are slightly affected by the different I^n_{th} in case of medium load, since the level of interference remains low. However, as IED load increases, the accumulated interference causes performance degradation for the D2D-capable IEDs which becomes even more severe when I^n_{th} is set to a more restrictive value. The impact of the performance parameters, $p_{c,\text{th}}$ and I^n_{th}, in the mode selection procedure is summarized in Table 4.8, where the fraction of IED links switching to D2D-overlay mode is quantified as a function of the IED load. It can be observed that the insights acquired from the observation of the rate figures are reflected in the amount of IED links transmitting in D2D-overlay mode.

Regarding the orthogonal partition of uplink cellular resources for cellular and D2D-

Table 4.8: Fraction of IED links in D2D-overlay mode with increasing IED traffic load.

Mode selection performance criteria	Fraction of IED links in D2D-overlay				
	IED access attempts/sec				
	200	400	600	800	1000
$p_{c,\text{th}} = 10^{-4}$, $I^n_{\text{th}} = 0$dB	0.41	1	0.92	0.73	0.51
$p_{c,\text{th}} = 10^{-3}$, $I^n_{\text{th}} = 0$dB	0.3	0.85	0.83	0.78	0.6
$p_{c,\text{th}} = 10^{-3}$, $I^n_{\text{th}} = 5$dB	0.28	0.91	0.86	0.82	0.69

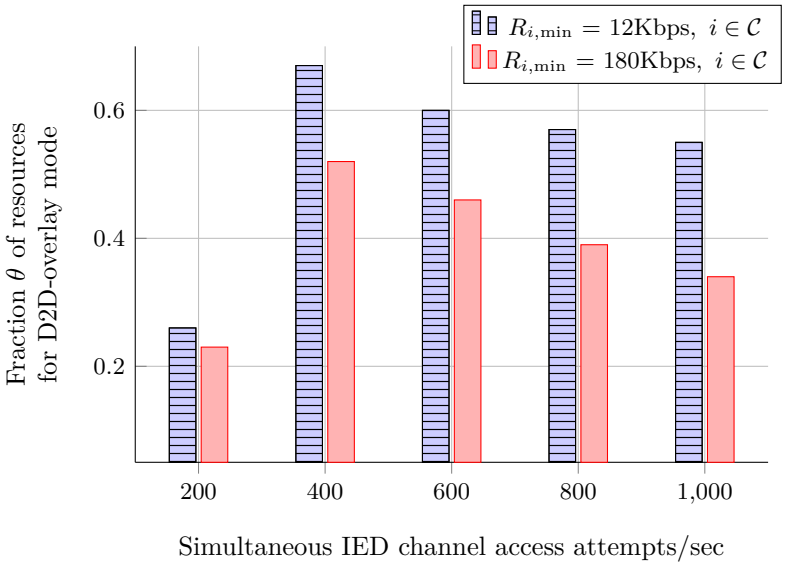

Figure 4.10: Fraction of resource block pairs allocated to IEDs in D2D-overlay mode for different minimum rate requirements of cellular UEs given $\{p_{c,\text{th}}, I^n_{\text{th}}\} = \{10^{-3}, 0dB\}$ and increasing IED traffic load for the MSRA scheme.

overlay modes, Figure 4.10 illustrates the fraction, θ in Eq. (4.7), of resource block pairs allocated to D2D-overlay mode as a function of the increasing IED load for different minimum rate requirements of the cellular UEs. In particular, it can be seen that θ initially increases since more and more IEDs switch to D2D-overlay mode. However, its value tends to decrease when the performance-protection requirement of cellular UEs is violated. This flexible resource utilization can yield improved spectral efficiency compared to traditional cellular communication. It is also worth noting that the decrease is more rapid in the case of demanding human-type services with higher minimum rate requirements, e.g., video services with GBR of 180Kbps instead of voice services with GBR equal to 12Kbps.

4.2.5 Summary

D2D communication is recognized as one of the promising radio enhancements of future cellular systems since it allows devices in physical proximity to communicate directly, bypassing the base station as in conventional cellular networks. However, the integration

of D2D capabilities in cellular networks poses new technical challenges and design problems. Transmission mode selection and resource allocation mechanisms are identified as key techniques to realize the full potential of this technology in scenarios where smart grid traffic coexists with human-type traffic. Mode selection for IEDs should be jointly performed with resource allocation decisions and their joint optimization generally leads to challenging problem formulations. In this section of Chapter 4, a joint MSRA mechanism was introduced for the support of event-driven substation automation traffic in cellular-enabled power distribution grids. In our proposed load- and interference-aware MSRA scheme, unsynchronized IEDs may seamlessly switch to D2D-overlay mode for data transmission, thus achieving higher transmission rates with respect to the conventional cellular mode, even in network overload conditions. In addition, the orthogonal resource allocation between cellular and D2D-overlay links is performed in a way that prevents the underutilization of the scarce cellular spectrum. The numerical evaluation of our proposed scheme under different performance criteria demonstrates the significant rate gains compared to traditional cellular communication. Useful design insights can thus be drawn for the applicability of D2D-overlay communication in substation automation scenarios.

Chapter 5

Conclusions and Future Work

5.1 Concluding Remarks

Cellular networks constitute a promising enabler for emerging smart grid operations associated with demanding communication requirements. In this context, this thesis has investigated RAN problems that arise when smart grid communication is integrated in LTE-based networks. In particular, we have focused on MAC and RRM issues related to random access and resource scheduling in future cellular networks. This thesis has proposed several protocols to enable massive and reliable smart grid data exchange and suggested fundamental RAN design guidelines for handling smart grid communication. As 3GPP standardization work is underway towards fulfilling the stringent MTC requirements, the results of this thesis are expected to provide novel insights towards massive and reliable MTC connectivity. In addition, the proposed original analysis may have the potential to substantially steer future protocol design principles by identifying robust techniques that lead to higher protocol performance. In what follows, we elaborate on the main conclusions drawn.

In Chapter 3, we have studied the congestion problem in LTE random access for massive smart grid communication with reliability guarantees. We have first identified the connectivity limitations of the standard LTE random access procedure due to high number of devices in large-scale smart metering and wide-area monitoring scenarios. In the latter case, the performance degradation becomes even more severe due to the event-based traffic activation patterns and the higher arrival intensity of monitoring messages. These observations call for the design of an efficient access mechanism to handle the traffic surge of simultaneous channel access requests and meet the strict latency requirements of mission-critical messages. To this end, we have introduced an adaptive radio access mechanism for the seamless integration of IEC-61850 communication services. Our proposed scheme properly modifies the network configuration parameters (i.e., preamble partition, barring rate) in traffic-overload conditions and exploits the spatial proximity of geographically adjacent devices to shed unnecessary preamble transmissions. It is worth noting that RACH congestion can be alleviated without significantly degrading the performance experienced by regular LTE subscribers.

While our focus so far had been on addressing the stringent latency constraints imposed by automation traffic, in the next part of Chapter 3 we turn our attention on the

reliability analysis of the LTE random access procedure for the support of the challenging event-based smart grid monitoring traffic. In particular, by leveraging tools from Markov chain theory, we have introduced a tractable analytical model of the contention-based LTE random access enhanced with a barring scheme for the connection establishment of a high number of monitoring devices. Since the random access procedure in emerging 3GPP enhancements, i.e., LTE-M, NB-IoT and NR, follows the same principles as in LTE-based systems, the rationale of the proposed analytical model can also be applicable for the performance analysis of smart grid monitoring traffic using other cellular IoT technologies. An accurate traffic model has been further proposed to capture the varying traffic behavior of IEDs. The developed framework allowed us to derive the analytical expression of the achieved reliability whose accuracy is validated with the aid of extensive simulations. A performance assessment reveals the impact of the monitoring traffic characteristics and RACH/barring parameters in the achieved reliability. The numerical results confirm that as the frequency of an IED traffic burst increases, the reliability decreases due to the higher arrival intensity in the alarm state which leads to a surge of channel access attempts. In addition, as the duration of each burst increases, the reliability decreases since the IEDs remain longer in the alarm state.

We have further observed that the availability of orthogonal random access preambles which, in turn, reflects the number of opportunities for channel access, severely affects the RACH reliability. This motivated us investigating the relation between the cell size and the availability of orthogonal preambles in a single LTE cell. The preambles are generated from a single or multiple ZC root sequences and their cyclic shifts. The larger the cell radius, the larger the cyclic shift required to generate orthogonal preambles, and consequently, the smaller the number of orthogonal preambles constructed by a single root sequence. Thus, as the cell radius increases, a higher number of ZC root sequences is necessary to provide the 64 required preambles in an LTE cell. However, preambles obtained from cyclic shifts of different root sequences are not orthogonal and induce intra-cell interference in the preamble reception. To this end, using our analytical expression of the RACH reliability per cell, we have introduced an interference- and load-aware cell planning mechanism that efficiently allocates the root sequences among multiple cells and regulates the traffic load via a barring parameter to guarantee reliable support of substation automation traffic. Our proposed mechanism employs a spatial ZC root sequence allocation scheme based on the preamble-decoding distance in an effort to mitigate the inter-cell interference. Since substation automation communication often involves the transmission of highly space- and time-correlated messages, we proposed a realistic traffic model to accurately capture the interdependent and non-exponential interarrival times. The numerical evaluation of our proposed mechanism has demonstrated its superiority in terms of RACH reliability with respect to benchmarking network deployment schemes.

Finally, we have studied the impact of RACH reliability on the state estimation accuracy performance in wide-area monitoring systems. Unlike the majority of existing literature where imperfect underlying communication, e.g., reliability limitations, is either neglected or limitedly considered for PMU information acquisition, we have assessed the state estimation accuracy performance based on the achieved reliability per PMU attained with *i*) increasing number of contending devices in the system and *ii*) varying cell coverage range. The numerical results reveal that the installation of additional PMUs not only helped reduce the state estimation uncertainty but also desensitized the

estimation error to the effect of the lower communication reliability caused by the increased background traffic load. On the other hand, we have observed that the achieved reliability per PMU severely degrades with the increasing cell radius, leading to a state estimation accuracy degradation that cannot be counterbalanced by a higher number of available synchronized measurements. The consideration of imperfect communication can thus provide useful insights for the design of reliability-aware state estimators for wide-area monitoring. In order to exploit the accuracy gains of PMUs' installation, network planning and cell size dimensioning need to be carefully configured.

Chapter 4 has been devoted to the problem of resource sharing and scheduling for smart grid and human-type traffic in shared LTE networks. We have first introduced an appropriate LTE scheduler for the integration of IEC-61850 data transmissions. The scheduling scheme applies traffic prioritization on smart grid data flows over human-type communication and rigorously considers the latency and throughput constraints in the resource allocation process. The simulation results of network-overload scenarios showed that our proposed scheduler can efficiently support automation services with minimum impact on background traffic.

The integration of D2D communication into cellular networks appears as a promising solution for enhancing the performance of next-generation networks. In an effort to exploit the benefits of D2D communication in event-driven substation automation scenarios, we have investigated the potential of IED direct information exchange over dedicated cellular resources, i.e., D2D-overlay mode. The joint problem of mode selection and resource allocation has been formulated as a sum-rate maximization problem using an analytical framework that captures both uplink communication phases, i.e., random access and data transmission. We have then proposed a mechanism that ensures *i*) seamless IED transition from cellular (i.e., communication via the eNodeB) to D2D-overlay mode upon detection of traffic overload and *ii*) efficient orthogonal resource partition for cellular and D2D links. Resource allocation has been performed in a way that prevents spectrum underutilization and guarantees a minimum rate requirement for the coexisting cellular users. The numerical evaluation of our proposed scheme has demonstrated that improved rate gains could be achieved for substation automation traffic.

Besides realizing the full potential of the smart grid paradigm, the research findings of this thesis may also prove useful for other emerging applications envisioned for 5G involving MTC, i.e., intelligent transportation, industrial control/automation and mobile health-care services. These applications are often associated with demanding requirements in terms of *i*) massive number of connected devices, *ii*) very high link reliability and *iii*) real-time operation (i.e., low latency). An example use case where our proposed RAN design solutions could be potentially applied is vehicle-to-everything (V2X) connectivity. To achieve low-latency and high-reliability for V2X services, the widely-deployed LTE-based systems have been considered as a promising solution to achieve ubiquitous cell coverage, controllable latency and high data rates. To this end, some of the radio access techniques discussed in this thesis could help mitigate RACH congestion in dense and rapidly-changing vehicular environments whereas our proposed RRM framework could improve the timely scheduling of mission-critical data transmissions in shared LTE-based vehicular networks, e.g., road safety and vulnerable user protection scenarios. In addition, vehicles could leverage the dynamic switch to direct D2D transmission mode to achieve lower latency and higher performance gains.

5.2 Future Work

Although many open issues and future works are suggested throughout the thesis, we hereby provide some additional research directions in which the work presented in this thesis can be extended:

- *Extensions of the RACH analytical framework*: The modeling approach for the LTE random access procedure adopted in this thesis could be properly extended to account for the packet transmission errors that may occur due to the wireless channel. We have further assumed that if two or more packets collide, then none of the packets can be decoded at the eNodeB, i.e., there is no capture effect. In addition, the failures of the connection request message due to insufficient physical downlink control channel resources could be also considered in our modeling approach as an additional limitation besides the contention in the uplink preamble transmission. Therefore, the theoretical framework to compute the RACH reliability could be extended by including also these signaling considerations.

- *Tradeoffs in uplink shared resources*: An interesting topic for future work is the investigation of the resource tradeoffs in the physical uplink shared channel. In LTE-based systems, part of the shared uplink resources are allocated for the transmission of connection request messages in the random access procedure whereas another part of the shared resources is devoted to the actual uplink data transmission. A resource management scheme needs to balance this tradeoff by properly dimensioning the resources when the number of contending devices becomes high and the available bandwidth is constrained.

- *Spectral efficiency considerations*: The dynamic spectrum usage and the efficient utilization of the radio resources are essential for the accommodation of dense deployments. Motivated by the emerging non-orthogonal multiple access, non-orthogonal random access schemes should be further pursued in future research as a means to increase system capacity and spectrum efficiency. The idea of relaxing the orthogonality constraint would enable a better handling of the increased smart grid demand for the scarce resources, since the number of supported devices would be no longer limited by the orthogonal resources. The challenge here mainly resides in the development of efficient successive interference cancellation techniques. Similarly, the D2D-underlay transmission mode could be investigated as an additional option for IEDs in Section 4.2 with the development of appropriate interference mitigation schemes with low computational overhead for the D2D-capable devices.

- *Artificial intelligence and machine learning*: Since massive random access problems deal with extremely large state spaces and actions, reinforcement learning methods could be substantially beneficial for online resource allocation decisions as they require low computation. Machine learning techniques could be used to infer smart grid traffic activation patterns in event-triggered substation automation scenarios and, in turn, allow the eNodeB to timely detect/predict potential network congestion in the RACH.

Bibliography

[1] C. Kalalas, L. Thrybom, and J. Alonso-Zarate, "Cellular Communications for Smart Grid Neighborhood Area Networks: A Survey," *IEEE Access*, vol. 4, pp. 1469–1493, April 2016.

[2] A. Rico-Alvarino, M. Vajapeyam, H. Xu, X. Wang, Y. Blankenship, J. Bergman, T. Tirronen, and E. Yavuz, "An overview of 3GPP enhancements on machine to machine communications," *IEEE Communications Magazine*, vol. 54, pp. 14–21, June 2016.

[3] M. Cosovic, A. Tsitsimelis, D. Vukobratovic, J. Matamoros, and C. Antón-Haro, "5G Mobile Cellular Networks: Enabling Distributed State Estimation for Smart Grids," *IEEE Communications Magazine*, vol. 55, pp. 62–69, October 2017.

[4] A. Laya, C. Kalalas, F. Vazquez-Gallego, L. Alonso, and J. Alonso-Zarate, "Goodbye, ALOHA!," *IEEE Access*, vol. 4, pp. 2029–2044, April 2016.

[5] C. Kalalas, F. Vazquez-Gallego, and J. Alonso-Zarate, "Handling mission-critical communication in smart grid distribution automation services through LTE," in *IEEE International Conference on Smart Grid Communications (SmartGridComm)*, pp. 399–404, November 2016.

[6] C. Kalalas and F. Vazquez-Gallego and J. Alonso-Zarate, "Performance Evaluation of the Contention-Based Random Access of LTE Under Smart Grid Traffic," in *Smart Grid Inspired Future Technologies* (Lau E. et al. (eds), ed.), vol. 203 of *Lecture Notes of the Institute for Computer Sciences, Social Informatics and Telecommunications Engineering*, pp. 172–181, Springer, Cham, August 2017.

[7] C. Kalalas and J. Alonso-Zarate, "Reliability analysis of the random access channel of LTE with access class barring for smart grid monitoring traffic," in *IEEE International Conference on Communications Workshops (ICC Wkshps)*, pp. 724–730, May 2017.

[8] C. Kalalas and J. Alonso-Zarate, "Efficient Cell Planning for Reliable Support of Event-Driven Machine-Type Traffic in LTE," in *IEEE Global Communications Conference (GLOBECOM)*, pp. 1–7, December 2017.

[9] A. Tsitsimelis, C. Kalalas, J. Alonso-Zarate, and C. Antón-Haro, "On the Impact of LTE RACH Reliability on State Estimation in Wide-Area Monitoring Systems,"

in *IEEE Wireless Communications and Networking Conference (WCNC)*, pp. 1–6, April 2018.

[10] Ericsson White Paper, "LTE for Utilities, Supporting Smart Grids," September 2013.

[11] C. Kalalas, L. Gkatzikis, C. Fischione, P. Ljungberg, and J. Alonso-Zarate, "Enabling IEC 61850 communication services over public LTE infrastructure," in *IEEE International Conference on Communications (ICC)*, pp. 1–6, May 2016.

[12] C. Kalalas, J. Alonso-Zarate, and G. Bag, "On the Transmission Mode Selection for Substation Automation Traffic in Cellular Networks," in *IEEE International Conference on Smart Grid Communications (SmartGridComm)*, pp. 1–7, October 2017.

[13] F. Vazquez-Gallego, C. Kalalas, L. Alonso, and J. Alonso-Zarate, "Contention Tree-Based Access for Wireless Machine-to-Machine Networks With Energy Harvesting," *IEEE Transactions on Green Communications and Networking*, vol. 1, pp. 223–234, June 2017.

[14] A. Pouttu, J. Haapola, P. Ahokangas, Y. Xu, M. Kopsakangas-Savolainen, E. Porras, J. Matamoros, C. Kalalas, J. Alonso-Zarate, F. D. Gallego, J. M. Martín, G. Deconinck, H. Almasalma, S. Clayes, J. Wu, M. Cheng, F. Li, Z. Zhang, D. Rivas, and S. Casado, "P2P model for distributed energy trading, grid control and ICT for local smart grids," in *European Conference on Networks and Communications (EuCNC)*, pp. 1–6, June 2017.

[15] J. Haapola and S. Ali and C. Kalalas and J. Markkula and N. Rajatheva and A. Pouttu and J. M. Martín Rapún and I. Lalaguna and F. Vazquez-Gallego and J. Alonso-Zarate and G. Deconinck and H. Almasalma and J. Wu and C. Zhang and E. Porras Muñoz and F. David Gallego, "Peer-to-Peer Energy Trading and Grid Control Communications Solutions' Feasibility Assessment based on Key Performance Indicators," in *IEEE Vehicular Technology Conference (VTC-Spring), Workshop on Enabling Internet via Machine type Wireless Communications*, pp. 1–6, June 2018.

[16] A. P. Dempster and N. M. Laird and D. B. Rubin, "Maximum likelihood from incomplete data via the EM algorithm," *Journal of the Royal Statistical Society, Series B*, vol. 39, pp. 1–38, January 1977.

[17] C. F. Jeff Wu, "On the Convergence Properties of the EM Algorithm," *The Annals of Statistics*, vol. 11, pp. 95–103, March 1983.

[18] 3GPP TR 37.868 v11.0.0, "Study on RAN improvements for Machine-Type Communications," Release 11, September 2011.

[19] Q. Yang, J. Barria, and T. Green, "Communication Infrastructures for Distributed Control of Power Distribution Networks," *IEEE Transactions on Industrial Informatics*, vol. 7, pp. 316–327, May 2011.

[20] A. Timbus, M. Larsson, and C. Yuen, "Active Management of Distributed Energy Resources Using Standardized Communications and Modern Information Technologies," *IEEE Transactions on Industrial Electronics*, vol. 56, pp. 4029–4037, October 2009.

[21] P. Parikh, T. Sidhu, and A. Shami, "A Comprehensive Investigation of Wireless LAN for IEC 61850-Based Smart Distribution Substation Applications," *IEEE Transactions on Industrial Informatics*, vol. 9, pp. 1466–1476, August 2013.

[22] G. Zhabelova and V. Vyatkin, "Multiagent Smart Grid Automation Architecture Based on IEC 61850/61499 Intelligent Logical Nodes," *IEEE Transactions on Industrial Electronics*, vol. 59, pp. 2351–2362, May 2012.

[23] V. Vyatkin, G. Zhabelova, N. Higgins, K. Schwarz, and N. Nair, "Towards intelligent Smart Grid devices with IEC 61850 Interoperability and IEC 61499 open control architecture," in *IEEE Power Energy Society Transmission and Distribution Conference and Exposition*, pp. 1–8, April 2010.

[24] R. Mackiewicz, "Overview of IEC 61850 and Benefits," in *IEEE PES Transmission and Distribution Conference and Exhibition*, pp. 376–383, May 2006.

[25] IEC, "IEC 61850-90-5 TR Ed.1: Communication networks and systems for power utility automation - Part 90-5: Use of IEC 61850 to transmit synchrophasor information according to IEEE C37.118," 2011.

[26] IEC, "IEC 61850-90-1: Communication networks and systems for power utility automation - Part 90-1: Use of IEC 61850 for the communication between substations," 2010.

[27] V. Gungor, D. Sahin, T. Kocak, S. Ergut, C. Buccella, C. Cecati, and G. Hancke, "Smart Grid Technologies: Communication Technologies and Standards," *IEEE Transactions on Industrial Informatics*, vol. 7, pp. 529–539, November 2011.

[28] W. Meng, R. Ma, and H.-H. Chen, "Smart grid neighborhood area networks: a survey," *IEEE Network*, vol. 28, pp. 24–32, January 2014.

[29] S. Sesia, I. Toufik, and M. Baker, *LTE: The UMTS Long Term Evolution from theory to practice*. John Wiley & Sons Ltd., February 2009.

[30] 3GPP, "Evolved Universal Terrestrial Radio Access (E-UTRA); Physical Channels and Modulation," March 2010.

[31] S.-B. Lee, I. Pefkianakis, A. Meyerson, S. Xu, and S. Lu, "Proportional Fair Frequency-Domain Packet Scheduling for 3GPP LTE Uplink," in *IEEE International Conference on Computer Communications (INFOCOM)*, pp. 2611–2615, April 2009.

[32] 3GPP TS 23.203 v14.3.0, "Policy and charging control architecture," Release 14, December 2017.

[33] E. Dahlman, S. Parkvall, and J. Skold, *4G: LTE/LTE-Advanced for Mobile Broadband*. Academic Press, May 2011.

[34] 3GPP TS 22.368 v12.1.0, "Service requirements for Machine-Type Communications (MTC) Stage 1," Release 12, December 2012.

[35] P. Phunchongharn, E. Hossain, and D. Kim, "Resource allocation for device-to-device communications underlaying LTE-advanced networks," *IEEE Wireless Communications*, vol. 20, pp. 91–100, August 2013.

[36] G. Fodor, E. Dahlman, G. Mildh, S. Parkvall, N. Reider, G. Miklós, and Z. Turányi, "Design aspects of network assisted device-to-device communications," *IEEE Communications Magazine*, vol. 50, pp. 170–177, March 2012.

[37] M. Eriksson, M. Armendariz, O. Vasilenko, A. Saleem, and L. Nordstrom, "Multiagent-Based Distribution Automation Solution for Self-Healing Grids," *IEEE Transactions on Industrial Electronics*, vol. 62, pp. 2620–2628, April 2015.

[38] N. Cheng, N. Lu, N. Zhang, T. Yang, X. . Shen, and J. W. Mark, "Vehicle-Assisted Device-to-Device Data Delivery for Smart Grid," *IEEE Transactions on Vehicular Technology*, vol. 65, pp. 2325–2340, April 2016.

[39] N. Maskey, S. Horsmanheimo, and L. Tuomimaki, "Analysis of latency for cellular networks for smart grid in suburban area," in *IEEE Power Energy Society Innovative Smart Grid Technologies Conference Europe (ISGT-Europe)*, pp. 1–4, October 2014.

[40] S. Horsmanheimo, N. Maskey, and L. Tuomimaki, "Feasibility study of utilizing mobile communications for smart grid applications in urban area," in *IEEE International Conference on Smart Grid Communications (SmartGridComm)*, pp. 440–445, November 2014.

[41] P. Ferrari, A. Flammini, M. Loda, S. Rinaldi, D. Pagnoncelli, and E. Ragaini, "First experimental characterization of LTE for automation of Smart Grid," in *IEEE International Workshop on Applied Measurements for Power Systems (AMPS)*, pp. 108–113, September 2015.

[42] J. Brown and J. Khan, "Performance comparison of LTE FDD and TDD based Smart Grid communications networks for uplink biased traffic," in *IEEE International Conference on Smart Grid Communications (SmartGridComm)*, pp. 276–281, November 2012.

[43] J. Brown and J. Khan, "Performance analysis of an LTE TDD based smart grid communications network for uplink biased traffic," in *IEEE Global Communications Conference Workshops (GC Wkshps)*, pp. 1502–1507, December 2012.

[44] P. Cheng, L. Wang, B. Zhen, and S. Wang, "Feasibility study of applying LTE to Smart Grid," in *2011 IEEE International Workshop on Smart Grid Modeling and Simulation (SGMS)*, pp. 108–113, October 2011.

[45] J. Markkula and J. Haapola, "Impact of smart grid traffic peak loads on shared LTE network performance," in *IEEE International Conference on Communications (ICC)*, pp. 4046–4051, June 2013.

[46] J. Markkula and J. Haapola, "LTE and hybrid sensor-LTE network performances in smart grid demand response scenarios," in *IEEE International Conference on Smart Grid Communications (SmartGridComm)*, pp. 187–192, October 2013.

[47] O. Al-Khatib, W. Hardjawana, and B. Vucetic, "Queuing analysis for Smart Grid communications in wireless access networks," in *IEEE International Conference on Smart Grid Communications (SmartGridComm)*, pp. 374–379, November 2014.

[48] M. Gerasimenko, V. Petrov, O. Galinina, S. Andreev, and Y. Koucheryavy, "Energy and delay analysis of LTE-Advanced RACH performance under MTC overload," in *IEEE Global Communications Conference Workshops (GC Wkshps)*, pp. 1632–1637, December 2012.

[49] C. Hagerling, C. Ide, and C. Wietfeld, "Coverage and capacity analysis of wireless M2M technologies for smart distribution grid services," in *IEEE International Conference on Smart Grid Communications (SmartGridComm)*, pp. 368–373, November 2014.

[50] R. Ratasuk, S. Iraji, K. Hugl, L. Wang, and A. Ghosh, "Performance of Low-Cost LTE Devices for Advanced Metering Infrastructure," in *IEEE Vehicular Technology Conference (VTC Spring)*, pp. 1–5, June 2013.

[51] C. Muller, M. Putzke, and C. Wietfeld, "Traffic engineering analysis of smart grid services in cellular networks," in *IEEE Third International Conference on Smart Grid Communications (SmartGridComm)*, pp. 252–257, November 2012.

[52] C. Karupongsiri, K. Munasinghe, and A. Jamalipour, "Random access issues for smart grid communication in LTE networks," in *International Conference on Signal Processing and Communication Systems (ICSPCS)*, pp. 1–5, December 2014.

[53] M. R. Souryal and N. Golmie, "Analysis of advanced metering over a Wide Area Cellular Network," in *IEEE International Conference on Smart Grid Communications (SmartGridComm)*, pp. 102–107, October 2011.

[54] C.-H. Wei, R.-G. Cheng, and F. Al-Taee, "Dynamic radio resource allocation for group paging supporting smart meter communications," in *IEEE International Conference on Smart Grid Communications (SmartGridComm)*, pp. 659–663, November 2012.

[55] C. Karupongsiri, K. S. Munasinghe, and A. Jamalipour, "Smart meter packet transmission via the control signal of LTE networks," in *IEEE International Conference on Communications (ICC)*, pp. 2991–2996, June 2015.

[56] S. Andreev, A. Larmo, M. Gerasimenko, V. Petrov, O. Galinina, T. Tirronen, J. Torsner, and Y. Koucheryavy, "Efficient small data access for machine-type communications in LTE," in *IEEE International Conference on Communications (ICC)*, pp. 3569–3574, June 2013.

[57] G. C. Madueño, N. K. Pratas, C. Stefanović, and P. Popovski, "Massive M2M access with reliability guarantees in LTE systems," in *IEEE International Conference on Communications (ICC)*, pp. 2997–3002, June 2015.

[58] K. Zhou and N. Nikaein, "Packet aggregation for machine type communications in LTE with random access channel," in *IEEE Wireless Communications and Networking Conference (WCNC)*, pp. 262–267, April 2013.

[59] J. Brown and J. Khan, "Reflection: An efficient technique for implementing an LTE based wireless network control system for smart grid and other applications," in *IEEE International Conference on Communications (ICC)*, pp. 4052–4057, June 2013.

[60] M. Shahab, A. Hussain, and M. Shoaib, "Smart grid traffic modeling and scheduling using 3GPP LTE for efficient communication with reduced RAN delays," in *International Conference on Telecommunications and Signal Processing (TSP)*, pp. 263–267, July 2013.

[61] G. Karagiannis, G. Pham, A. Nguyen, G. Heijenk, B. Haverkort, and F. Campfens, "Performance of LTE for Smart Grid Communications," in *Measurement, Modelling, and Evaluation of Computing Systems and Dependability and Fault Tolerance* (K. Fischbach and U. Krieger, eds.), vol. 8376 of *Lecture Notes in Computer Science*, pp. 225–239, Springer International Publishing, March 2014.

[62] E. Yaacoub and A. Kadri, "LTE radio resource management for real-time smart meter reading in the smart grid," in *IEEE International Conference on Communications Workshops (ICC Wkshps)*, pp. 2000–2005, June 2015.

[63] C. Karupongsiri, M. Hossain, K. Munasinghe, and A. Jamalipour, "A novel scheduling technique for Smart Grid data on LTE networks," in *International Conference on Signal Processing and Communication Systems (ICSPCS)*, pp. 1–5, December 2013.

[64] A. Gotsis, A. Lioumpas, and A. Alexiou, "Evolution of packet scheduling for Machine-Type communications over LTE: Algorithmic design and performance analysis," in *IEEE Global Communications Conference Workshops (GC Wkshps)*, pp. 1620–1625, December 2012.

[65] Z. Ruiyi, Y. Jian, and S. Zhang, "An adaptive resource allocation scheme in LTE uplink transmission for smart grid," in *Chinese Control Conference (CCC)*, pp. 8857–8862, July 2013.

[66] N. Afrin, J. Brown, and J. Y. Khan, "A delay sensitive LTE uplink packet scheduler for M2M traffic," in *IEEE Globecom Workshops (GC Wkshps)*, pp. 941–946, December 2013.

[67] M. N. Hindia, A. W. Reza, and K. A. Noordin, "A Novel Scheduling Algorithm Based on Game Theory and Multicriteria Decision Making in LTE Network," *International Journal of Distributed Sensor Networks*, Article ID 604752, pp. 1–8, January 2015.

[68] M. Carlesso, A. Antonopoulos, F. Granelli, and C. Verikoukis, "Uplink scheduling for smart metering and real-time traffic coexistence in LTE networks," in *IEEE International Conference on Communications (ICC)*, pp. 820–825, June 2015.

[69] Y. Xu and C. Fischione, "Real-time scheduling in LTE for smart grids," in *International Symposium on Communications Control and Signal Processing (ISCCSP)*, pp. 1–6, May 2012.

[70] S. Chen, "A novel TD-LTE frame structure for heavy uplink traffic in smart grid," in *IEEE Innovative Smart Grid Technologies - Asia (ISGT Asia)*, pp. 158–163, May 2014.

[71] S. Louvros, M. Paraskevas, V. Triantafyllou, and A. Baltagiannis, "LTE uplink delay constraints for smart grid applications," in *IEEE International Workshop on Computer Aided Modeling and Design of Communication Links and Networks (CAMAD)*, pp. 110–114, December 2014.

[72] A. Awad, S. Moarrab, and R. German, "QoS implementation inside LTE networks to support time-critical smart grid applications," in *IEEE International Conference on Environment and Electrical Engineering (EEEIC)*, pp. 1204–1209, June 2015.

[73] N. Saxena and A. Roy, "Exploiting multicast in LTE networks for smart grids demand response," in *IEEE International Conference on Communications (ICC)*, pp. 3155–3160, June 2015.

[74] M. Garau, M. Anedda, C. Desogus, E. Ghiani, M. Murroni, and G. Celli, "A 5G cellular technology for distributed monitoring and control in smart grid," in *IEEE International Symposium on Broadband Multimedia Systems and Broadcasting (BMSB)*, pp. 1–6, June 2017.

[75] K. D. Lee, S. Kim, and B. Yi, "Throughput comparison of random access methods for M2M service over LTE networks," in *IEEE Global Communications Conference (GC Wkshps)*, pp. 373–377, December 2011.

[76] J. P. Cheng, C. h. Lee, and T. M. Lin, "Prioritized Random Access with dynamic access barring for RAN overload in 3GPP LTE-A networks," in *IEEE Global Communications Conference Workshops (GC Wkshps)*, pp. 368–372, December 2011.

[77] 3GPP TS 36.331 V10.5.0, "Evolved Universal Terrestrial Radio Access (E-UTRA); Radio Resource Control (RRC)," March 2012.

[78] M. Angjelichinoski, M. Cosovic, C. Kalalas, R. Lliuyacc, M. Zeinali, J. Alonso-Zarate, J. Manuel Mauricio, P. Popovski, C. Stefanovic, J. S Thompson, D. Vukobratovic, "Overview of research in the ADVANTAGE project," in *Smarter Energy: from Smart Metering to the Smart Grid*, Energy Engineering, pp. 335–379, Institution of Engineering and Technology, October 2016.

[79] A. Asadi, Q. Wang, and V. Mancuso, "A Survey on Device-to-Device Communication in Cellular Networks," *IEEE Communications Surveys Tutorials*, vol. 16, pp. 1801–1819, Fourthquarter 2014.

[80] L. B. Le, "Fair resource allocation for device-to-device communications in wireless cellular networks," in *IEEE Global Communications Conference (GLOBECOM)*, pp. 5451–5456, December 2012.

[81] M.-H. Han, B.-G. Kim, and J.-W. Lee, "Subchannel and Transmission Mode Scheduling for D2D Communication in OFDMA Networks," in *IEEE Vehicular Technology Conference (VTC Fall)*, pp. 1–5, September 2012.

[82] L. Su, Y. Ji, P. Wang, and F. Liu, "Resource allocation using particle swarm optimization for D2D communication underlay of cellular networks," in *IEEE Wireless Communications and Networking Conference (WCNC)*, pp. 129–133, April 2013.

[83] D. Feng, L. Lu, Y. Yuan-Wu, G. Li, G. Feng, and S. Li, "Optimal resource allocation for device-to-device communications in fading channels," in *IEEE Global Communications Conference (GLOBECOM)*, pp. 3673–3678, December 2013.

[84] H. Min, J. Lee, S. Park, and D. Hong, "Capacity Enhancement Using an Interference Limited Area for Device-to-Device Uplink Underlaying Cellular Networks," *IEEE Transactions on Wireless Communications*, vol. 10, pp. 3995–4000, December 2011.

[85] X. Chen, L. Chen, M. Zeng, X. Zhang, and D. Yang, "Downlink resource allocation for Device-to-Device communication underlaying cellular networks," in *IEEE International Symposium on Personal Indoor and Mobile Radio Communications (PIMRC)*, pp. 232–237, September 2012.

[86] B. Kaufman and B. Aazhang, "Cellular networks with an overlaid device to device network," in *Asilomar Conference on Signals, Systems and Computers*, pp. 1537–1541, October 2008.

[87] T. Peng, Q. Lu, H. Wang, S. Xu, and W. Wang, "Interference avoidance mechanisms in the hybrid cellular and device-to-device systems," in *IEEE International Symposium on Personal, Indoor and Mobile Radio Communications (PIMRC)*, pp. 617–621, September 2009.

[88] P. Janis, C. Yu, K. Doppler, C. Ribeiro, C. Wijting, K. Hugl, O. Tirkkonen, and V. Koivunen, "Device-to-Device Communication Underlaying Cellular Communications Systems," *International Journal of Communications, Network and System Sciences*, vol. 2, pp. 169–178, June 2009.

[89] N. Lee, X. Lin, J. Andrews, and R. Heath, "Power Control for D2D Underlaid Cellular Networks: Modeling, Algorithms, and Analysis," *IEEE Journal on Selected Areas in Communications*, vol. 33, pp. 1–13, January 2015.

[90] K. Vanganuru, S. Ferrante, and G. Sternberg, "System capacity and coverage of a cellular network with D2D mobile relays," in *Military Communications Conference (MILCOM)*, pp. 1–6, October 2012.

[91] J. Han, Q. Cui, C. Yang, M. Valkama, and X. Tao, "Optimized power allocation and spectrum sharing in device to device underlaying cellular systems," in *IEEE Wireless Communications and Networking Conference (WCNC)*, pp. 1332–1337, April 2014.

[92] F. Wang, L. Song, Z. Han, Q. Zhao, and X. Wang, "Joint scheduling and resource allocation for device-to-device underlay communication," in *IEEE Wireless Communications and Networking Conference (WCNC)*, pp. 134–139, April 2013.

[93] P. Janis, V. Koivunen, C. Ribeiro, J. Korhonen, K. Doppler, and K. Hugl, "Interference-Aware Resource Allocation for Device-to-Device Radio Underlaying Cellular Networks," in *IEEE Vehicular Technology Conference (VTC Spring)*, pp. 1–5, April 2009.

[94] M. Zulhasnine, C. Huang, and A. Srinivasan, "Efficient resource allocation for device-to-device communication underlaying LTE network," in *IEEE International Conference on Wireless and Mobile Computing, Networking and Communications (WiMob)*, pp. 368–375, October 2010.

[95] R. Zhang, X. Cheng, L. Yang, and B. Jiao, "Interference-aware graph based resource sharing for device-to-device communications underlaying cellular networks," in *IEEE Wireless Communications and Networking Conference (WCNC)*, pp. 140–145, April 2013.

[96] M. Botsov, M. Klugel, W. Kellerer, and P. Fertl, "Location dependent resource allocation for mobile device-to-device communications," in *IEEE Wireless Communications and Networking Conference (WCNC)*, pp. 1679–1684, April 2014.

[97] K. Doppler, M. Rinne, C. Wijting, C. Ribeiro, and K. Hugl, "Device-to-device communication as an underlay to LTE-advanced networks," *IEEE Communications Magazine*, vol. 47, pp. 42–49, December 2009.

[98] K. Zheng, F. Hu, W. Wang, W. Xiang, and M. Dohler, "Radio resource allocation in LTE-advanced cellular networks with M2M communications," *IEEE Communications Magazine*, vol. 50, pp. 184–192, July 2012.

[99] B. Guo, S. Sun, and Q. Gao, "Graph-Based Resource Allocation for D2D Communications Underlying Cellular Networks in Multiuser Scenario," *International Journal of Antennas and Propagation*, vol. 2014, pp. 1–6, August 2014.

[100] C. Xia, S. Xu, and K. S. Kwak, "Resource Allocation for Device-to-Device Communication in LTE-A Network: A Stackelberg Game Approach," in *IEEE Vehicular Technology Conference (VTC Fall)*, pp. 1–5, September 2014.

[101] Q. Ye, M. Al-Shalash, C. Caramanis, and J. Andrews, "Distributed Resource Allocation in Device-to-Device Enhanced Cellular Networks," *IEEE Transactions on Communications*, vol. 63, pp. 441–454, February 2015.

[102] Q. Ye, M. Al-Shalash, C. Caramanis, and J. Andrews, "Resource Optimization in Device-to-Device Cellular Systems Using Time-Frequency Hopping," *IEEE Transactions on Wireless Communications*, vol. 13, pp. 5467–5480, October 2014.

[103] X. Lin, J. Andrews, and A. Ghosh, "Spectrum Sharing for Device-to-Device Communication in Cellular Networks," *IEEE Transactions on Wireless Communications*, vol. 13, pp. 6727–6740, December 2014.

[104] C. Xu, L. Song, Z. Han, D. Li, and B. Jiao, "Resource allocation using a reverse iterative combinatorial auction for device-to-device underlay cellular networks," in *IEEE Global Communications Conference (GLOBECOM)*, pp. 4542–4547, December 2012.

[105] C. Xu, L. Song, Z. Han, Q. Zhao, X. Wang, and B. Jiao, "Interference-aware resource allocation for device-to-device communications as an underlay using sequential second price auction," in *IEEE International Conference on Communications (ICC)*, pp. 445–449, June 2012.

[106] X. Xiao, X. Tao, and J. Lu, "A QoS-Aware Power Optimization Scheme in OFDMA Systems with Integrated Device-to-Device (D2D) Communications," in *IEEE Vehicular Technology Conference (VTC Fall)*, pp. 1–5, September 2011.

[107] M. Belleschi, G. Fodor, and A. Abrardo, "Performance analysis of a distributed resource allocation scheme for D2D communications," in *IEEE Global Communications Conference Workshops (GC Wkshps)*, pp. 358–362, December 2011.

[108] Y. Li, D. Jin, F. Gao, and L. Zeng, "Joint optimization for resource allocation and mode selection in Device-to-Device communication underlaying cellular networks," in *IEEE International Conference on Communications (ICC)*, pp. 2245–2250, June 2014.

[109] Z. Chen and M. Kountouris, "Distributed SIR-aware opportunistic access control for D2D underlaid cellular networks," in *IEEE Global Communications Conference (GLOBECOM)*, pp. 1540–1545, December 2014.

[110] A. Gotsis, A. S. Lioumpas, and A. Alexiou, "Analytical modelling and performance evaluation of realistic time-controlled M2M scheduling over LTE cellular networks," *Transactions on Emerging Telecommunications Technologies*, vol. 24, pp. 378–388, March 2013.

[111] K. Zhou, N. Nikaein, R. Knopp, and C. Bonnet, "Contention Based Access for Machine-Type Communications over LTE," in *IEEE Vehicular Technology Conference (VTC Spring)*, pp. 1–5, May 2012.

[112] C. Lee, S.-M. Oh, and A.-S. Park, "Interference avoidance resource allocation for D2D communication based on graph-coloring," in *International Conference on Information and Communication Technology Convergence (ICTC)*, pp. 895–896, October 2014.

[113] B. Cho, K. Koufos, and R. Jantti, "Spectrum allocation and mode selection for overlay D2D using carrier sensing threshold," in *International Conference on Cognitive Radio Oriented Wireless Networks and Communications (CROWNCOM)*, pp. 26–31, June 2014.

[114] B. Zhou, H. Hu, S.-Q. Huang, and H.-H. Chen, "Intracluster Device-to-Device Relay Algorithm With Optimal Resource Utilization," *IEEE Transactions on Vehicular Technology*, vol. 62, pp. 2315–2326, June 2013.

[115] X. Lin and J. Andrews, "Optimal spectrum partition and mode selection in device-to-device overlaid cellular networks," in *IEEE Global Communications Conference (GLOBECOM)*, pp. 1837–1842, December 2013.

[116] Q. Ye, M. Al-Shalash, C. Caramanis, and J. Andrews, "A tractable model for optimizing device-to-device communications in downlink cellular networks," in *IEEE International Conference on Communications (ICC)*, pp. 2039–2044, June 2014.

[117] B. Zhou, S. Ma, J. Xu, and Z. Li, "Group-wise channel sensing and resource preallocation for LTE D2D on ISM band," in *IEEE Wireless Communications and Networking Conference (WCNC)*, pp. 118–122, April 2013.

[118] J. Bai, C. Liu, and A. Sabharwal, "Increasing Cellular Capacity Using ISM Band Side-channels: A First Study," in *Proceedings of the 4th Workshop on All Things Cellular: Operations, Applications and Challenges*, AllThingsCellular '14, (New York, NY, USA), pp. 9–14, ACM, 2014.

[119] T.-S. Kim, R. Oh, S.-J. Lee, S.-H. Yoon, C.-H. Cho, and S.-W. Ryu, "Vertical Handover Between LTE and Wireless LAN Systems Based on Common Resource Management (CRRM) and Generic Link Layer (GLL)," in *International Conference on Interaction Sciences: Information Technology, Culture and Human*, ICIS '09, (New York, NY, USA), pp. 1160–1166, ACM, 2009.

[120] L. Nithyanandan and I. Parthiban, "Seamless vertical handoff in heterogeneous networks using IMS technology," in *International Conference on Communications and Signal Processing (ICCSP)*, pp. 32–35, April 2012.

[121] S. J. Bae, M. Y. Chung, and J. So, "Handover triggering mechanism based on IEEE 802.21 in heterogeneous networks with LTE and WLAN," in *International Conference on Information Networking (ICOIN)*, pp. 399–403, January 2011.

[122] J. M. Rodríguez Castillo, "Energy-Efficient Vertical Handovers," KTH Royal Institute of Technology, September 2013.

[123] A. Miyim, M. Ismail, R. Nordin, and G. Mahardhika, "Generic vertical handover prediction algorithm for 4G wireless networks," in *IEEE International Conference on Space Science and Communication (IconSpace)*, pp. 307–312, July 2013.

[124] A. Laya, L. Alonso, P. Chatzimisios, and J. Alonso-Zarate, "Reliable Machine-to-Machine Multicast Services with Multi-Radio Cooperative Retransmissions," *Mobile Networks and Applications*, pp. 1–11, February 2015.

[125] W. Yoon and B. Jang, "Enhanced Non-Seamless Offload for LTE and WLAN Networks," *IEEE Communications Letters*, vol. 17, pp. 1960–1963, October 2013.

[126] F. Rebecchi, M. Dias de Amorim, and V. Conan, "Flooding Data in a Cell: Is Cellular Multicast Better Than Device-to-device Communications?," in *ACM MobiCom Workshop on Challenged Networks*, CHANTS '14, (New York, NY, USA), pp. 19–24, ACM, September 2014.

[127] J. Sachs, N. Beijar, P. Elmdahl, J. Melen, F. Militano, and P. Salmela, "Capillary networks - a smart way to get things connected," Ericsson Review, September 2014.

[128] H. Heffes and D. Lucantoni, "A Markov Modulated Characterization of Packetized Voice and Data Traffic and Related Statistical Multiplexer Performance," *IEEE Journal on Selected Areas in Communications*, vol. 4, pp. 856–868, September 1986.

[129] W. Fischer and K. Meier-Hellstern, "The Markov-modulated Poisson Process (MMPP) Cookbook," *Performance Evaluation*, vol. 18, pp. 149–171, September 1993.

[130] M. F. Neuts, *Structured Stochastic Matrices of M/G/1 Type and Their Applications*. New York: Marcel Dekker, July 1989.

[131] A. Laya, L. Alonso, and J. Alonso-Zarate, "Is the Random Access Channel of LTE and LTE-A Suitable for M2M Communications? A Survey of Alternatives," *IEEE Communications Surveys Tutorials*, vol. 16, pp. 4–16, First Quarter 2014.

[132] IEC, "IEC 61850 Part 5: Communication requirements for functions and device models," 2002.

[133] IEC, "IEC 61850 Part 8-1: Specific Communication Service Mapping (SCSM) - Mappings to MMS (ISO 9506-1 and ISO 9506-2) and to ISO/IEC 8802-3," 2004.

[134] The ns-3 network simulator. [Online], "Available: http://www.nsnam.org/."

[135] IEC, "IEC 61850 Part 90-12: Wide area network engineering guidelines," Technical Report, July 2015.

[136] R. G. Cheng, J. Chen, D. W. Chen, and C. H. Wei, "Modeling and Analysis of an Extended Access Barring Algorithm for Machine-Type Communications in LTE-A Networks," *IEEE Transactions on Wireless Communications*, vol. 14, pp. 2956–2968, June 2015.

[137] I. Leyva-Mayorga, L. Tello-Oquendo, V. Pla, J. Martinez-Bauset, and V. Casares-Giner, "Performance analysis of access class barring for handling massive M2M traffic in LTE-A networks," in *IEEE International Conference on Communications (ICC)*, pp. 1–6, May 2016.

[138] G. Madueño, J. Nielsen, D. Kim, N. Pratas, C. Stefanović, and P. Popovski, "Assessment of LTE Wireless Access for Monitoring of Energy Distribution in the Smart Grid," *IEEE Journal on Selected Areas in Communications*, vol. PP, pp. 1–1, February 2016.

[139] V. Paxson and S. Floyd, "Wide area traffic: the failure of Poisson modeling," *IEEE/ACM Transactions on Networking*, vol. 3, pp. 226–244, June 1995.

[140] X. Lin, A. Adhikary, and Y. P. E. Wang, "Random Access Preamble Design and Detection for 3GPP Narrowband IoT Systems," *IEEE Wireless Communications Letters*, vol. 5, pp. 640–643, December 2016.

[141] A. Laya, L. Alonso, and J. Alonso-Zarate, "Efficient Contention Resolution in Highly Dense LTE Networks for Machine Type Communications," in *IEEE Global Communications Conference (GLOBECOM)*, pp. 1–7, December 2015.

[142] A. Ilori, Z. Tang, J. He, K. Blow, and H. H. Chen, "A random channel access scheme for massive machine devices in LTE cellular networks," in *IEEE International Conference on Communications. (ICC)*, pp. 2985–2990, June 2015.

[143] H. Okamura, T. Dohi, and K. S. Trivedi, "Markovian Arrival Process Parameter Estimation With Group Data," *IEEE/ACM Transactions on Networking*, vol. 17, pp. 1326–1339, August 2009.

[144] E. Grigoreva, M. Laurer, M. Vilgelm, T. Gehrsitz, and W. Kellerer, "Coupled markovian arrival process for automotive machine type communication traffic modeling," in *IEEE International Conference on Communications (ICC)*, pp. 1–6, May 2017.

[145] V. Kekatos and G. B. Giannakis, "Distributed Robust Power System State Estimation," *IEEE Transactions on Power Systems*, vol. 28, pp. 1617–1626, May 2013.

[146] M. Göl and A. Abur, "A Fast Decoupled State Estimator for Systems Measured by PMUs," *IEEE Transactions on Power Systems*, vol. 30, pp. 2766–2771, September 2015.

[147] J. Zhang, S. Nabavi, A. Chakrabortty, and Y. Xin, "ADMM Optimization Strategies for Wide-Area Oscillation Monitoring in Power Systems Under Asynchronous Communication Delays," *IEEE Transactions on Smart Grid*, vol. 7, pp. 2123–2133, July 2016.

[148] A. Abur and A. Gómez Expósito, *Power System State Estimation: Theory and Implementations*. CRC Press, March 2004.

[149] H. Zhu and G. B. Giannakis, "Power System Nonlinear State Estimation Using Distributed Semidefinite Programming," *IEEE Journal on Selected Topics in Signal Processing*, vol. 8, pp. 1039–1050, December 2014.

[150] J. Matamoros, A. Tsitsimelis, M. Gregori, and C. Antón-Haro, "Multiarea state estimation with legacy and synchronized measurements," in *IEEE International Conference on Communications (ICC)*, pp. 1–6, May 2016.

[151] M. Cosovic and D. Vukobratovic, "Distributed state estimation in power system using belief propagation: Algorithms and performance," *CoRR*, vol. abs/1702.05781, October 2017.

[152] N. M. Manousakis and G. N. Korres, "A Weighted Least Squares Algorithm for Optimal PMU Placement," *IEEE Transactions on Power Systems*, vol. 28, pp. 3499–3500, August 2013.

[153] R. D. Zimmerman, C. E. Murillo-Sanchez, and R. J. Thomas, "Matpower: Steady-state operations, planning, and analysis tools for power systems research and education," *IEEE Transactions on Power Systems*, vol. 26, pp. 12–19, February 2011.

[154] EIT ICT Activity 14145 LTE 4 Smart Energy, "Deliverable D1: Use Cases & Requirements," February 2014.

[155] H. C. Tijms, *Stochastic Modeling and Analysis: A Computational Approach*. Wiley Series in Probability and Mathematical Statistics, 1986.

[156] D. Bertsekas, *Network Optimization Continuous and Discrete Models*. Athena Scientific, May 1998.

[157] Cisco Systems Inc, "Measuring Delay, Jitter, and Packet Loss with Cisco IOS SAA and RTTMON," October 2005.

[158] K. Doppler, C. H. Yu, C. B. Ribeiro, and P. Janis, "Mode Selection for Device-To-Device Communication Underlaying an LTE-Advanced Network," in *IEEE Wireless Communications and Networking Conference (WCNC)*, pp. 1–6, April 2010.

[159] M. Jung, K. Hwang, and S. Choi, "Joint Mode Selection and Power Allocation Scheme for Power-Efficient Device-to-Device (D2D) Communication," in *IEEE Vehicular Technology Conference (VTC Spring)*, pp. 1–5, May 2012.